UNIVERSITÀ DEGLI STUDI DI TRIESTE

UNIVERSITÀ DEGLI STUDI DI TRIESTE

XXXV CICLO DEL DOTTORATO DI RICERCA IN

SCIENZE DELLA RIPRODUZIONE E DELLO SVILUPPO

Isolation and characterization of monoclonal antibodies against ICOSL

Settore scientifico-disciplinare: BIO/13

DOTTORANDO
Andrea Lanza

COORDINATORE
Prof. Paolo Gasparini

SUPERVISORE DI TESI
Prof. Daniele Sblattero

TUTOR DI TESI
Prof. Alberto Tommasini

ANNO ACCADEMICO 2021/2022

UNIVERSITÀ
DEGLI STUDI
DI TRIESTE

UNIVERSITÀ DEGLI STUDI DI TRIESTE

XXXV CICLO DEL DOTTORATO DI RICERCA IN

SCIENZE DELLA RIPRODUZIONE E DELLO SVILUPPO

Isolation and characterization of monoclonal antibodies against ICOSL

Settore scientifico-disciplinare: BIO/13

DOTTORANDO
Andrea Lanza

COORDINATORE
Prof. Paolo Gasparini

SUPERVISORE DI TESI
Prof. Daniele Sblattero

TUTOR DI TESI
Prof. Alberto Tommasini

ANNO ACCADEMICO 2021/2022

Table of Contents

Riassunto

L'osso è un tessuto connettivo che è continuamente rimodellato dall'interazione tra cellule del sistema immunitario e cellule dell'osso. In particolare i due attori principali sono gli osteoblasti (deputati all formazione di nuovo osso) e gli osteoblasti (deputati al riassorbimento osseo). Per mantenere l'omeostasi del tessuto l'attività di queste due cellule deve essere in equilibrio. Quando l' equilibrio viene interrotto si va in contro a patologie come l'osteoporosi. Essa è caratterizzata da un eccessivo riassorbimento osseo dato dalla non regolazione dell'attività osteoclastica. Infatti, l'osteoporosi è caratterizzata da perdita della densità ossea, con conseguente aumento del rischio di fratture. Ad oggi esistono diverse terapie per il trattamento della patologia, ma esse non sono definitive e inoltre presentano diversi effetti collaterali. Ad oggi è stata studiata una nuova via di segnalazione coinvolta nel processo di rimodellamento: ICOS/ICOSL. In particolare è staato visto che trattando gli ostoclasti con una molecola ricombinante chiamata ICOS-Fc (creata da Novaicos) è possibile innescare ICOSL sulla superficie degli osteoclasti, determinane una inibizione dell'attività e della maturazione sia in test in vitro che in vivo.

Il progetto mira, in collaborazione con Novaicos, alla sostituzione della molecola ICOS-Fc con un anticorpo monoclonale che sia in grado di legare ICOSL sugli osteoclasti e causarne l'inibizione della maturazione e dell'attività. Per far ciò sono state utilizzate le tecnologie in vitro di isolamento degli anticorpi. In particolare è stata usata una combinazione del phage e dell' yeast display per unire gli aspetti positivi delle due tecniche e dimunuirne gli svantaggi. Infatti, è stato possibile sfruttare la capacità di formare delle librerie anticorpali di grandi dimensioni tramite phage display ma anche sfruttare le modifiche post traduzionali e i processi di selezioni effettuati in tempo reale tramite yeast display.

Tramite phage display è stato possibile isolare, a partire da una libreria naive di frammenti anticorpali, di isolare un anticorpo monoclonale chiamato G10. Il clone isolato ha mostrato specifitaà di legame verso la molecola ICOSL e anche una buona affintà (calcolata tramite BLI: Biolayer interferometry). Inoltre, per comprendere meglio la capacità del clone di legare ICOSL nella sua conformazione nativa, sono state effettuate delle analisi citofluorimetriche su diversi tipi cellulari $ICOSL^+$. Da questi esperimenti è stato dimostrato che il clone riconosce ICOSL sulla superficie cellulare.

Viste le ottime caratteristiche di questo clone, si è deciso di migliorare ulteriormente l'affinità attraverso la tecnica di 'Affinity maturation'. Per far ciò la regione variabile della catena pesante (V_H) del cone G10 è stata mantenuta costante e successivamente associata casualmente con una libreria di V_L (regione variabile della catena leggera). La nuova libreria è stata clonata all'interno di un vettore che permette l'espressione del frammento anticorpale sulla proteina del lievito. Infatti per l'isolamento di cloni ad affinità migliorata è stata usata la tecnica dell'yeast display. Tramite FACS è stato possibile selezionare in real-time i cloni con migliore affinità. Questo ha portato all'isolamento di 4 cloni. La corretta riuscita dell' 'Affinity maturation' è stata verificata attraverso il calcolo della costante di dissociazione (k_D). Tutti i nuovi cloni presentano una k_D inferiore rispetto a quella del clone parentale G10 dimostranto il successo della tecnica.

Il clone G10 è stato inoltre caratterizzato per la sua capacità di inibire la maturazione e l'attivià degli osteoclasti. Test condotti in collaborazione con Novaicos hanno evidenziato un comportamento del clone G10 analogo a quello di ICOS-Fc. Infatti, il clone G10 appare essere in grado di inibire l'osteoclastogenesi e quindi la maturazione degli osteoclasti. Questi dati sono confermati anche dalla riduzione dell'espressione di geni cruciali per lo sviluppo degli osteoclasti.

Invece, la riduzione dell'attività osteoclastica è stata valutata, quantificando l'enzima TRAP, all'interno degli osteoclasti trattati con l'anticorpo G10. I dati hanno mostrato una riduzione della proteina TRAP negli osteoclasti trattati con il clone G10 che è paragonabile a quella degli osteoclasti trattati con ICOS-Fc.

Abstract

Bone is a connective tissue that is continuously remodeled by the interaction between the cells of the immune system and the cells of the bone. In particular, the two main actors are osteoblasts (responsible for forming new bone) and osteoblasts (responsible for bone resorption). To maintain tissue homeostasis, these two cells' activity must be balanced. When the balance is hampered, pathologies like osteoporosis can occur. It is characterized by excessive bone resorption due to the non-regulation of osteoclastic activity. Osteoporosis is characterized by a loss of bone density, resulting in an increased risk of fractures.

To date, there are several therapies for treating the disease, but they are not definitive and have different side effects. Recently, a new signaling pathway involved in the remodeling process has been studied: ICOS / ICOSL. In particular, it has been seen that by treating the osteoclasts with a recombinant molecule called ICOS-Fc (created by Novaicos), it is possible to trigger ICOSL on the surface of the osteoclasts, with consequent inhibition of their activity and maturation both in vitro and in vivo tests.

In collaboration with Novaicos, the project aims to replace the ICOS-Fc recombinant molecule with a monoclonal antibody capable of binding ICOSL on osteoclasts, inhibiting their maturation and activity. To do this, in vitro antibody isolation technologies were used. In particular, a combination of phage and yeast visualization was used to combine the positive aspects of the two techniques and reduce their disadvantages. It was possible to exploit the ability to form large libraries of antibodies via phage display and to exploit post-translational modifications and selection processes carried out in real-time via yeast display. Through the phage display technique, it was possible to isolate, starting from a naïve library of antibody fragments, to isolate a monoclonal antibody called G10. The isolated clone showed specific binding to the ICOSL molecule and also good affinity (calculated by BLI: Biolayer interferometry). Furthermore, to better understand the ability of the clone to bind ICOSL in its native conformation, flow cytometric analyzes were performed on different ICOSL + cell types. From these experiments, it was shown that the clone recognizes ICOSL on the cell surface.

Given the promising characteristics of this clone, it was decided to further improve the affinity through the 'Affinity Maturation' technique. To do this, the heavy chain variable region (V_H) of clone G10 was kept constant and subsequently randomly associated with a library of V_L (light chain variable region).

The new library was cloned into a vector that allows the expression of the antibody fragment on the yeast surface. Indeed, the yeast display technique was used to isolate clones with improved affinity. Through FACS, it was possible to select the clones with the best affinity in real-time. This led to the isolation of 4 clones. The ‘Affinity maturation' success was verified by calculating the dissociation constant k_D (BLI) for all clones. All new clones have a lower kD than the parental clone G10, demonstrating the technique's success.

Clone G10 was also characterized as inhibiting osteoclast maturation and activity. Tests conducted in collaboration with Novaicos showed a behavior of clone G10 similar to that of ICOS-Fc. Clone G10 appears to inhibit osteoclastogenesis and, therefore, the maturation of osteoclasts. These data are also confirmed by the reduction of the expression of genes crucial for the development of osteoclasts.

The reduction of osteoclastic activity was assessed by quantifying the TRAP enzyme within the osteoclasts treated with the G10 antibody. The data showed a decrease of TRAP protein in G10-treated osteoclasts comparable to that of ICOS-Fc-treated osteoclasts.

Introduction

1 The Immune System: an Overview

The immune system (IS) discriminates between self and not-self and defends itself from pathogenic microorganisms [1]. The immune system is composed of humoral factors such as complement proteins, as well as immune cells that lead to the production of antibodies, cytokines/chemokines, and growth factors (Fig. 1 [2]) [1, 3].

In this vision, in the IS, it is possible to distinguish two different types of immune response: the innate response and the adaptive (or acquired) response [3].

Within a few seconds after overcoming the anatomical and physiological barriers (epithelial cells, sebaceous glands, and mucus) and the consequent exposure to the pathogen, the innate immune system generates an anti-inflammatory response [3, 4].

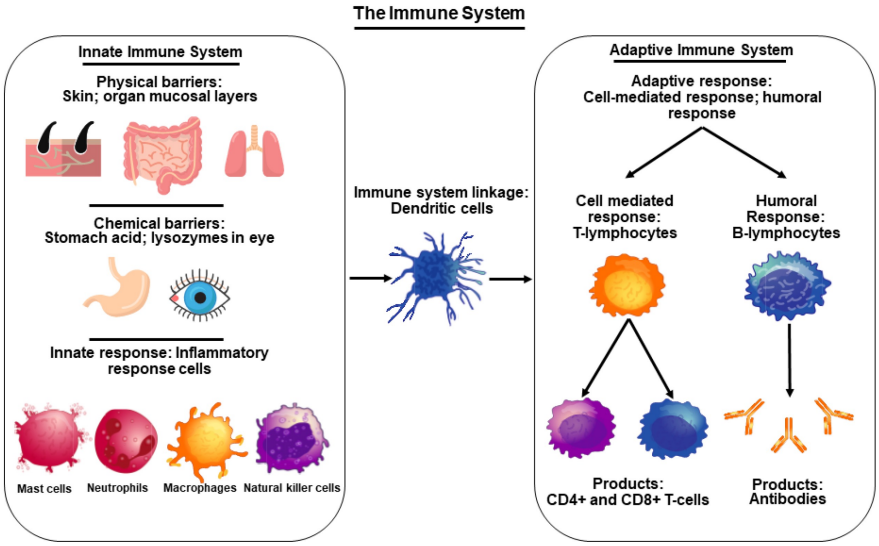

Fig.1 *Schematic figure of the components of the immune system. It is composed of the innate immune system (physical and chemical barriers and inflammatory response cells) and the adaptive immune system (cell-mediated response and humoral response). Figure taken from [2].*

This kind of response has evolved to rapidly eliminate a wide range of pathogens, but the pathogenic molecular patterns it can recognize are limited [5].

On the contrary, adaptive immunity is characterized by the interaction between the antigen-presenting cells and T and B lymphocytes, leading to more specific immunologic effector pathways, generation of immunologic memory, and regulation of host immune homeostasis [3, 5].

T lymphocytes differentiate into two types of cells: T helper and T cytotoxic. In detail, T helper regulates the immune response depending on the pathogen, whereas T cytotoxic has an effector function against pathogens [3, 6].

T lymphocytes must be activated through 3 signals mediated by Ligand-receptor interaction to perform their functions.

In detail, the first activation signal is mediated by the interaction between the T cell receptor (TCR) and the antigen carried by the MHC (major histocompatibility complex) expressed by the antigen-presenting cells (APC). The second signal foresees the interaction between the costimulatory molecules B7.1 (CD80) and B7.2 (CD86) on the APC and the CD28 molecules on the T cell. Notably, the absence or interruption of the second signal leads to an anergic or apoptotic state.

The third phase is called polarization. At this stage, APC cells and T lymphocytes release specific cytokines that direct the T lymphocytes to cytotoxic or helper lymphocytes [7, 8]. Another CD28 family receptor is the cytotoxic T-lymphocytes-associated antigen 4 (CTLA-4). This has an opposite function (inhibitory) than CD28 and interacts with the same ligand of CD28 (B7.1-B7.2) but with a higher affinity [8]. The balance between the CD28 and CTLA-4 molecules is crucial for maintaining a state of immunological tolerance and maximizing the immune response [9].

Instead, the main characteristic of B lymphocytes, once they have become plasma cells, is to produce antibodies. They have several duties, such as complement activation, bacterial opsonization, toxin neutralization, and preventing organisms from adhering to the mucosa surface [10].

1.1 ICOS/ICOSL Pathway

As mentioned before, T-cell activation is a complex process that involves different signals mediated by receptor-ligand interaction. Another molecule belonging to CD28/ CTLA-4 family is expressed upon T-cell activation: ICOS (inducible T costimulator) [11]. The ICOS signal triggered by its ligand ICOSL leads to increased proliferation, survival, and differentiation of T cells (Fig.2 [12]) [13]. Moreover, ICOS can co-induce the secretion of several cytokines like IL-4, IL-5, IL-6, IL-10, IL-21, Interferon-gamma, and TNF-α [14]. Its ligand ICOSL (B7h2) is a monomeric transmembrane glycoprotein of 60 kDa belonging to the B7 costimulatory superfamily. It comprises an extracellular domain

of 240 aa, a transmembrane domain of 19 aa, and an intracytoplasmatic domain of 23 aa [15] [11].

The extracellular part of ICOSL contains two different immunoglobulin domains: the IgV domain responsible for its binding with the receptor ICOS and the IgC domain that maintains the structural integrity of the molecule [15]. The IgC portion of ICOSL is also important for binding with another interacting molecule: OPN (osteopontin). This binding appears to play an important role in tumor development [16].

The B7h2 molecule, differently from its receptor ICOS, is expressed by several cell

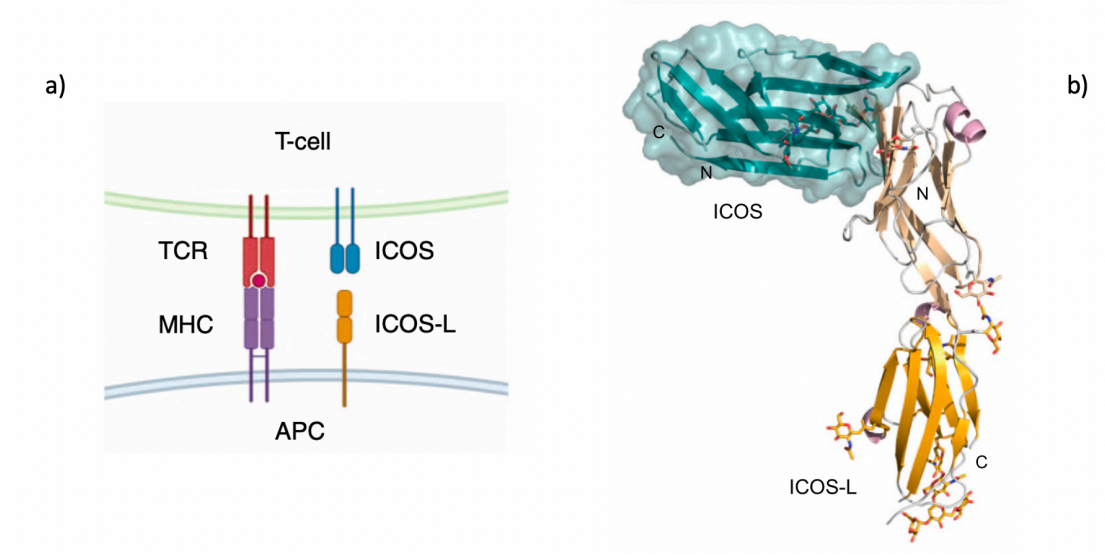

Fig. 2 *a) Schematic representation of the binding between the ICOS receptor (T cells) and ICOS ligand (APC). b) side view of the secondary structure cartoon of ICOS/ICOSL complex. Figure taken from [12]*

types. In particular, it is constitutively expressed by B cells, macrophages, dendritic cells (DCs), and monocytes (the expression is upregulated after activation). But it is also expressed by epithelial cells, fibroblasts, vascular endothelial cells, and some tumor cells [17, 18].

The widespread expression of ICOSL suggests that its role in the activation of T lymphocytes occurs not only in the lymphoid organs but also in sites of inflammation far from them [18].

New studies have demonstrated that the binding ICOS/ICOSL may trigger a bidirectional signal that modulates the response of cells bearing ICOSL [19]. In particular, Dianzani et al. [20, 21] have demonstrated that the triggering of the ICOSL molecule by a soluble molecule ICOS-Fc (a recombinant molecule composed of the extracellular part of ICOS fused with the Fc fragment of human IgG) inhibits

adhesiveness and migration of HUVECs (human umbilical vein endothelial cells) and several cancer cell lines, and improve cutaneous wound healing (increasing angiogenesis and recruiting reparative macrophages [22]. Another effect of ICOSL triggering by ICOS-Fc is hampering the development of experimental lung metastases in B16 melanoma models. Moreover can cause the migration and adhesion of dendritic cells (DC) but also modulate the release of cytokine and antigen cross-presentation in MHC I [23].

1.2 ICOS/ ICOSL in tumor

The interaction between ICOS-ICOSL, as a pathway involved in the regulation of SI, plays a role in oncogenesis. Several studies have shown dual behavior in cancer progression. The co-stimulatory signal mediated by the ICOS-ICOSL interaction participates in an antitumor response of T lymphocytes but also shows pro-tumor characteristics linked to the immunosuppressive activity of activated Treg (regulatory T lymphocytes) [13]. Studies have seen that in metastatic melanoma, ICOS is expressed by Tregs in tumor-infiltrating lymphocytes [24], while ICOSL is expressed by melanoma cells [25]. The signaling pathway triggered by ICOSL on melanoma cells determines the expansion of $ICOS^+$ Tregs, causing the tumor cells to escape immunity. A similar situation exists in other solid tumors like renal clear cell carcinoma [26], gastric cancer [27], and primary breast cancer [28], in which the presence of Tregs $ICOS^+$ correlates with an immunosuppressive environment and poor prognosis.

On the other hand, in different hematologic malignancies, Treg $ICOS^+$ is associated with a favorable prognosis [29].

Therefore, the therapeutic modulation of ICOS/ICOSL could be used to treat tumors. Depending on cancer and the microenvironment, it is possible to use antagonist or agonist mAbs. Antagonist antibodies could be used if cancer presents TILs $ICOS^+$ Tregs. For example, MEDI-570 is an antagonistic mAb directed against ICOS, which binds and eliminates ICOS-expressing cells in preclinical in vivo models [30].

In contrast, if ICOS is expressed on the surface of cytotoxic lymphocytes, a mAb agonist could be used to enhance the immune response [13]. Preclinical models of mouse melanoma and prostate cancer have demonstrated that ICOS agonists cannot independently induce a potent immune response. However, a synergic treatment with

mAb anti-CTLA-4 enhanced the function of antitumor T effector cells [31]. Two agonist mAb are currently under investigation: GSK3359609 and JTX-20011 [13].
Finally, since the ICOS/ICOSL pathway presents a bidirectional signal that has pro-inflammatory and anti-tumor abilities, it is necessary to investigate the use of mAbs targeting ICOSL.

2 ICOS/ICOSL and Bone

2.1 Bone tissue: an overview

Recent findings [32] have demonstrated the involvement of the ICOS/ICOSL pathway in the regulation of bone turnover.
Bone tissue is a rigid tissue that performs essential functions in our body. It involves locomotion, protects soft tissue, supports, and covers the bone marrow. However, it is also involved in biological processes; in fact, it allows the storage of calcium and phosphate, allowing them to regulate their concentration in the bloodstream through bone remodeling. Despite an apparently rigid and inert structure, bone is a highly dynamic organ, continuously remodeled according to the stimuli and stress signals it receives [33, 34]. Bone remodeling is not always constant throughout life. In childhood, there is a high bone turnover that progressively decreases with aging, up to a net bone loss in older subjects [34].
The bone extracellular matrix is composed of 60% of inorganic material (calcium phosphate), 25% of organic material (collagen, proteoglycans, and osteocalcin), and 5% of water [35].
Inside the bone structure is possible to distinguish four different cell types clearly: osteoblasts, osteocytes, lining cells, and osteoclasts (Fig 4) [34].
Osteoblasts represent 4-6% of the total bone cells and are specialized fibroblast-like cells derived from MSCs (Fig. 4a) [36]. Osteoblasts are mainly responsible for the formation of new bone and its mineralization. In detail, the synthesis of the bone matrix involves a first phase in which the organic matrix is formed through the release of collagen (mainly type I), osteonectin, osteopontin, and proteoglycans by the osteoblasts [37]. Finally, thanks to the formation of hydroxyapatite crystals (calcium phosphate), the mineralization process of the bone will take place [38]. At this stage, the osteoblast can go into apoptosis or become osteocytes or lining cells [37]

Bone lining cells are quiescent flat-shaped osteoblasts located on the surface of bone

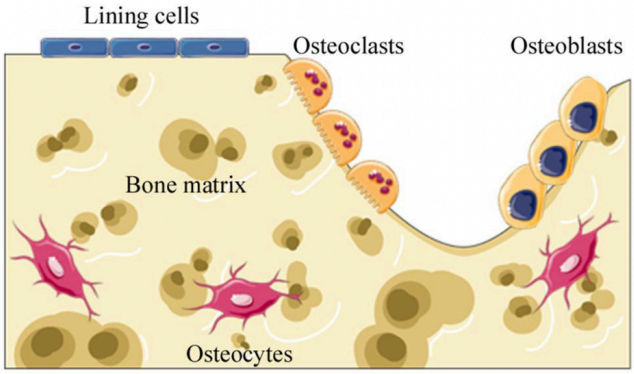

***Fig.3 Schematic representation of bone tissue cells**. The lining cells are found on the surface of the bone; osteocytes are trapped within the bone matrix they have formed; osteoclasts are cells involved in the formation of new bone; osteoclasts are cells responsible for bone resorption*

whose function is not entirely understood. However, studies have shown a protective behavior, hampering the interaction between the bone matrix and the osteoclasts when bone resorption should not occur [37]. Furthermore, findings show their involvement in osteoclast differentiation through the production of osteoprotegerin (OPG) and RANKL (receptor activator of nuclear factor kappa-B ligand) [39].

Osteocytes are the most abundant cells in the bone tissue (90-95%), with a lifespan of up to 25 years. The osteocytes are osteoblasts incorporated into the bone matrix after the mineralization process [40]. Osteocytes are the orchestrators of bone remodeling; by acting as mechanosensory, they can respond to mechanical pressure and forces, regulating the activity of osteoblasts and osteoclasts [41].

Finally, osteoclasts are end-differentiated multinucleated cells involved in bone resorption. They derive from the hematopoietic stem cell, and osteoclast differentiation is a complex process involving several factors. The first factor that comes into play is the M-CSF (macrophage colony-stimulating factor), secreted by the osteoprogenitor mesenchymal cells and the osteoblasts (Fig. 4b). Once M-CSF binds, its receptor (cFMS) on the osteoclast stimulates their proliferation and inhibits apoptosis [42, 43]. RANKL is another crucial factor; it is expressed by osteoblasts, osteocytes, and stromal cells, and when it binds to its receptor on the osteoclast induces the osteoclastogenesis process [44].

Moreover, the interaction between RANK/RANKL promotes the expression of other factors, such as NFATc1 and DC-STAMP. The first is crucial for expressing essential

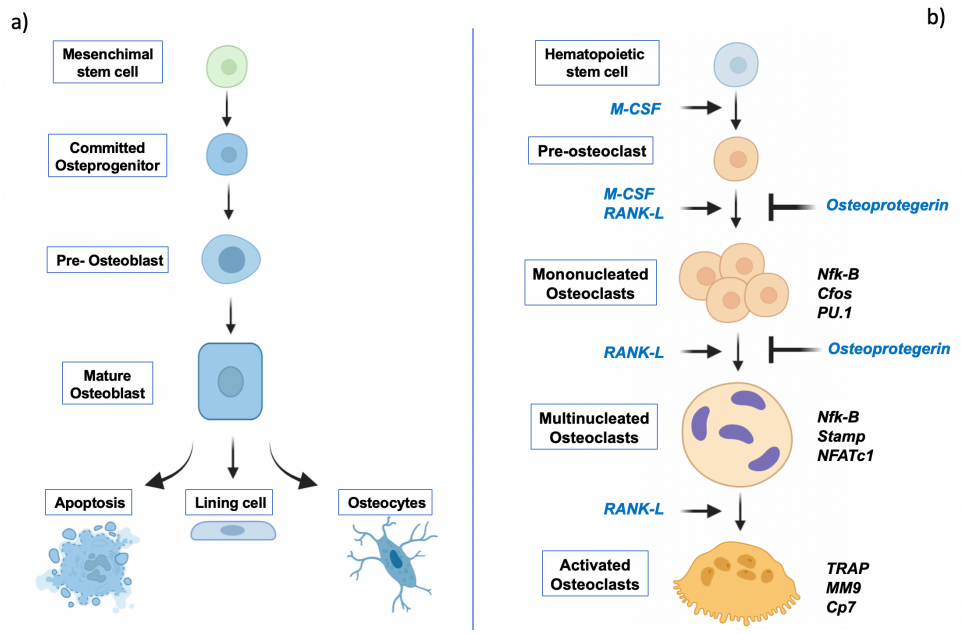

***Fig.4 Schematic representation of the maturation process of osteoblasts and osteoclasts**: a) Osteoblasts develop from the mesenchymal stem cell through intermediate maturation stages. Once they have produced the bone matrix, the osteoblasts either go into apoptosis or become osteocytes or lining cells; b)osteoclasts derive from the hematopoietic stem cell. The osteoclastogenesis process involves several stages highly regulated by factors such as M-CFS, RANKL (pro maturation) and Osteoprotegerin (inhibitor of maturation). This leads to the activation of transcription factors (Nfk-B, Stamp, NFATc1) which will allow the formation of multinucleated cells with active bone resorption capacity. Figure created with BioRender.com*

enzymes involved in bone resorption (TRAP and Cathepsin K). Instead, DC-STAMP is necessary to form multinucleated cells, allowing osteoclast precursor fusion [45]. On the other hand, the osteoclastogenesis process must be inhibited to avoid excessive bone resorption, which would cause a weakening of the bone structure. To do this, osteoclasts and stromal cells produce a factor called osteoprotegerin, which binds RANKL preventing it from binding to its receptor and inducing osteoclastogenesis [46].

2.2 Osteoporosis

As mentioned above, the bone remodeling mechanism is a complex process based on the balance between the formation of new bone (osteoblasts) and bone resorption (osteoclasts). Therefore, when this balance is impaired, bone pathologies can occur. In particular, Osteoporosis is a “progressive systemic skeletal disease characterized by low bone mass and microarchitectural deterioration of bone tissue, with a consequent increase in bone fragility and susceptibility to fracture” [47] due to excessive bone

resorption [48]. It has been estimated that about 200 million men and women worldwide have osteoporosis: one in three women and one in five men over 50 years old will experience osteoporotic fractures. Notably, more than 8.9 million fractures occur yearly, one every three seconds [48]. Given the progressive increase in life expectancy, more and more people will be affected by this disease, thus increasing the economic burden and weighing on the health system of many countries; in fact, it has been estimated that the direct cost of treating osteoporotic fractures is between 5000-6500 billion USD in Canada USA and Europe [49]. For these reasons, it is crucial to understand the molecular mechanism better to use the proper approach to cure this pathology.

2.3 Osteoporosis: treatments

To date, several therapeutic approaches against osteoporosis have been used, targeting essential factors involved in bone remodeling at different levels.

The first compound widely used since the 1990s is Bisphosphonates (BPS); thanks to its core structure of P-C-P bounds, it is able to bind the hydroxyapatite, which is taken up by di osteoclasts during the bone resorption process. This molecule inhibits osteoclast activity by inducing apoptosis [48]. However, BPs can be described for less than five years because of their side effects: gastrointestinal and renal complications [50, 51], atypical femoral fractures, and risk of osteomalacia [52].

Another effective molecule is strontium ranelate. It has a double effect by preventing bone resorption (interfering with osteoclast differentiation) and promoting bone formation (stimulating osteoblast differentiation). But it can only be used in severe cases of osteoporosis or where other treatments have failed, as its use increases the risk of heart problems [53].

The monoclonal antibody Denosumab is also used for the treatment of osteoporosis. Its mechanism foresees the inhibition of the osteoclasts by binding RANKL, thus, preventing its binding with the RANK receptor on the surface of the osteoclasts [54].

Since RANKL is also expressed by dendritic cells and activated T lymphocytes, using an antagonist monoclonal antibody could affect the IS [55].

A different approach is used with the SERMs (Selective Estrogen Receptor Modulators). A previous study has shown how estrogen regulates the survival of mature osteoclasts [56] by interacting with the RANK/RANKL/OPG system, causing decreased bone resorption [57]. Among the best-known SERMs, there is Raloxifene, which binds

to estrogen receptors and produces estrogen-like effects on bone, causing the reduction of bone loss in postmenopausal women [58].
However, these drugs are not recommended as a first-line treatment for osteoporosis in postmenopausal women, as they present a risk of thromboembolism and stroke [48].

2.4 ICOS-Fc: The innovative treatment

Bone remodeling is quite a complex process, managed by osteoclasts and osteoblasts but also by the immune system through a regulation mediated by cytokines and surface receptors. As previously mentioned, the ICOS/ICOSL pathway is involved in bone remodeling [32]. Furthermore, the binding of ICOS to ICOSL triggers a signaling pathway not only in ICOS-expressing cells but also in ICOSL-expressing cells [19]. To fully understand the involvement of the ICOS/ICOSL pathway in bone remodeling, a new recombinant molecule was created; it is formed by the extracellular part of ICOS

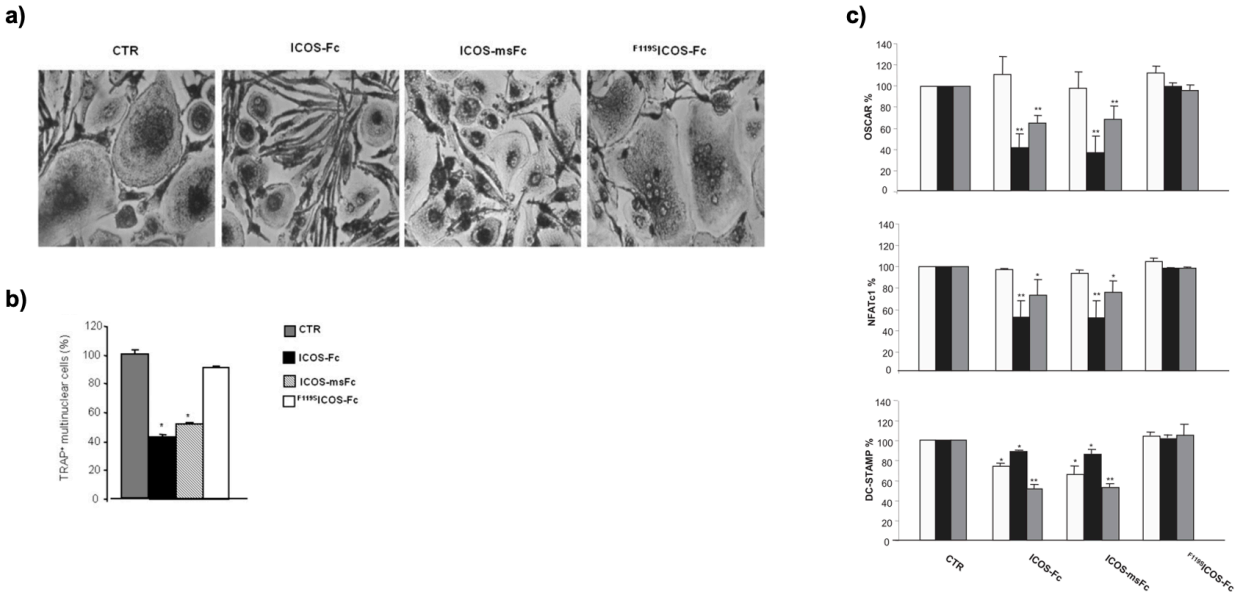

Fig.5 *a) Microphotographs of MDOCs stained with TRAP. The cells were treated with F119S ICOS-Fc (mutated and non-functional form), with recombinant molecule ICOS-Fc and ICOS-mFc (ICOS molecule fused with a mouse Fc). It is possible to observe a reduction in the number of osteoclasts (giant cells) and in the quantity of TRAP enzyme inside them (black colouration) in cells treated with ICOS-Fc and ICOS-mFc. b) Bar graphs show the percentage of the multinuclear TRAP+ cells. c) Histogram representing the gene expression level of NFATc1, OSCAR and DC-STAMP. ICOS-Fc and ICOS-mFc treatments reduce the expression of genes important in osteoclast development and maturation. Figure taken from [32]*

fused with the Fc fragment of IgG [18]. It has been seen that the triggering of ICOSL on

MDOCs (human monocytes-derived osteoclast-like cells) using ICOS-Fc can impair their maturation and differentiation (Fig.5 a) [32]. In agreement with these results, it was observed that ICOS-Fc-treated cells exhibited a decreased expression level of TRAP, DC-STAMP, OSCAR, and NFATc1, as well as inhibited osteolytic activity in vitro (Fig.5 b,c). All these findings align with the in vivo results, in which the treatment whit ICOS-Fc strikingly inhibits bone resorption in mice models of osteoporosis [32]. Other studies currently aim to combine the inhibition of ICOS-Fc osteoclast activity and differentiation with the ability of strontium to promote osteoblast replication and stimulate the formation of new bone [59]. In particular, treatment of cells with Sr-containing MBGs(mesoporous bioactive glasses) functionalized with ICOS-Fc shows similar behavior to ICOS-Fc treatment. This treatment has shown an inhibitory effect on osteoclast differentiation, proved by a decreased expression level of osteoclast differentiation genes (DC-STAMP, NFATc1, and OSCAR) [59].

3 Antibody: Structure and Function

3.1 Antibody : an overview

As mentioned before, the plasma cells can produce the antibodies continuously.
Antibodies, also known as Immunoglobulins (Igs), are molecules able to recognize a specific portion of exogenous entity (photogenic, toxins, etc.) [10, 60].
Immunoglobulins belong to the Immunoglobulin superfamily and share structural elements [60, 61]. Each immunoglobulin is composed of 2 heavy (H) and two light (L) chains connected by disulfide bonds (Fig. 5) [60, 61].
The light chain is composed of one variable domain (V_L) and one constant domain (C_L), whereas the heavy chain presents one variable domain (V_H) and three-four constant domains (C_H1-C_H2-C_H3; C_H4 only for IgM and IgE). Each V and C domain has about 110-130 amino acids (25 kDa), which gives the immunoglobulin a total molecular weight of about 150 kDa [3, 60, 61].
In the antibody, we can find two types of light chains: k and λ. These chains are present in a 2:1 ratio, and there would appear to be no functional difference between them [3, 61, 62].
Differently, an antibody's class and the effector function are defined by the constant region of the heavy chain. It is possible to distinguish five main classes of heavy chain:

IgM, IgD, IgG, IgA, and IgE. Moreover, are present also subclasses for IgG (IgG1-IgG2-IgG3-IgG4) and IgA (IgA1-IgA2) [3, 61].

Since the modular nature of the Igs, the study of the structure and function of the antibody was possible thanks to the use of proteases that cut the antibody into well-defined portions.

Papain, for instance, cuts the molecule at the amino-terminal level of the disulfide bonds, releasing two identical fragments called Fab (fragment antigen binding) and a fragment called Fc (fragment crystallizable) (Fig.6 b) [2, 8].

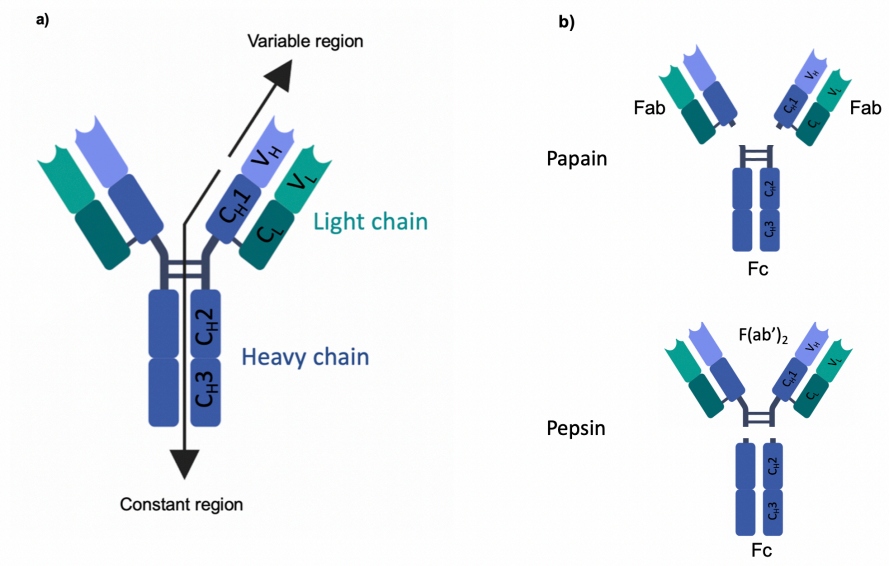

***Fig.6 Basic structure of antibody**: a) The immunoglobulins are composed of two heavy chains (blu) and two light chains (green). The variable region of the light (V_L) and heavy chain (V_H) form the Fv (fragment variable) involved in the antigen's binding. b) Papain separates the immunoglobulin in 2 identical Fab and one Fc, instead, pepsin digestion leads to the formation of one F(ab')2 and one Fc fragment. Figure created with BioRender.com*

The Fab fragment contains a complete light chain (V_L-C_L) bonds to V_H and C_H1 of the heavy chain; this is responsible for binding with the antigen. The Fc region (CH2-CH3) is the molecule's effector part, and functional differences depend on the various Ig subclasses.

On the other side, pepsin cuts at the carboxy-terminal level of the disulfide bonds. This leads to the release of fragment $F(ab')_2$ and fragmented Fc fragment (Fig.6 b) [3, 61, 62]. The variable regions (V_L-V_H) of the Fab fragment are called Fv (fragment variable) and are the portion of the antibody in charge of binding the antigen [3, 61, 63].

The variable regions of an antibody are unique compared to those of the other antibodies. This is due to the presence in the sequence of highly variable regions called hypervariable regions (or Complementarity Determining Regions: CDR) [2, 10].
There are three hypervariable regions for each variable region: H1-H2-H3 for V_H and L1-L2-L3 for V_L, and the most variable region in composition (with 10^{23} diverse sequences) and length (6-24 amino acids) is CDRH3 [64, 65].
Among the CDRs, some regions present lower variability, the framework regions (FR) that have a structural function allowing the correct folding of the CDRs.
Interestingly, the folding of the V_L and V_H brings the CDRs together, allowing them to form the antigen-binding site, also known as the paratope [2, 8, 10].

3.2 Antibody Fragments

It is possible to exploit the antibody molecule's modular nature through biochemical or genetic means to create optimized therapies with specific characteristics for targeted biological applications [66, 67].
Thanks to this, it was possible to develop smaller antibody fragments that combine correct folding with the binding specificity of a full-size-Ig [68].

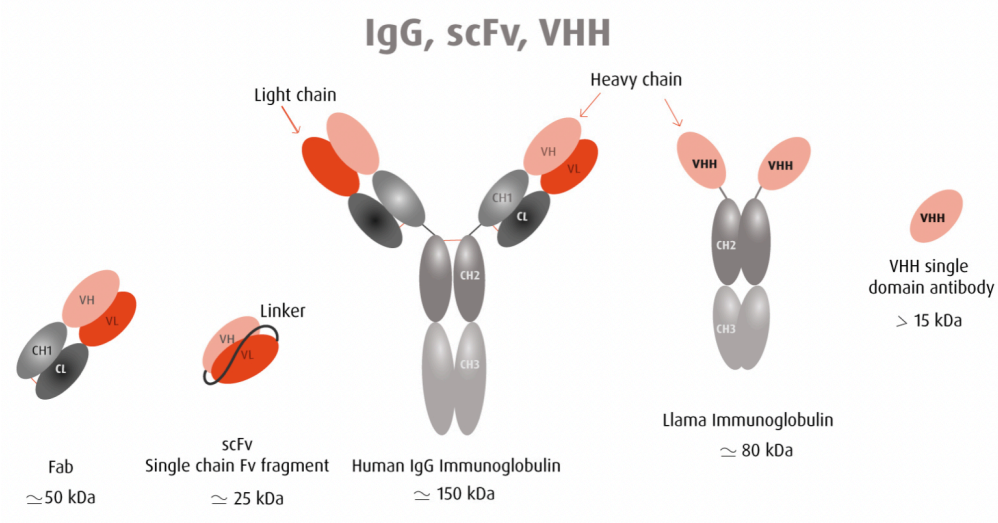

***Fig. 7 Schematic representation of antibody fragments**. FAb fragments are heterodimers composed of V_H-C_H1 and V_L-C_L bonded through a disulfide bond. scFv is composed of V_H-V_L and is the smallest part of an antibody that has binding capacity. VHH has the same function as conventional Fab but is derived from the heavy chain of Camelidae antibodies. From Hybribody. com*

The principal antibody fragments are the Fab and the scFv. The Fab (~50kDa) is a heterodimeric protein composed of V_H-C_H1 and V_L-C_L linked tighter through a disulfide

bond (Fig.6). The scFv (~ 25 kDa) is the smallest part of an antibody that retains the binding capacity. It is composed of the variable region of the heavy and light chain (V_H-V_L) joined by a flexible polypeptide of approximately 15 amino acids which helps the molecule to fold; usually, the sequence of the linker is (Gly4Ser)3 (Fig.7) [66, 67, 69].
Furthermore, it is possible to create multivalent scFv molecules reducing the linker's length (between 0 to 5 amino acids) and favoring the aggregation; in this way, it is possible to obtain diabodies (2 scFv, ~50kDa), triabodies (3 scFv, ~ 75kDa) and tetrabodies (4 scfv, ~ 110kDa) [66, 67].
Another type of antibody fragment that has caught the attention for the characteristics it possesses is VHH (or nanobodies) which derives from the heavy-chain antibodies (HCAbs) found in sera of Camelidae (Fig. 7).
In particular, the VHH has the same function as conventional antibodies' Fab fragment [70, 71]. The altered physiochemical features of these molecules give them several possible uses. For instance, their smaller size allows them to penetrate otherwise inaccessible tissues; this could be important in diagnosis and therapy. Besides, they can interact with cryptic epitopes as enzyme active sites not reachable by the full-length antibody.[66, 67, 71, 72].On the other hand, lacking the Fc domain leads to increased degradation and, consequently, to a decreased circulating half-life. The antibody fragment lacking the Fc portion cannot perform an effector function, so the therapeutic effect can be effective only by binding either ligand or receptor [11, 12]. Their smaller size allows them to be expressed to a high level in prokaryotic organisms (*Escherichia coli),* and this made the antibody fragments worthwhile for the creation of an antibodies library for the in Vitro Display Technology [69, 73, 74]

4 Monoclonal antibodies generation

4.1 Antibodies in Therapy

Their ability to bind a specific target with high affinity and specificity makes monoclonal antibodies an excellent tool for therapeutic and diagnostic applications.
In particular, the number of therapeutic mAbs has dramatically increased since the first approval, by the FDA, of the therapeutic monoclonal antibody (Muromonab-CD3, trade name Orthoclone OKT3) [75] in 1985. In fact, they have become the fastest-growing drug class in history [76].

Over the years, monoclonals have proven to be really effective in the treatment of pathologies like cancer and inflammatory disorders [77] [78]. Their essential therapeutic efficacy has now made them the most purchased drugs in the world (most of the top 10 drugs for global sales are antibody therapies) [79], thus, making monoclonals antibodies the main income factor of the pharmaceutical market [80].
In 2018, the market was estimated at around US $ 115 billion, with growth estimated at around US $ 300 billion in 2025 [81]. To date, around 80 mAbs have been approved in the US and EU, and 79 more are in late-stage clinical trials [82].
Given their versatility, various technologies have been developed over time to find mAbs with suitable affinity, specificity, and functionality characteristics. Among them, there are the Hybridoma Technology and the in vitro display system (phage, yeast, ribosome) [81]. These techniques will be discussed in the following chapters.

4.2 Hybridoma technology

The Hybridoma technique was a milestone for producing monoclonal antibodies (mAbs). Invented by Georges Köhler and Cesar Milstein in 1975, this technique allows the isolation and production of mAbs by creating a particular cell, the so-called Hybridoma (Fig.7) [83]. Even today, the hybridoma technique is widely used to produce monoclonal antibodies; today, more than 90% of the antibodies approved by the FDA are produced with this method [84, 85].

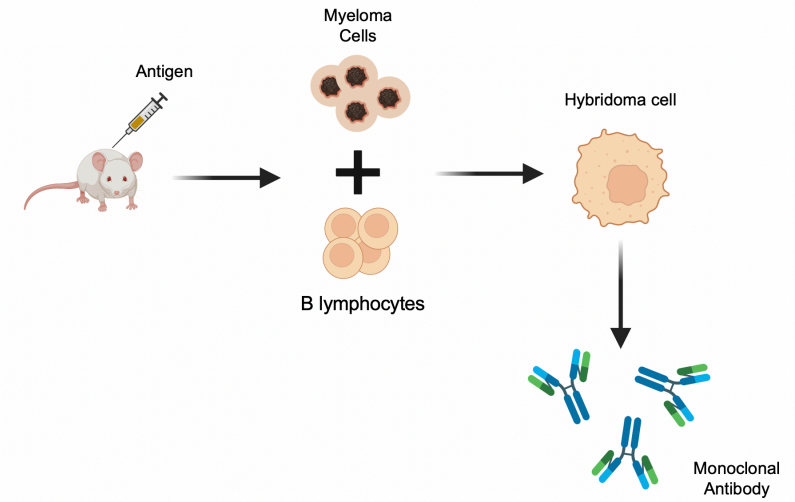

Fig.8 *The hybridoma technique involves animal immunization with an antigen of interest by stimulating the host's immune response. Subsequently, the B lymphocytes extracted from the animal's spleen are fused with immortal myeloma cells to form the hybridoma. Each hybridoma cell will be able to produce a specific monoclonal antibody against the antigen of interest. Figure created with biorender.com*

Hybridoma cell is formed by fusing B lymphocytes with immortal myeloma cells [84]. Each hybridoma cell can create one specific antibody (Fig.8). To obtain B lymphocytes that produce antibodies with high specificity and affinity, the technique exploits the immune system of the host animals.

B lymphocytes are isolated from the spleen after immunization with a specific antigen of a host animal (mouse, rabbit, and chicken are the most used) which provokes the immune response and triggers the maturation process of B lymphocytes [85].

Despite the widespread use of this methodology, the technique has several drawbacks. First, it is a quite demanding and time-consuming technique whose effectiveness in generating an appropriate humoral response depends on the proper activation of the immune system. This leads to the impossibility of this technique in providing antibodies against self-antigens or toxic antigens [86, 87].

Furthermore, due to the instability of the hybridoma cells, there could be a risk of losing the clone with the selected immunoglobulin, resulting in reproducibility problems [88].

However, antibodies produced through hybridoma technology show a different Fc than humans. Therefore, if the antibody is used in human therapy, it can induce an immune reaction against it and render the treatment ineffective [89].

This problem was overcome thanks to genetic engineering by creating two different molecules; the first is a "chimeric" antibody in which the Fc domain is replaced with a constant human domain, and the second is a "humanized" antibody in which only the antigen / CDR binding site is not human [90] [91].

Furthermore, it is possible to use transgenic animals, often mice and rats, that bear the human immunoglobulin loci while their loci are knocked out. Consequently, the immunoglobulin produced will be human after immunization [89].

However, recombinant DNA technologies provide another way to overtake the hybridoma problems. This has led to the development of an in vitro display method for producing mAbs.

5 *In vitro* antibody display technologies

In vitro antibody display technologies enable the isolation of specific antibodies with different applications: mainly therapeutic and diagnostic.

The critical factor is that the phenotype is coupled to the genotype, allowing the antibody sequence to be easily and quickly traced [80]. The three main display methods widely used to isolate mAbs are ribosome, phage, and yeast display.[73].

The ribosome display is a method in which the antibody is produced in vitro, exploiting the prokaryotic or eukaryotic cell-free expression systems [92]. In the ribosome display, it is necessary to respect certain conditions that make the environment suitable for producing antibodies. In detail, the reaction environment must have a high concentration of magnesium ions, low temperature, and plasmid without a stop codon. The presence of these elements allows the ribosome to slow down at the end of mRNA while the emerging antibody is folded and displayed [73].

A good advantage of this technique is the possibility to rapidly generate an extensive library because the transformation of a vast amount of plasmids into a host is no longer required [92]. The ribosome display is a challenging technique due to several drawbacks that limit its effectiveness. Some problems are associated with the mRNA, which is easily degraded by RNAse, with the possible premature cessation of antibody generation, or dissociating of the synthesized peptide from the ribosome during translation [73, 92].

The phage and yeast display will be discussed in the following chapters.

5.1 Phage Display Technology

The phage display is a tool for isolating mAbs [74] based on the work of George Smith in 1985 [93]. Over the years, this technique has become one of the most potent and effective for isolating antibodies [94, 95]. The phage display technique has allowed, over time, the isolation of several mAbs to treat cancer, inflammatory, immunological, and infectious diseases [96]. Some examples are Adalimumab (Humira®: treatment of rheumatoid arthritis), Atezolizumab (Tecentriq™:treatment of urothelial carcinoma (UC) and metastatic lung cancer), Belimumab (Benlysta®: treatment systemic lupus erythematosus) and Avelumab (Bavencio®: treatment of metastatic Merkel cell carcinoma in adults and pediatric patients) [96].

This method is based on the link between phenotype and genotype, which guarantees the permanent availability of the antibody selected over time[97].

Phage display relies on the expression, on the surface of the bacteriophage M13, of an antibody library [98]containing several million variants used for the selection of antibodies with the desired characteristics of affinity and specificity[69].

5.2 Filamentous Bacteriophage M13

The filamentous bacteriophage M13 belongs to a group called Ff phages [99] that only infect *Escherichia coli* strains that express the F pilus (Fig.9 [87]) [100]) [98].

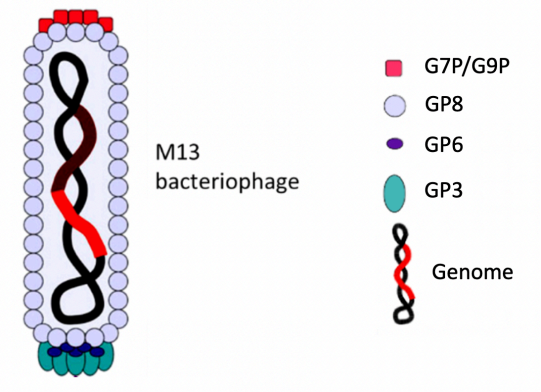

Fig.9 Schematic representation of filamentous bacteriophage M13*. Phage DNA is covered by 5 coat proteins: G3P, G6P, G7P and G9P Figure adapted from [87].*

The life cycle of M13 is neither temperate nor lytic but establishes a persistent infection by continuously producing new phage particles. The M13 phage has a width of 6,5nm and a length of 900nm[98].

Single-stranded phage DNA (ssDNA) has a length of 6407 bp [101]which encodes 11 different proteins: 5 are coat proteins, and 6 are proteins involved in the replication process and assembly of the phage particles [98]. The five coat proteins are G3P, G6P, G7P, G8P, and G9P. The envelope is mainly composed of G8P with approximately 2700 protein units; instead, the other proteins are each present in about five copies [98, 102]. The replicative cycle of the M13 begins with the adsorption process, in which the N2 domain of the G3P protein binds the F pilus on the surface of 'male' E. coli [103]. After interacting with the pilus, the DNA is introduced into the bacterial cell thanks to the N1 domain of the G3P that binds the TolA protein, which, together with the other TolR and TolQ proteins, depolymerizes the phage coat (Fig. 10 [104]) [103]. Once the ssDNA is inside the bacterium, it is converted, by the host DNA replication machinery, into the double-stranded plasmid termed the replicative form (RF) [98]. The ssDNA plasmid

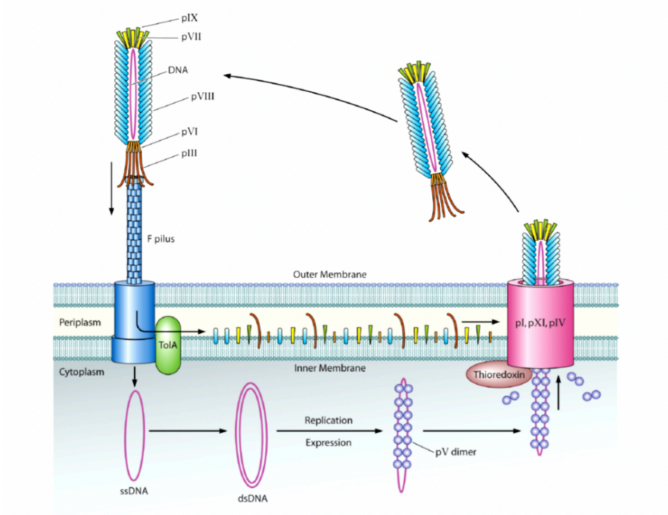

Fig.10 *Filamentous phage infection, phage particles assembly and release from the host cell. Figure taken from [109]*

serves as a template for the production of the protein coat (G3P and G8P). Finally, the new phage particles are assembled by packaging the ssDNA inside the coat protein and released through the bacterial membrane [69].

5.3 Display strategy

Previous works have shown how the phage library could be generated as a fusion with all five protein coatings (G3P, G6P, G7P, G8P, G9P), but most antibodies and peptides are displayed fused with G3P and G8P [94, 105, 106]. Nevertheless, most phage libraries are expressed as a fusion with protein G3P because the functionality of G8P protein is maintained only with small no-cysteine peptides of 5-6 amino acids [107]. Moreover, the protein G8P is present in about 2700 copies, which can have an avidity effect at the expense of affinity [108].

5.4 Phage and Phagemid library

For the construction of the antibodies library, two different strategies are used. The first one foresees that the genes of the antibody library are cloned directly inside the phage genome, while in the second case, the phagemid vector is used.

In the first method, the phage genome carries all the genes fundamental for infection, replication, assembly, budding, and the G3P-scFv fusion gene. This leads to a multivalent display of antibody-G3P proteins [98].

The phagemid vector, instead, is based on a plasmid in which three key elements must be present: 1) antibiotic marker (for selection and propagation), 2) G3P-antibody gene, and 3) origin of replication for phage and its host (*E.coli)* (Fig. 11) [109] [98].

However, the phagemid lacks the gene required for replication and generation of functional phage particles; to do this, it is necessary to use a helper phage (M13KO7 or VCSM13) which bears all the structural proteins and a defective origin of replication [94].

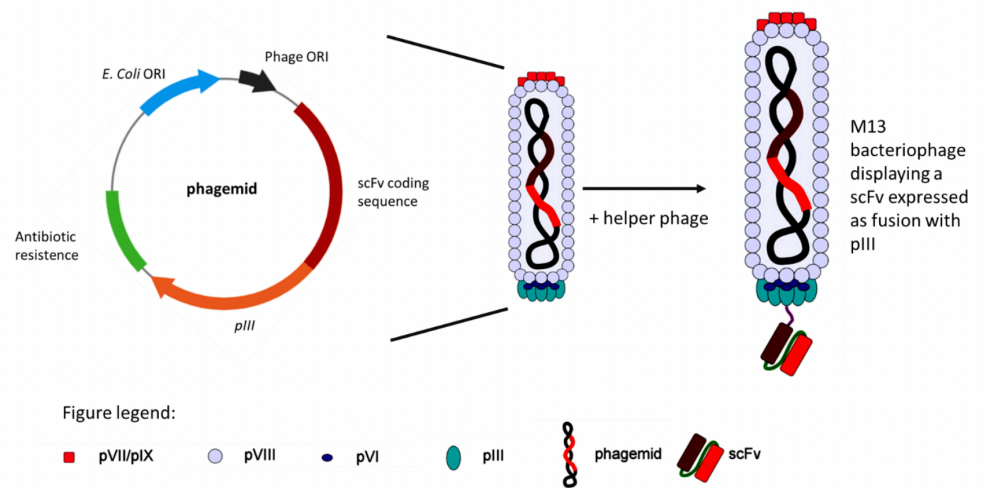

***Fig.11 Schematic picture of a phagemid**: the bacterial and viral replication origins are represented in blue and black, respectively. The scFv coding sequence is in red and is fused with the coat protein G3P coding sequence (orange). The antibiotic resistance is in green. In the middle, the M13 bacteriophage bearing a phagemid. On the right, the M13 displaying a scFv as a fusion product with the minor viral coat protein pIII. Image adapted from [87] and partially created with BioRender.com.*

The helper phage infects *E.coli* that hosts the phagemid and, at the formation of the phage particle, the wild-type G3P (carried by the helper phage) competes with G3P-scFv (held by the phagemid) [94].

As a result, the phage particles will have wild-type G3P and G3P-scFv. The ratio between them may be 1 to 9 and 1 to 1000 depending on the phagemid, polypeptide type, growth condition, and proteolytic cleavage [110].

Although libraries built with phage vectors have shown greater diversity of antibody ligands, phagemid is more widely used [111]. This may be because phagemids are

more stable than phages' genomes, and it is possible (thanks to the higher efficiency of transformation in *E.coli*) to create large libraries more efficiently [112]. In general, the larger the library, the higher the possibility of selecting antibodies with high affinity [97].

5.5 Phage display selection

The phage display selection, or panning, is a high throughput method that allows the isolation of antibodies against a specific antigen. This process comprises different steps in which unspecific antibodies are eliminated, and only the specific ones can be selected [73]. In detail, the process foresees the phage library incubation with the antigen of interest (antigen presentation), washes for the elimination of unspecific unbound phages, and the final amplification of the selected clones through *E.coli* infection [98].

Theoretically, only one selection cycle is necessary, but due to the clones' unspecific binding, 2-4 rounds of selection are required (Fig. 12) [69].

The presentation of the antigen is a crucial step because the characteristics of the selected antibodies depend on it. The simplest way is to passively absorb the antigen with an activated surface into the tube. However, adsorption presents several hurdles. Small organic molecules or short peptides are not efficiently adsorbed to the surface and, therefore, must be conjugated with transport proteins like KLH (Keyhole Limpet Hemocyanin) or BSA (Bovine serum albumin). Above all, passive adsorption is accompanied by a diverse degree of antigens' structural change and a reduction of the antigen-exposed area [98]. This can lead to isolating antibodies that recognize linear epitopes and may not bind the antigen in its proper conformation [113, 114]. It is possible to overcome this problem by using a steptavidin-biotin capture system. In this case, the streptavidin coated on the tube binds the biotinylated antigen; thus, the antigen will be lifted from the surface. This allows the antigen to maintain its native conformation and have more surfaces available for interaction with the antibody [98, 115].

The principal disadvantage of this system is the over-biotinylation; indeed, it can alter the physic-chemical proprieties of the antigen causing side effects such as antigen aggregation or decreasing the available surface, hampering the binding. A further downside to this system is the possibility of nonspecific bonds between phages and

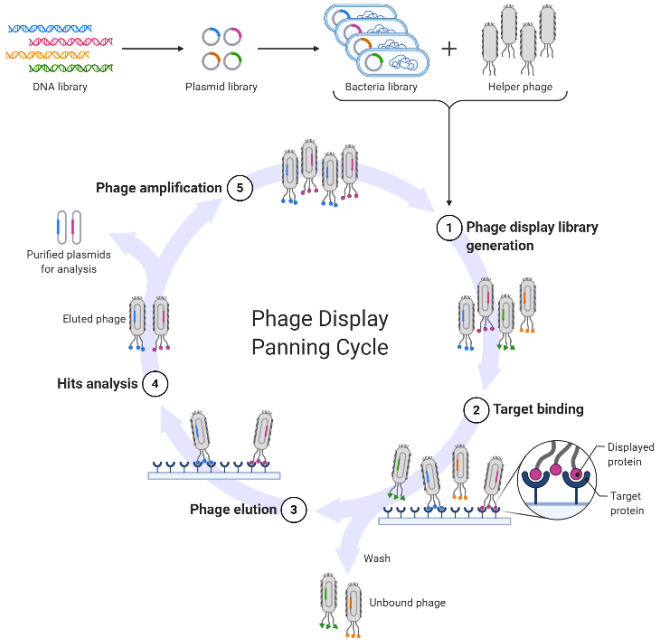

***Fig.12 Schematic representation of the selection process**. During biopanning the generated phage library is put in contact with the antigen of interest. Washes will be useful in eliminating non-specific clones or those that bind weakly to the target. Positive clones will be eluted and amplified for a new selection cycle. Adapted from "Phage Display Panning", by Biorender.com*

biotin; thus, a negative selection must be added to the antibody selection process to avoid the problem [98].

Another method that allows for the maintenance of the native conformation of the antigen during the selection process is the selection in solution. This technique involves the use of paramagnetic beads functionalized with streptavidin. As explained above, the biotinylated antigen will be bound by the antibody fragments, and through a magnet, it will be possible to isolate the positive clones from the negative ones. Again, a negative selection step must be included in the selection process to eliminate the clones that bind the beads or biotin [69].

6 Yeast Display

Despite some studies showing that yeast display was used in the past only in the affinity maturation process of pre-existing antibodies, recent studies have demonstrated the validity of this technology in isolating antibody fragments.

As with the other two display technique, the primary advantage is the direct linkage between the genotype and phenotype [73].

The antibody libraries are expressed on the surface of the Saccharomyces cerevisiae yeast strain, and the antibodies of interest are selected through FACS and MACS techniques [106] [116].

6.1 Saccharomyces cerevisiae

Saccharomyces cerevisiae (*S.cerevisiae*) (Fig.13a,[117]) is a model organism belonging to the kingdom of *Fungi.* Its genome was the first wholly sequenced eukaryotic genome [118, 119]. It is composed of 12068 kilobases (kb) organized in 16 chromosomes that contain approximately 5570 protein-encoding genes [118, 120]. The density within the

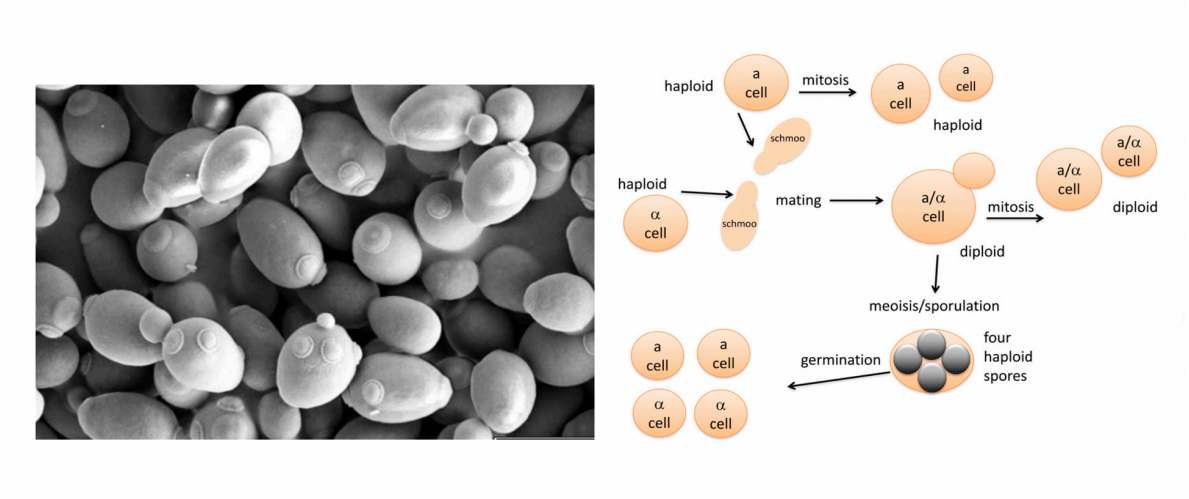

Fig.13 *a) SEM of yeast Saccharomyces cerevisiae [117]; b) Schematic life cycle diagram of budding yeast. Haploid yeast cells can be: MAT**a** (**a** cell) or MAT**α** (**α**cell). These cells can undergo mitotic cell division through budding, producing daughter cells. In favorable condition, and in precence of partners of opposite mating type, a dipoid cell can be formed (MAT**a**/MAT**α** (a/**α**cell). Diploid cells also divide mitotically by budding to produce genetically identical daughter cells. Under nutrient-poor conditions, diploids are induced to undergo meiosis, forming four haploid spores, which can germinate into two MAT**a** cells and two MAT**α** cells. Figure taken from [119]*

genome of protein-coding genes is relatively high (one gene every ~2kb) compared to that of man (~50-fold higher). This can be due to the low number of genes that contain introns which are ~ 4% [119].

It is a unicellular organism of ~ 5 μm with a replication time of approximately 90 minutes under optimized laboratory conditions. Moreover, it presents a 200nm thick cell wall composed of mannoproteins and B-linked glucans [121].

S. Cerevisiae is also called “budding yeast” because of its replication methods; indeed, during replication, small daughter cells bud from the mother cell [119].

The budding Yeast is a microorganism capable of living well both in a haploid and diploid state and passes from one to the other only if precise environmental conditions occur. It is possible to recognize two different mating types: haploid **a** and haploid **α.** During a nutrient-poor phase, the cell undergoes a sporulation process, in which the cell, through meiosis, forms four haploid spores, with two cells belonging to each mating type [119]**.** The mating type is determined by two different alleles (MAT a and α: mating-type locus) found in the middle of the right arm of chromosome III (Fig.13 b) [122].

However, in favorable conditions, in the presence of partners with the opposite mating type, the cells undergo conjugation. This event involves cell fusion and the formation of the diploid zygote (Fig. 12b, [119]) [123]. To do this, cells of the opposite mating type adhere through proteins called agglutinins on the yeast cell wall [124].

The agglutinin consists of two subunits, Aga1 (73kDa) and Aga2 (9kDa). In particular, Aga1 is secreted by the cell and covalently binds to β-glucan in the yeast cell wall extracellular matrix. In contrast, Aga2 binds to Aga1 via two disulfide bonds and, after the secretion, remains attached to the cell via Aga1 [125]. Every yeast cell can display 10^4 to 10^5 agglutinins [119, 126].

6.2 Antibody Fragment Display

The yeast display technique is based on expressing a pool of antibody fragments, whose sequences are cloned into specific plasmid vectors fused to the C-terminus of the Aga2 protein [127].

The yeast strain used for the yeast display contains the Aga1 gene stably integrated into the chromosome, and the expression of Aga1 and Aga2 is controlled by the galactose-inducible GAL1 promoter (Fig. 14).

When galactose is present, the antibody fragment is expressed on the surface of yeast cells fused to the Aga2 subunit. The inducible promoter GAL1 plays a crucial role in the quality of antibody display. It allows the expression of antibody fragments to be activated only after the growth phase, thus eliminating the possibility that potential antibodies toxic to the cell can be selected negatively [116]. One of the main advantages of this technique relies on the quality antibody displayed. The reason is due to the post-translation modification. For example, yeast has a similar glycosylation

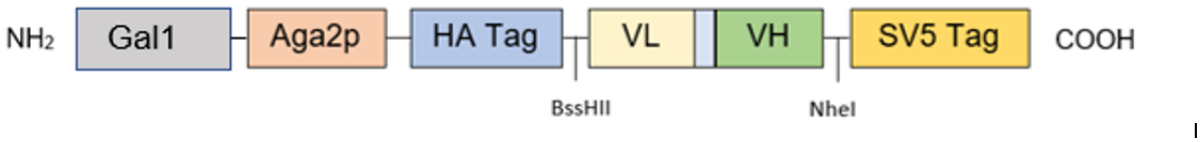

Fig.14 Schematic representation of the scFv expression system. *it is regulated by the inducible promoter GAL1, which in the presence of galactose allows the expression of the scFv fused with the Aga2 protein. Note the presence of two tags (HA tag) and SV5*

pattern to the mammalian system that improves antibody solubility. Moreover, the presence of molecular chaperon protein within the yeast endoplasmatic reticulum allows the elimination of clones with unstable sequences but also the expression of clones to complex for procaryotic system (*E.coli* in phage display) [126]

The main bottleneck of yeast surface display is the smaller library size (from 10^7 to 10^9) than phage (from 10^6 to 10^{11}) and ribosome (from 10^{11} to 10^{13}) display [116].

Another disadvantage can be given by the presence of thousands of copies of the antibody fraction on the surface of the yeast. Indeed, it may be possible to isolate clones based on avidity rather than affinity during the selection process. This mechanism is emphasized during the selection of oligomeric antigens in which multivalent binding can occur [126].

6.3 Selection process: FACS

The most significant advantage of the yeast display technology is the possibility of controlling in real time the progress of the selection through the use of FACS (fluorescent-activated cell sorting) [125].

This is not possible with the phage display technique, where the quality of the selection process is not clear until the screening of individual clones [128].

The cell sorter is an instrument (flow cytometer) capable of measuring each cell's optical and fluorescent characteristics. Parameters such as fluorescence size and granularity are chosen to differentiate and sort the cells of interest [129].

To select positive clones (which can bind antigen), yeast cells are incubated with antigen, and binding is detected through 2 fluorescent markers [116]. First, it is necessary to recognize the yeast cell that shows the antibody fragments on the surface

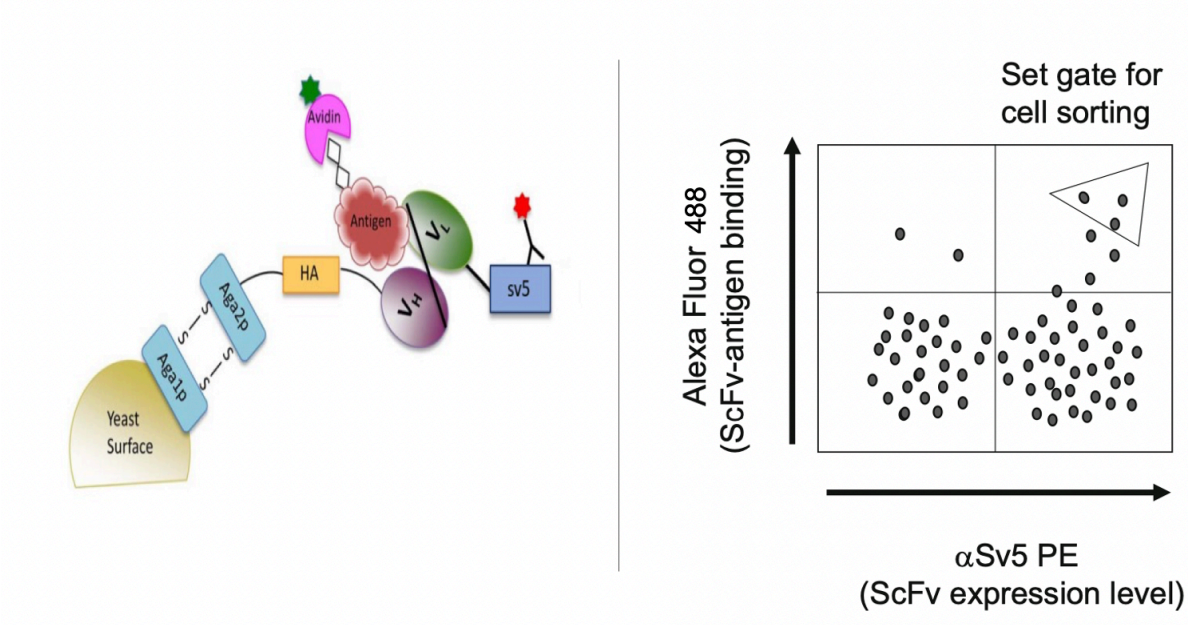

Fig. 15 *a) schematic representation of scFv expression on the yeast surface. Two fluorescent markers are used to assess scFv expression level and antigen binding. Figure adapted from [106]; b) Schematic representation of a flow cytometric dot plot representing a yeast population incubated with antigen .By cytometry it is possible to identify double positive clones (4_{th} quadrant) and set a gate to sort the clones of our interest. Figure taken from [128].*

from the ones that don't. This is possible thanks to a conjugated mAb (usually labeled with PE: phycoerythrin) that identifies a tag at the end of the V_L of the antibody fragment. The second marker (usually Streptavidin-Alexa Fluor 488) recognizes the biotinylated antigen (Fig. 15 a) [128]. With this construct, it is possible to sort only the cells of interest that exhibit both fluorescences (Fig. 15b).

Different rounds of selection are necessary to select antibodies with determined parameters. Typically, in the first selection round, the gate is opened on the 5% double positive population to preserve the diversity of the antibody fragments. However, in the following rounds (usually 2-3), the gate is narrowed up to 0.1% to 1% of double positive cells, trying to take the most affinity clones (Fig.15 b [128]) [116]. Finally, from the enriched population, the single clones are characterized one by one in terms of affinity and functionality via flow cytometry without subcloning [80].

7 Antibody display libraries

The crucial point for the display technology is the creation of high-quality antibody fragment libraries. For this reason, there are different strategies for library generation. In

particular, it is possible to distinguish four kinds of libraries: Immune Library, Naïve Library, and Synthetic / Semi-synthetic Library.
Independently from the V gene sources, the library's construction is the same. The B-cells are isolated, and the V(D)J rearranged domains are amplified through PCR using oligonucleotides covering the diversity of antibody sequence [130].

7.1 Immune Library

The immune library is usually generated from V genes (variable genes) of IgG (another isotype library with IgA and IgE [73]) mRNA from B cells from immunized animals [69] like mice, chickens, rabbits, bovine, non-human primates, sheep, and camel (Fig.16) [74]. However, it can also derive from patients previously exposed to a specific disease or infection [73].
The main characteristics of this kind of library are the enriched antigen-specific antibodies population and high-affinity antibodies since the antibodies have undergone affinity maturation [69, 73]. Indeed, the selected high-affinity antibodies may be directly used in diagnostic and humanized applications (therapeutics)[74].
The Immune library, however, has several setbacks; the need for immunization renders this library animal-dependent and time-consuming. Moreover, a new library must be generated for each new antigen. Besides, since the immune library relies on the immune system's natural response, there are difficulties in isolating self or toxin antigens [69, 74].

7.2 Naïve Library: “single pot library.”

The Naïve Library or single pot library is generated starting from rearranged V-gene from B-cell of non-humanized donors [102], generally isolated from bone marrow, tonsil peripheral blood lymphocytes, and spleen (Fig.16) [73, 131]. In particular, IgM mRNA is usually used, even if IgD has been used [132].
The naïve library has a bigger size (10^7-10^{10} clones) than the immune library because the B-cell genes have not undergone the affinity maturation process [74].
As mentioned before [133], the library’s size can have a considerable impact on the affinity of selected antibodies; studies have shown how it is possible to isolate

micromolar to nanomolar from a library of 10^7-10^8 size and sub-nano molar to picomolar from large libraries of 10^{10}-10^{11} [74].

The crucial point of this library, different from the immune library, is that it can be used to select antibodies versus all the antigens: self, non-immunogenic and toxic.[69]

7.3 Synthetic and Semi-synthetic libraries

As the previous chapter (1.2) mentioned, the binding specificity is mainly due to the light and heavy chain CDR regions. Since they play a crucial role in antigen-binding site formation, the synthetic and semi-synthetic libraries are generated through the randomization of the CDR regions (Fig. 16) (especially CDRH3, which presents the highest diversity) [11-12].

CDR regions are randomized in synthetic phage libraries and inserted/grafted into fully synthetic framework sequences. Instead, semisynthetic phage libraries are based on a limited number of randomizations, typically in heavy chain CDR3. They are generated from non-rearranged pre-B cell V genes or using an antibody framework. A CDRH3 is randomly mutated using oligonucleotide-directed mutagenesis or PCR-based methods, or all six CDR are mutated and cloned into one defined antibody framework [74].

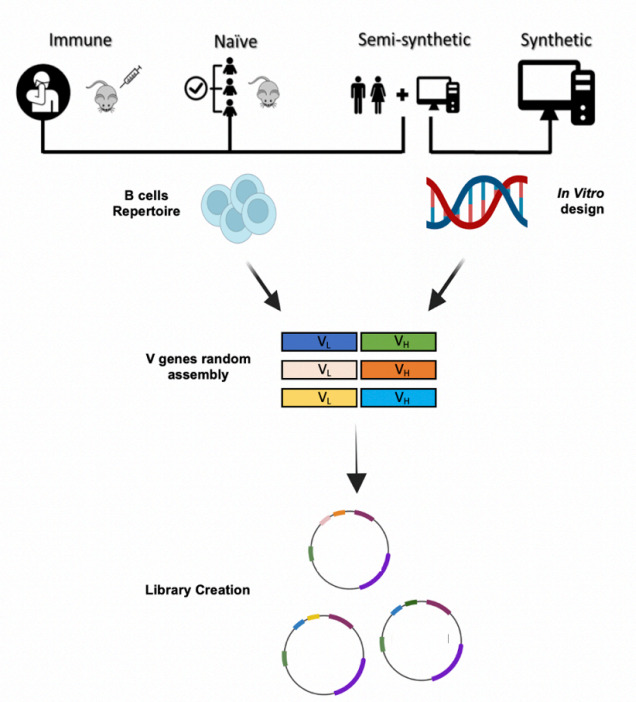

***Fig.16 Library creation**: Depending on the type of library, the coding sequences of the V genes can be recovered from B lymphocytes or they can be designed de novo. Finally, the V genes are randomly assembled and cloned into plasmids for the creation of libraries. Figure partially created with BioRender.com.*

Due to their nature, these libraries have the advantage of being independent of a natural immune response repertoire. They also work as a naive library that allows the selection of antibodies against several antigen types.
However, the construction of these libraries has a high cost, which makes them inaccessible to most researchers [73].

7.4 Clones optimization

In vivo, high-affinity antibodies are generated by somatic hypermutation. It consists of the insertion of mutations in the variable regions of the antibody. The in vitro display technologies, in combination with mutagenesis, can be used to improve the affinity of the clones directly selected from the library. Among the techniques used, there are random mutagenesis, chain shuffling, and site-specific mutation (Fig.17) [98, 134].
Random mutagenesis (Fig. 17b) is based on introducing mutations within the coding sequence of the antibody. Generally, this occurs randomly within predetermined regions, such as the CDR regions. A well-established technique of random mutagenesis involves the use of error-prone PCR that exploits the normal error rate of a low-fidelity DNA polymerase [135]; in particular, after selecting the ideal antibody for affinity maturation, PCR amplification with low-fidelity polymerase is performed to introduce mutations in the CDR to generate a new small library of mutants [136]. However, this technique may lead to mutations in the entire sequence, including the framework regions, with consequences that can be positive such as increasing the stability and affinity of the antibody, but also negative with the destruction of the site of interaction with the antigen [134].
In contrast, site-specific mutagenesis (Fig.17c) is an approach capable of modifying a gene locus or a DNA sequence in a targeted manner used to generate limited libraries of specific variants. The positions where diversity must be introduced are predicted to contribute to antigen binding. Structural data is required to perform this type of affinity maturation, but improvement in affinity is very likely, and there is little chance of creating problems with scFv stability [137].
Chain shuffling (Fig.17a) consists of keeping the V_H or the V_L antibody domain constant and subsequently combining one of the two with the entire repertoire of the opposite variable domain used for constructing the naïve library. This domain exchange mimics the hypersomatic mutation process that occurs in vivo [134]. This leads to the

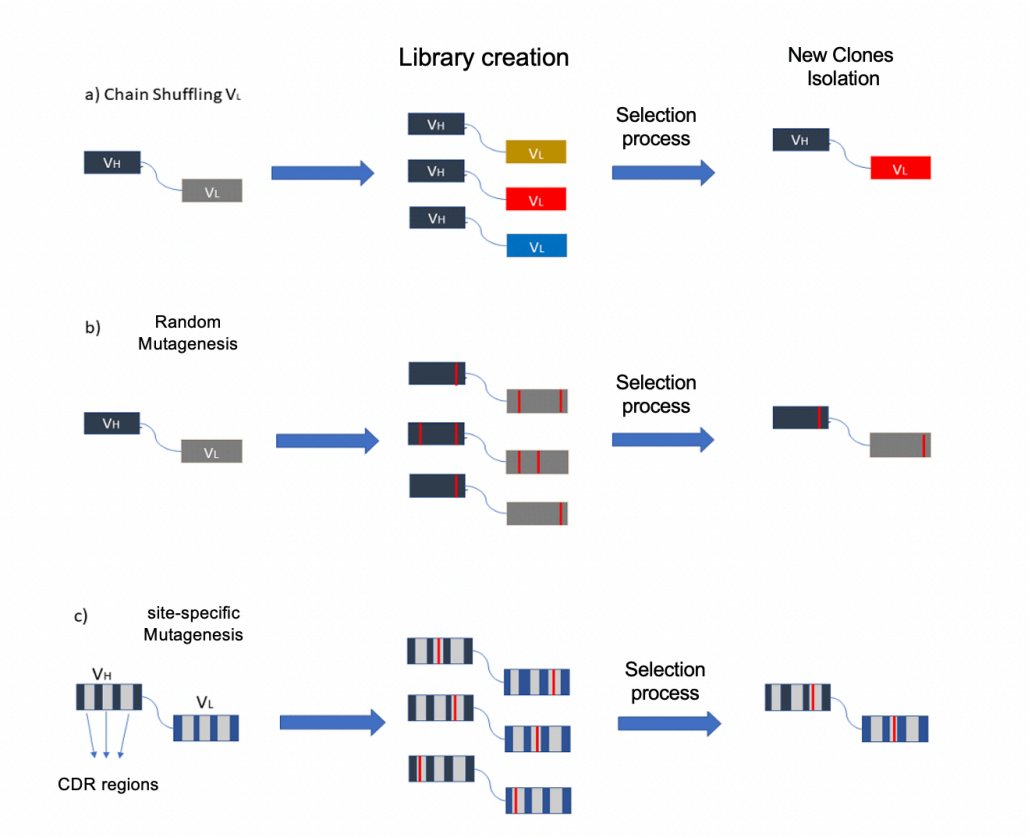

***Fig.17 Schematic representation of affinity maturation methods**. a) chain shuffle: the V_H or V_L are kept constant and combined with the entire repertoire of the opposite variable domain. b) Random Mutation: Mutations in CDRs are randomly inserted through error-prone PCR. c) site-specific mutagenesis: mutations are inserted in specific regions. It needs structural data to insert mutations that contribute to antigen binding*

generation of a new library that will have to undergo another selection process to identify the best clones [98].

Aim

Osteoporosis is a disease of the skeletal system caused by excessive bone resorption. This leads to an unregulated loss of bone density resulting in an increased risk of fractures. This disease not only has a dramatic impact on the quality of life, but it also has a significant impact on the health system. Therefore, it is necessary to understand better the mechanism underlying this pathology in order to find therapeutic solutions that improve the quality of life and affect the health system less. ICOS-Fc is a recombinant molecule created by the NOVAICOS company that has been shown to be effective in inhibiting osteoclast maturation and activity, both in vitro and in vivo tests, through the triggering of ICOSL on the surface of the osteoclasts. However, since ICOS-Fc is a recombinant molecule, it may present some problems in the validation and approval phase. Consequently, it is necessary to find an alternative to this treatment.
In light of this, this project has two aims: 1) the isolation of monoclonal antibodies against the ICOSL and 2) and determine the inhibition of osteoclast maturation and activity. The planned strategies and the related main points to reach the proposed purposes are summarized below:

1) **Isolation of monoclonal antibodies against ICOSL:** This phase aims at the screening of a naïve library and at the subsequent characterization (test of specificity and affinity) of the isolated clones.

2) Evaluation of the functional effect of the antibody: Once the clones have been isolated, they are evaluated for their ability to recognize ICOSL on the cell surface of different cell types (flow cytometry). Furthermore, their functionality will be evaluated in functional tests (wound healing assay, osteoclastogenesis, and TRAP assay)

3) Improvement in antibody characteristics: The third phase aims to improve the performance of the isolated clones through the affinity maturation technique called chain shuffling. The use of phage display technology for the screening of high-affinity antibodies has also been envisaged

Materials and Methods

List of abbreviations

AP: Alkaline Phosphatase

BCIP: 5-Bromo-4-chloro-3-indolyl phosphate HRP: Horseradish Peroxidase

NBT: Nitrotetrazolium Blue chloride

TMB: 3,3',5,5'-Tetramethylbenzidine

IDA: Iodoacetamide

DTT: Dithiothreitol

MTT: 3-(4,5-dimethylthiazol-2-yl)-2,5-diphenyltetrazolium bromide

1. Materials

1. Bacterial strains used are:
   Escherichia coli DH5α [F'/endA1 hsd17(rK_mKþ) supE44 thi-1 recA1gyrA (Nalr) relA1 _(lacZYA-argF) U169 deoR (F80dlacD-(lacZ) M15)];
2. *S.cerevisiae* for scFv display: **EBY100** (ATCC #MYA-4941): MATa AGA1::GAL1-AGA1::URA3 ura3-52 trp1 leu2-delta200 his3-delta200 pep4::HIS3 prbd1.6R can1 GAL;
3. *S.cerevisiae* for antobody secretion: **YVH10** (ATCC #MYA-4940): MATalpha PDI1::GAPDH-PDI1::LEU2 ura3- 52 trp1 leu2-delta200 his3-delta200 pep4::HIS3 prbd1.6R can1 GAL.
4. GenEluteTM Plasmid Miniprep Kit (Sigma-Aldrich) for plasmid DNA preparation, following the manufacturer's instructions.
5. Stock solutions of antibiotics (Sigma-Aldrich) are prepared by dissolving kanamycin at 50 mg/ml in water and ampicillin at 100 mg/ml in water. Kanamycin and ampicillin stocks are filtered with a 0,22 μm filter device and stored at –20°C.
6. 2xTY liquid broth: 16 g bacto-tryptone, 10 g bacto-yeast, and 5 g NaCl to 1 L of ddH2O. Final pH 7,0. Agar plates are prepared by adding 1,5% bacto-agar to 2xTY broth.
7. Restriction endonucleases, T4 DNA ligase, and buffers are purchased from New England Biolabs and used according to the manufacturer's suggestions and standard molecular biology procedures.

8. GenEluteTM Gel Extraction Kit and GenElute PCR Clean-Up Kit (Sigma-Aldrich) for DNA purification from agarose gel, following the manufacturer's instructions.
9. The DNA Clean & ConcentratorTM-5 kit (Zymo Research) for purification and concentration of the ligation reaction, following the manufacturer's instructions.
10. Helper phage M13KO7 (New England Biolabs).
11. Solution for precipitation of phages: 20% (w/v) polyethylene glycol (PEG) 6000 in 2,5 M NaCl. The solution is filtered through a 0,22 μm filter before use.
12. PBS: 8 g NaCl, 0,2 g KCl, 1,44 g Na2HPO4, and 0,24 g KH2PO4 in 1 L H2O, final pH 7,4.
13. 2xTYAG: 2xTY liquid broth supplemented with 100 μg/ml ampicillin and 1% glucose.
14. 2xTYAK: 2xTY liquid broth supplemented with 100 μg/ml ampicillin and 50 μg/ml kanamycin.
15. YPDAK: YPD liquid broth supplemented with 15μg/ml ampicillin and 50 μg/ml kanamycin. For a solid plate, add 15g of Agar per liter
16. SD-CAA AK: SD-CAA Yeast Selective Growth media liquid broth supplemented with 15μg/ml ampicillin and 50 μg/ml kanamycin. For a solid plate, add 15g of Agar per liter
17. SG/R-CAA AK: SG/R-CAA Yeast Selective scFv induction media liquid broth supplemented with 15μg/ml ampicillin and 50 μg/ml kanamycin.
18. SGT AK: SGT Yeast Induction Media liquid broth supplemented with 15μg/ml ampicillin and 50 μg/ml kanamycin
19. PBS/Tween: PBS supplemented with 0,1% (v/v) of Tween-20.
20. 2% MPBS: 2 g non-fat milk powder/100 ml PBS.
21. 4% MPBS: 4 g non-fat milk powder/100 ml PBS.
22. EZ-Link™ Sulfo-NHS-SS-Biotinylation Kit (ThermoFisher) is used to biotinylate the target antigen
23. HRP-conjugated antibodies were all purchased from Jackson ImmunoResearch, except for the anti-human IgA and IgM antibodies purchased from Sigma-Aldrich.
24. Anti M13 HRP: the Ab was purchased from PROGEN and HRP-conjugated with a commercial kit from Abcam
25. SV5 antibody-PE: The Ab was produced by a hybridoma cell line and conjugated with PE/R-Phycoerythrin Conjugation Kit - Lightning-Link® (Abcam) following the manufacturer’s instructions
26. Streptavidin-Alexa Fluor 488 was purchased from Thermo Fisher

27. TMB ready-to-use, pre-mixed solution for colorimetric HRP-based ELISA detection (Sigma- Aldrich)
28. 2N sulfuric acid: 55,6 ml 97% H2SO4 diluted up to 1 L H20
29. AP-conjugated antibodies: anti-V5 antibody was purchased from ThermoFisher
30. Anti-human and mouse IgG antibodies were purchased from Jackson ImmunoResearch
31. POROS Mab Capture A Select (Applied Biosystems)
32. BCIP/NBT (Sigma-Aldrich)
33. MTT (Thermo Fisher)
34. DTT powder (Sigma-Aldrich)
35. IDA powder (Sigma-Aldrich)

2. Methods

2.1 Phage display library

2.1.1 Phage library production

1. Dilute the library glycerol stock in 15 ml of 2xTY. Read the OD600 and inoculate in 100 ml of 2xTYAG OD600=0,05 bacteria.
2. Grow with shaking (250 rpm) for about 1,5-2,5 hours at 37°C to an OD600 of 0,5.
3. Add a 20-fold excess of helper phage. Leave at 37°C for 45 min, standing with occasional shaking.
4. Spin the cells for 15 min at 4.000 rpm.
5. Discard the supernatant.
6. Resuspend the bacterial pellet in a volume 5 times greater than the initial culture volume of 2xTY Ampicillin + Kanamycin.
7. Grow shaking (250 rpm) overnight at 28°C, using enough flasks to ensure that the flask volume is five times greater than the culture volume.
8. The following day bacteria are centrifuged at 5000 rpm for 20 min at 4°C. The supernatant containing phages is collected and subject to PEG precipitation.

2.1.2 PEG precipitation of phagemid particles

1. Add 1/5 volume of PEG/NaCl solution to the cleared supernatant, mix well and leave for 30-60 min on ice. Successful precipitation can usually be seen after a few minutes as haziness.
2. Spin down at 4.000 g for 15 min at four °C; discard the supernatant. The pellet should be white. If it is brown, this is usually due to contamination with bacteria, and the PEG precipitation should be repeated.
3. Resuspend the phage pellet in 1/10 original volume with PBS.
4. Spin in a microcentrifuge (10 min, max speed) to remove the remaining bacteria; a small brown pellet could be visible.
5. Transfer the supernatant to a new tube.

2.1.3 Phage titration into E. coli

1. Make serial 10-100 fold dilutions of the phagemid solution in 1,5 ml tubes in 2xTY medium to final volumes of 1 ml.
2. Add two µl of the diluted phages to 1 ml of exponentially growing *E. coli*. Incubate without shaking at 37°C for 45 min.
3. Make five serial 10-fold dilutions of the infected *E.coli.* and make spots of all dilutions to understand the library dimension. Incubate the plate at 30°C O/N
4. As a control, uninfected *E. coli* should be plated and grown on a separate ampicillin plate. If colonies grow on this plate, it indicates possible contamination.
5. The next day, count the number of colonies and calculate the phage titer.

2.1.4 Selection Antigen immobilized on plastic surfaces

1. Add 1 ml antigen (at desired concentration) to a 75x12 mm Nunc-immunotube. Leave O/N at 4°C.
2. Next day, wash 3x with PBS.
3. Block the immunotube by adding 2% Milk-PBS 1X to the brim. Seal the tube with parafilm and leave for 45’ at RT. Meanwhile, pre-block PEG-concentrated phage in a final volume of 1 ml with 2% MPBS.
4. Wash the immunotube 1x with PBS, transfer the phage mix to the immunotube, and cover the tube with parafilm. Incubate for 30 min on a rotator and then for

1,5 hrs standing at room temperature. Wash tubes ten times with PBS-Tween-20, then ten times with PBS. Each washing step is performed by pouring buffer in and out immediately.

5. Elute phages from the tube by infecting *E. coli* cells at OD600 =0,5. Leave the tube at 37°C for 45 min with occasional shaking. Plate bacteria directly on 2 x 15 cm 2xTY agar plates added with ampicillin and grown O/N at 30°C.

2.2 Screening of isolated clones

2.2.1 Bacterial library growth

After two or three rounds of selection, individual colonies from the selection are tested for antigen binding by ELISA. A microtiter-well system can be used for individual phage preparation. The principle involving growth, helper phage infection, and phage production is the same as for the library, but it is applied to single clones in the 96-well plate format.

1. Put 100 µl of 2xTY Ampicillin+Glucose into each well of a round-bottomed 96-well plate. Inoculate a single colony in each well by touching the top of a colony with a sterile plastic tip. Grow with shaking (250 rpm) at 37°C for 3-5 hours
2. Use a 96-well sterile transfer device or pipet to inoculate ten µl per well from this plate to a new round-bottomed 96-well containing 120 µl 2xTY Ampicillin+Glucose per well. Grow to OD600 nm 0,5 at 37°C, shaking (1,5-2 hours).
3. Add 50 µl 2xTY Ampicillin+Glucose containing 1x109 pfu helper phage to each well. The ratio of phage to bacterium should be about 20:1. Stand for 45 min at 37°C.
4. After the incubation, spin at 2500 rpm for 20 min; then remove the supernatant.
5. Resuspend the bacterial pellet in 120 µl 2xTY Ampicillin+Kanamicin. Grow overnight at 28°C, shaking.
6. Next day, spin at 2500 rpm for 20 min and use 50 µl supernatant per well for phage ELISA.

2.2.2 Phage Elisa: Antigen directly coated on the solid surface

1. Coat the plate with 100 µl per well at the final antigen concentration of 10 µg/ml. Leave O/N at 4°C.
2. Discard the antigen solution, rinse wells twice with PBS, and block with 120 µl per well of 2% Milk-PBS 1x for at least 45 min at room temperature.
3. Wash wells twice with PBS 1x.
4. Add 50 µl 4% Milk-PBS1x and 50 µl culture supernatant containing the phage antibodies to the appropriate wells, and mix carefully. Leave approximately 1,5 hrs at room temperature.
5. Discard the solution, and wash out wells 3x with PBS-Tween-20 and 3x with PBS.
6. Add 100 µl properly diluted HRP-conjugated anti-M13 antibody. Incubate for 1 hr at room temperature.
7. Discard the solution and wash wells 3x with PBS-Tween-20 and 3x with PBS.
8. Dispense 100 µl TMB solution per well, and leave it at room temperature in the dark.
9. Quench by adding 50 µl stop solution 2N H2SO4.
10. Read at 450 nm.

2.3 Construction of the G10 antibody VL library

2.3.1 Assembly PCR

The *scFv* library is generated by mixing equal amounts (5 ng) of *VH* of G10 clone and *VL*l genes and performing a two-step overlapping PCR: 8 cycles of PCR without primers followed by 27 cycles in the presence of VLPT2-VHPT2 primers. Cycling parameters are 95°C for 15 sec (denaturation), 65°C for 30 sec (annealing), and 72°C for 60 sec (extension). Four assembly reactions of 50 µl should be set up and the product purified on a 1.5% agarose gel.

Table 1: Assembly PCR protocol

1	95°C	1’	
2	95°C	15’’	x 8
3	65°C	30’’	
4	72°C	1’	
5	Pause	-	
6	95°C	30’’	x 27
7	65°C	30’’	
8	72°C	40’’	
9	72°C	7'	
10	8°C	-	

2.3.2 Ligation and electroporation of *scFv* library

1. Both phagemid cloning vector pDAN5 and purified *scFv* fragments are sequentially digested with *Bss*HII restriction endonuclease for two h at 50°C and then with *Nhe*I for two h at 37°C. Vector is loaded on an agarose gel and gel purified using a purification kit; scfv inserts, instead, are purified using a clean-up kit.
2. Ligation reaction is prepared as follows: double-digested and purified vector 500 ng, double-digested and purified scFv 300 ng (phagemid: insert molar ratio of 1:3); T4 ligase. Incubate reactions at two h at 22°C and then at 16°C overnight.
3. Clean up and concentrate ligation using a commercial kit (Zymo research)
4. Elute the DNA in ultrapure H2O.
5. The ligation mix is electroporated into homemade electrocompetent *E.coli* cells following the manufacturer's instructions.
6. Transformations are pooled and plated on 2xTY Ampicillin 15 cm plates and grow O/N at 30°C to obtain a primary library. Make dilutions to estimate library diversity.
7. The following day colonies are scraped up in 2xTY 20% glycerol and frozen down in 1 ml aliquots.

2.3.3 Colony PCR amplification and DNA fingerprinting

1. Make up a PCR-Mastermix with 20 µl per clone. Use forward and back primers mapping external to the 5' and 3' end of the *scFv* insert.
2. Aliquot 19 µL of the Mastermix.
3. Add one µl of culture taken from the master plate into the PCR reaction
4. Perform 30 cycles of denaturation, annealing, and elongation steps using the temperature and incubation times indicated on the DNA Taq Polymerase datasheet.
5. Check two µl of the PCR reaction on a 1,5% agarose gel.
6. Make up a fingerprinting-Mastermix and add 15 µl to each PCR tube. Mastermix is as follows: *Bst*NI buffer (10x), *Bst*NI 1 unit per µg of DNA.
7. Digest samples at 60°C (*Bst*NI).
8. Load on a 2% agarose gel, run and compare the banding patterns of individual clones on a UV transilluminator.

2.4 Yeast Display

2.4.1 Yeast Display Selection

ScFv genes amplification from Phage Selection output and Yeast Display vector preparation

1. Obtain a pDAN5 [138] plasmid DNA miniprep from selection output and a pDNL6 [127] plasmid DNA miniprep from DH5α glycerol stock.

2. Dilute the pDAN5 plasmid DNA miniprep to 1ng/µL and use 1µL as a template for the PCR reaction.

3. Using the diluted template obtained above, set up the PCR reaction using a Taq polymerase and pDAN5topDNL6_5 and pDANtopDNL6_3 primers. Set up enough reactions to generate 2 µg of PCR product for each output.

4. Load the entire reaction volume on a 1.5 % agarose gel. Cut out the band of interest with a clean razor blade. Purify the PCR products using a Gel Extraction Kit and following manufacturer instructions. Elute in UltraPure H2O and measure concentration by spectrophotometer.

5. Digest the yeast display vector (pDNL6) with BssHII and NheI. Run the digested plasmid on 0.8 % agarose gel, and cut out the vector band (~6,000 bp) with a clean

razor blade. Isolate the digested vector with a Gel Extraction Kit. Elute in deionized H2O and measure concentration by spectrophotometer.

2.4.2 Transformation of EBY100 yeast competent cells

1. For each transformation, aliquot ten µL of 10 mg/mL boiled salmon testes DNA in a 1.5 mL tube.
2. Add 500 ng of digested vector and 1.5 µg of the purified PCR product to the tube or 500ng of pDNL6 (containing the scFv of interest as an insert) plasmid DNA miniprep (By taking advantage of the gap repair system of the yeast cell, the scFv is recombined into the yeast display vector).
3. Add 100 µL competent cells and vortex.
4. Add 600 µL of Yeast Plating Buffer and vortex.
5. Incubate for 30 min at 30°C with shaking.
6. Add 10 % volume (70 µL) of DMSO.
7. Heat shock for 15 min at 42°C in a water bath.
8. Spin for 5 sec. In micro-centrifuge and remove the supernatant.
9. Resuspend in 1 mL of ddH_2O.
10. Plate 10 µL of cell suspension on SD/CAA agar plates to estimate the library's size. Place the rest of the transformed cells into 10 mL selective SD/CAA liquid media and grow for 2-3 days at 30°C until colonies appear on the plate.

2.4.3 Induction and analysis of EBY100 yeast cells

DAY 1

1. Starting from the 10 mL culture of transformed yeast (which should have reached saturation at OD600 >4), prepare a 5 mL culture at OD600 = 0.5 in SG/R-CAA and grow at 20°C with shaking overnight. The culture reaches an OD600 of about 1/1.5. The induced library can be stored for a week at 4°C.

DAY 2

2. If necessary, dilute the culture into 1mL PBS to have a starting OD600=1. Spin down 100µL (10^6 cells) of the induced library at 10,000×*g* for 30 sec. Remove supernatant.
3. Wash with 1mL of Yeast Wash Buffer, vortex, and spin down again.

4. Resuspend cells in 100 µL of a 1:2000 dilution of mouse anti-SV5-PE antibody (1 mg/mL) in PBS and vortex. Incubate at four °C for 30 min in the dark and vortex every 10 minutes.
5. Wash with 1 mL of Yeast Wash Buffer, vortex, and spin down at 10,000×*g* for 30 sec.
6. Resuspend in 1 mL of PBS.
7. Store in ice until ready to analyze.
8. Analyze the cells by FACS and record 10,000 singlets.

2.4.4 scFvs Yeast library Selection (sorting)

1. Once analyzed the population by FACS, select the population of interest (clones that bind the antigen);
2. Sort between 5,000 – 20,000 events directly into 1 mL of SD-CAA media;
3. Dilute the sorted population in 10 mL of SD-CAA media and grow at 30°C with shaking at 250 rpm for 48 hours. The culture should reach saturation (OD600 >4).
4. Normally, 2-3 selection processes are necessary to reach the population of interest.
5. If no other sorts are required, plate the sorted cells on 1-2 large SD-CAA plates. The colonies are visible on the plates after three days at 30°C

2.4.5 Screening of individual clones

DAY 1

1. Pick individual colonies from the plate.
2. Inoculate the colonies in a tube with 1mL of SD-CAA.
3. Grow the colonies at 30°C with shaking at 250 rpm O/N.

DAY 2

4. Prepare a 1mL culture at OD600 = 0.5 in SG/R-CAA and grow at 20°C with shaking O/N (16/20h). The induced yeast can be stored for a week at 4°C.
5. To prepare a glycerol stock, follow the instruction previously reported on page 14.

DAY 3

6. If necessary, dilute the culture into 1 mL PBS to have a starting OD600=1. Spin down 100 mL (10^6 cells) of the induced library at 10,000×*g* for 30 sec. Remove supernatant.

7. Resuspend the cells in 100 µL PBS containing the desired concentration of biotinylated target antigen. Incubate for one h at room temperature with shaking.
8. Wash twice with Yeast Wash Buffer by spinning the cells for 30 sec at 10,000xg and carefully removing the supernatant.
9. Incubate the yeast with 100mL of PBS solution containing 1:2,000 diluted anti-SV5-PE (1mg/mL) and 1:400 Streptavidin-Alexa Fluor 488 (1ug/mL) for 30 min on ice in the dark (vortex every 10 minutes).
10. Wash the cells twice with Yeast Wash Buffer by spinning the cells for 30 sec at 10,000xg and carefully removing the supernatant.
11. Resuspend the yeast cells in 1mL of PBS.
12. Assess binding using a high-throughput flow cytometer.

Table 2: List of Primers

VHPT1 Forward	CCAGGCCCAGCAGTGGGTTTGGGATTGGTTTGCCGCTA
VHPTL Reverse	GGAGGGTCGACCATAACTTCGTATAATGTATACTATACGAAG TATCCTCGAGCGGTA
VHPT2 Forward	TGGTGATGGTGAGTACTATCCAGGCCCAGCAGTGGGTTTG
VLPTL Forward	ACCGCTCGAGGATAACTTCGTATAGTATACATTATACGAAGTT ATGGTCGACCCTCC
VLPT1 Reverse	CGCTGGATTGTTATTACTCGCAGCAAGCGGCGCGCATGCC
VLPT2 Reverse	TACCTATTGCCTACGGCAGCCGCTGGATTGTTATTACTC
pDAN_to_pDNL6 3’	ATCCAGGCCCAGCAGTGGGTTTGGGATTGGTTTGCC
pDAN_to_pDNL6 5’	TCTGGTGGTGGTGGTTCTGCTAGAGGCGCGGCAGCAAGC GGCGCGCATGCC
pPNL6 Forward	GTACGAGCTAAAAGTACAGTG
pPNL6 Reverse	TAGATACCCATACGACGTTC

2.5 BLI (Bio-layer interferometry)

2.5.1 Calculation of dissociation Constant

The instrument used is the OCTET® N1, purchased from the company Sartorius.
The software used to run the experiment is OCTET® N1 Software.

NB: *Before starting the experiment, hydrate the tip containing the biosensor in 250 µl of sample diluent for at least 10 minutes.*
NB: The biosensor used in the calculation of the dissociation constant is the OCTET® Sa Biosensor (functionalized with streptavidin)

1. Build an initial baseline by immersing the tip in 250 µl of sample diluent for 30’’;
2. Load the biotinylated antigen onto the biosensor by immersing the tip in a drop containing antigen solution concentrated at 10 µg/ml for 120’’;
3. (Baseline 2): eliminate excess antigen by washing the tip in 250µl of fresh sample diluent for 30’’;
4. (Association): incubate the biosensor with the antibody diluted in the sample diluent for 120’’. Make different concentrations of antibodies to get a more accurate measurement.
5. (Dissociation): Incubate the biosensor in 250µl of sample diluent for 120’’
6. Calculate the kD thanks to the OCTET® N1 Software.

Table 3: BLI program

Step	Time	Sample	Drop /Tube
Initial baseline	30”	Sample diluent	Tube
Loading	120”	Antigen	Drop
Baseline	30’'	Sample diluent	Tube
Association	120”	Antibody	Drop
Dissociation	120”	Sample diluent	Tube

2.6 Real-time PCR.

1. Isolate the total RNA from MDOCs using TRIzol reagent (Invitrogen);
2. Retrotranscribe 500ng of RNA using QunatiTect Reverse Transcription Kit (Qiagen, Hilden, Germany);
3. DC-STAMP, OSCAR, and NFATc1 expression was evaluated with gene expression assay (Assay-on Demand; Applied Biosystems, Foster City, CA);
4. Use the GAPDH gene for normalization of the cDNA amounts.
5. Perform the real-time PCR in 10µl of final volume with 1µl of diluted cDNA, 5ul of Taq Man Universal PCR Master Mix (Applied Biosystem), and 5µl of Assay-on Demand mix;
6. Analyze with ΔΔ threshold cycle method.

2.7 Wound Healing Assay

1. Plate the BxPc3 ($2x10^5$) in 12 well-plate and grow until confluence in 1ml of RPMI 1640 (Euroclone) with 10% FBS (Sigma-Aldrich), 1% glutamine (Sigma-Aldrich), and 1% P/S (Sigma-Aldrich);
2. Scratch with a pipette tip from left to right of the well
3. Remove the medium and wash two times with PBS 1X;
4. Add 2µg/ml of treatment in 1ml of RPMI 1%FBS, 1%glutamine (Sigma), and 1% P/S (penicillin-Streptomycin, Sigma) and incubate at 37°C for 24h.
5. Take three pictures for each well at 0 and 24h. Each condition was done in triplicate;
6. Calculate the migration difference via ImageJ/Fiji® plugin 'Wound_healing_size_tool

2.8 Trap Assay

According to the manufacturer's instructions, tartrate-resistant acid phosphatase (TRAP) activity was assessed using the Acid Phosphatase kit (Sigma-Aldrich).

- Cells were fixed with Citrate Solution 0.038 mol/L in 60% Acetone;
- Wash the cells and incubate them in a pre-warmed labeling solution (Fast Garnet GBC Base Solution 7 mg/mL dissolved in Acetate Solution 2.5 mol/L, pH 5.2, Naphthol AS-BI phosphoric acid solution12.5 mg/mL, Tartrate Solution 0.67 mol/L, pH 5.2) for 1 h at 37°C.

- Microphotographs of TRAP staining were acquired by EVOS FLoid Cell Imaging System (Life Technologies, Carlsbad, CA, USA).

2.9 Osteoclastogenesis assay

- Peripheral Blood Mononuclear Cells (PBMCs) were separated from human blood samples obtained from buffy coats, provided by the local Blood Transfusion Service (Novara, Italy), by density gradient centrifugation using the Ficoll–Hypaque reagent (Lympholyte-H; Cedarlane Laboratories, Burlington, ON, Canada).
- Monocyte-derived Osteoclasts (MDOCs) were prepared from CD14+ monocytes isolated with the Easy SepHuman CD14 Negative Selection Kit (STEMCELL Technologies, Vancouver, BC, Canada).
- The monocytes were plated in 6-well and cultured for 21 days in a differentiation medium composed of DMEM (Lonza, Basel, Switzerland), 2 mM of L-glutamine, 10% FBS (Invitrogen, Carlsbad, CA, USA), recombinant human M-CSF(25 ng/mL; R&D System, Minneapolis, MN, USA), and RANK-L (30 ng/mL; R&D System).
- The differentiation medium was changed every 3 days and, at different times
- Cells were treated with free ICOS-Fc at 2 µg/mL.
- Phase-contrast images were acquired by Axiovert 40 CFL microscope (Zeiss, Oberkochen, Germany)

2.10 MTT viability assay

- Grow the cells (BxPc3) in the 96-well plate until confluency is reached. Incubation at 37°C and 5% CO_2;
- . Used RPMI medium with 10% FBS, 1% glutamine, and 1% P/S.
- Remove the medium and wash two times with sterile PBS 1X;
- Add treatment at a concentration of 5 ug/ml in RPMI medium with 1% FBS, 1% glutamine, and 1% P/S for 24 at 37°C and 5% CO_2;
- Remove the medium and wash two times with sterile PBS 1X;
- Add MTT reagent in ratio 1 to 10 v/v (20µl MTT/200µl medium) for 4h 37°C and 5% CO_2;
- Centrifuge at 2500rpm for 5';
- Remove de medium and resuspend in 200µl of DMSO;
- Read the absorbance at 570 nm.

2.11 Common procedures

2.11.1 ExpiCHO cells culture and transfection

ExpiCHO cells have been expanded, transfected, and stored, complying with the manufacturer's instructions.

2.11.2 Purification of the scFv-Fc/Full-size Ig

The general protocol is the same for the Protein A-resin or the CaptureSelect XL resin. The technical details for the CaptureSelect XL resin are written between the brackets. Each scFv-Fc was purified from 2,5 ml of cell culture medium.

1. The collected medium is filtered through a 0,22 µm filter device and mixed with 1/10 of the final volume of 1 M Tris/HCl pH 8 (PBS 10x pH 7,4).
2. Wash 50 µl-100 µl of the resin, the volume depending on its binding ability, twice by transferring it into a tube containing 8 ml of 0,1 M of Tris/HCl pH 8 (PBS pH 7,4) and centrifuging for 5 min at 800 x g, 10°C.
3. Incubate the resin was the medium on rotation O/N at 10°C.
4. Transfer the medium into a plastic column allowing the package of the resin.
5. After flowing the medium, add 10 ml of 0,1 M Tris/HCl pH 8 (PBS pH 7,4) to wash the resin.
6. Elute the resin-linked scFv-Fc (or full-size Ig) molecule by flowing 1 ml of 0,1 M Glycine pH 3 (0,1M Glycine pH 2) through the resin, collecting 3-5 fractions of 200 µl each.

2.11.3 DNA electrophoresis, SDS-PAGE, and Western Blot

All these procedures were performed according to the manufacturer's protocols and the standard molecular biology or biochemistry techniques (61 J. Sambrook i D. W. Russell. Molecular cloning: a laboratory manual, III. Red. New York: Cold Spring Harbor Laboratory Press (2001)), Western blots are detected with AP-labeled secondary antibodies and BCIP and NBT solutions.

Results and Discussion

Based on the isolation and characterization of antibodies against ICOSL, this work consists of three interconnected phases.

The first phase involved the use of phage display technology for the isolation and screening of specific antibody fragments against ICOSL. The second phase, instead, focused on the functional evaluation of the antibody and its ability to inhibit the maturation and function of the osteoclasts. Finally, the third phase, thanks to the display yeast technology, was focused on improving the affinity of the isolated antibody (Fig.18)

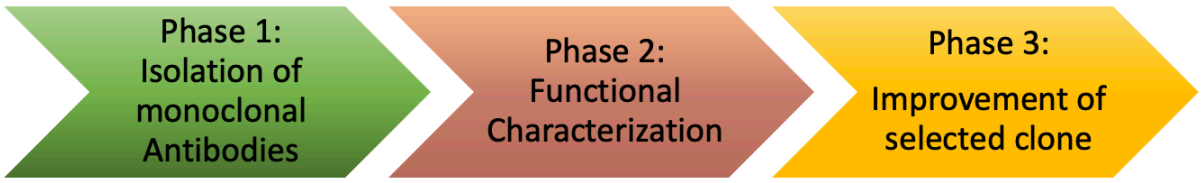

Fig. 18 *flowchart representing all stages of this work; starting from the isolation phase by phage display, passing through the functional characterization and concluding with the improvement of the isolated clone*

1 Isolation of monoclonal antibodies.

1.1 Phage Library

The whole process for isolating recombinant monoclonal antibodies started with validating a preexistent naïve library previously created in our laboratory.

The naive antibody phage display library was created from 25 healthy donors of different ages and genders. The cDNA resulting from the RNA reverse transcription of the genes of the variable regions (V genes) was used to selectively amplify some families of V genes with a well-established set of primers described in [139].

Subsequently, the variable regions were randomly assembled and inserted inside the phagemid (pDan5) for the construction of an scFv library. The phagemid library was, thus, electroporated into TG1 *E. coli* electrocompetent cells, and a final library was created.

1.2 Naive phage Library Validation

The bacterial cultures, *E. coli*, containing the antibody library were thawed and cultured to produce virions particles expressing the scFvs. After infection with the helper phage (M13KO7), the viral particles were collected from the supernatant, purified, and concentrated through the use of poly(ethylene)glycol (PEG), able to precipitate proteins from an aqueous solution [140].

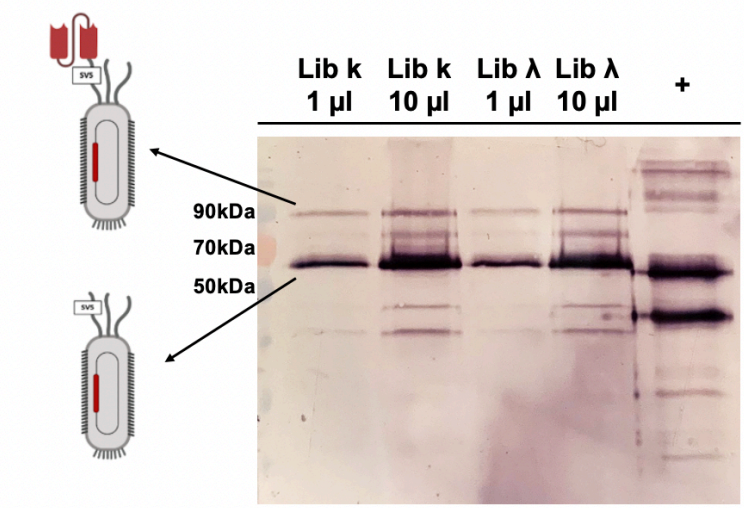

Fig.19 Validation of library production by western blot. *Loaded two different amounts of each library and evaluate the expression level with the anti-SV5 antibody. the band relative to the display has an apparent size of 90kDa. The level of visualization is comparable to that of the positive control (+). Partially created with biorender.com*

The display level of the library was assessed through Western Blot (WB) analysis. As it is possible to see from Fig.19, the display level was evaluated separately for the two light chains: k and λ. G3P-scFv was detected with an anti-SV5 secondary antibody since the phagemid pDAN5 has the SV5 tag coding sequence between the G3P and the scFv sequence.

The molecular weight of G3P is about 45 kDa, but the presence of the glycine-rich linker makes the protein migrate with an apparent molecular weight of about 65-70 kDa [101]. The display level is observable from the band with an apparent size of approximately 90kDa. This is the sum of the G3P protein and the scFv (molecular weight 27.5 kDa). Both libraries present a comparable level of display with positive control. In addition, according to Wen et al. [141], the display of the antibody fragment is

around 10% of the total phages. To know the phage concentration, both libraries were titer tested.

1.3 Antigen Validation

Before the selection process, the antigen was validated. ICOSL has been provided by NOVAICOS s.r.l.s. as a purified recombinant protein produced in HEK 293 cells. The antigen was supplied as a fusion protein between the extracellular portion of human ICOSL and the Fc fragment of a human IgG. Another form of ICOSL was also provided with His tag. In addition, the recombinant molecule ICOS-Fc was also provided and used in tests as a control (produced in HEK293) (Fig. 20). All the antigens are validated on the SDS page in reducing conditions to assess quality and quantity.

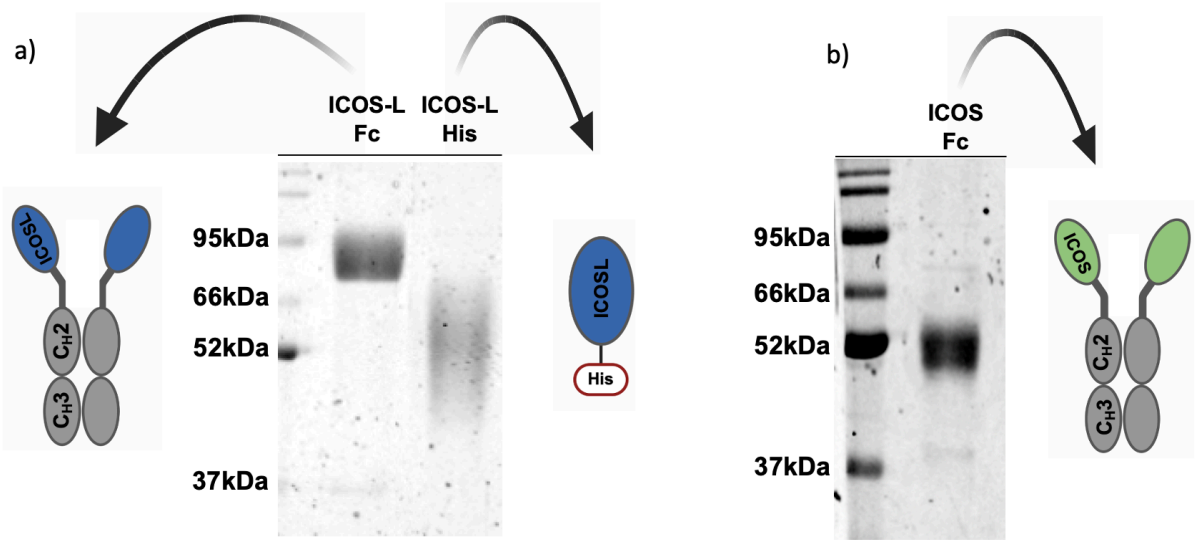

***Fig.20 Validation of antigens**: a) SDS page under reducing conditions of ICOSL-Fc and ICOSL-His. 1µg was loaded for both proteins. Both have a characteristic pattern due to glycosylations. ICOSL-Fc has a spread band from 70kDa to 95kDa, while ICOSL-His from 45 to 70kDa. b) SDS page under reducing condition of 1,5 µg of ICOS-Fc that present a smeared band from 45 to 55 kDa.*

The extracellular portion of ICOSL is about 27 kDa (240aa) [15], while the Fc fragment weighs about 25 kDa [3]. However, as it is possible to observe from Fig.20 (a), ICOSL presents a smeared band from 70kDa to 95kDa. This pattern is characteristic of glycosylated proteins, and ICOSL is a glycosylated protein. ICOSL with His tag also has the smeared band but with a lower molecular weight due to the absence of the Fc

fragment. The same pattern is present in ICOS-Fc protein (Fig 20 b), a glycosylated protein that runs with an apparent molecular weight of about 45-55 kDa.

1.4 Selection Strategy and Screening

Once validated, the antigen was used to select antibodies starting from a Phage Naïve library. The selection process was performed on a solid phase. In particular, ICOSL was coated in an immunotube, as shown in Fig. 21, and subsequently incubated with the phage library. This process was repeated twice. The output of the first round of selection (selected library) was used as input for the second round. Finally, from the

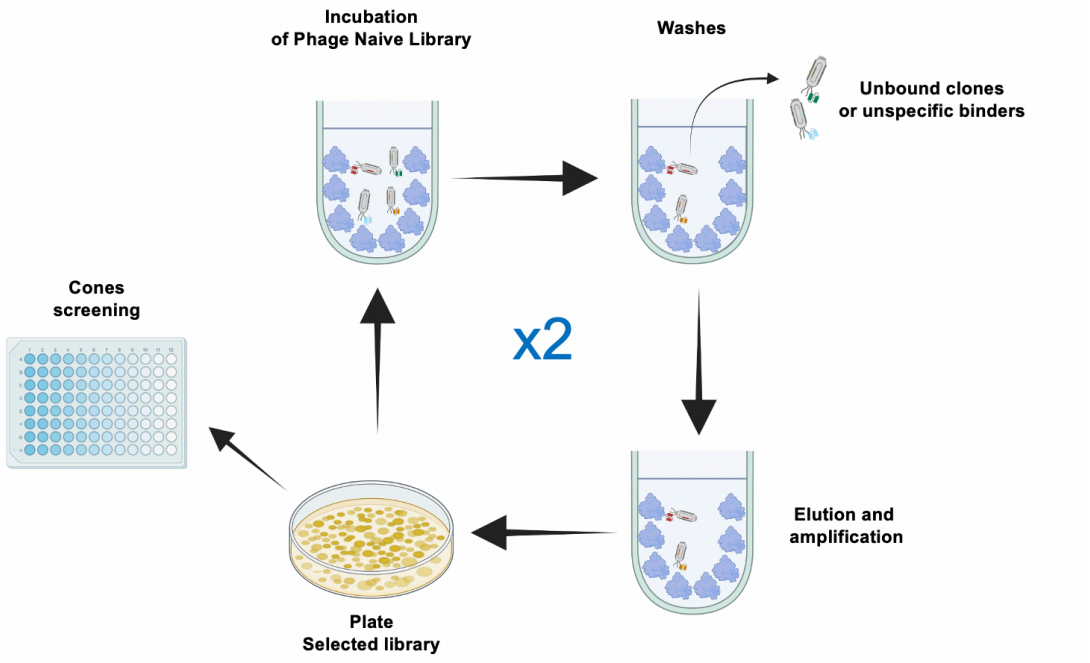

***Fig 21 Schematic representation of the selection strategy on solid phase**. During the first round of selection the naïve phage antibody library has been incubated with the antigen coated at 10 µg/ml. The output of the first round of biopanning has been used as input for the second round, were the antigen was coated at 5 µg/ml. After the second cycle of selection 300 random E. coli colonies have been picked and tested for antigen recognition.*

second output, random single *E. coli* colonies have been picked to be screened by phage ELISA for antigen recognition.

In detail, for the first round of selection, ICOSL-Fc was coated on the immunotube at the final concentration of 10 µg/ml; instead, for the second round, the concentration was 5µg/ml. The use of a decreased amount of coated antigen helps in selecting antibody fragments with increased affinity. Since ICOSL-Fc was used for the selection process,

the selection strategy involved a negative selection step to eliminate clones that bind the Fc portion of the antigen.

To do this, the library was incubated with ICOS-Fc at a concentration 10-fold higher than the antigen. This step was performed in both selection rounds. In addition, stringent washes were performed during the second panning cycle to remove poorly reactive or unspecific clones.

After two selection cycles, about 300 random clones were checked on the ICOSL-Fc antigen by phage-ELISA. To facilitate screening, clones showing an OD_{450nm} greater

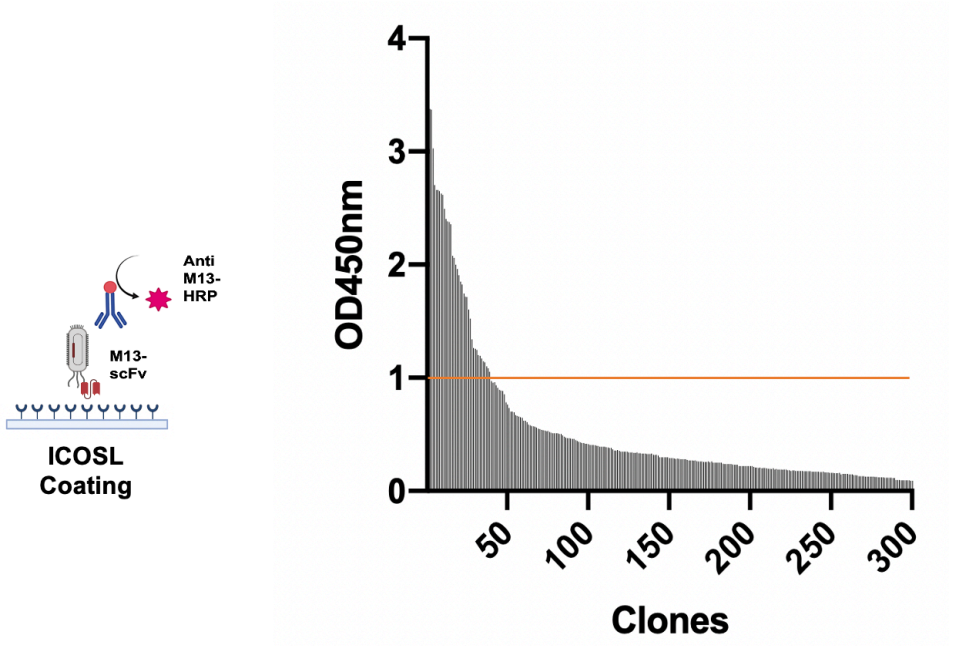

Fig.22 *Output of 300 random clones tested by phage-ELISA assay on ICOSL-Fc antigen after two cycles of selection. Clones showing an* OD_{450nm} *greater than 1 were considered positive*

than 1 were considered positive. The obtained output (Fig. 22) showed that almost 13% (40 clones) of the tested clones resulted positive for the target.

1.5 Analysis of selected clones

Therefore, the isolated anti-ICOSL-Fc clones were first analyzed by PCR reaction by amplifying the scFv fragment. Among the 40 clones analyzed, 20 were confirmed for the full length of the scFv, while the other 20 clones had PCR products of lower length, probably due to the loss of a single variable domain.

To determine the specificity of the selected antibodies, the 20 positive clones were tested in Phage-ELISA. The test was performed with ICOSL-Fc directly coated on a solid surface at a 5 µg/ml concentration. As a negative control and to assess the

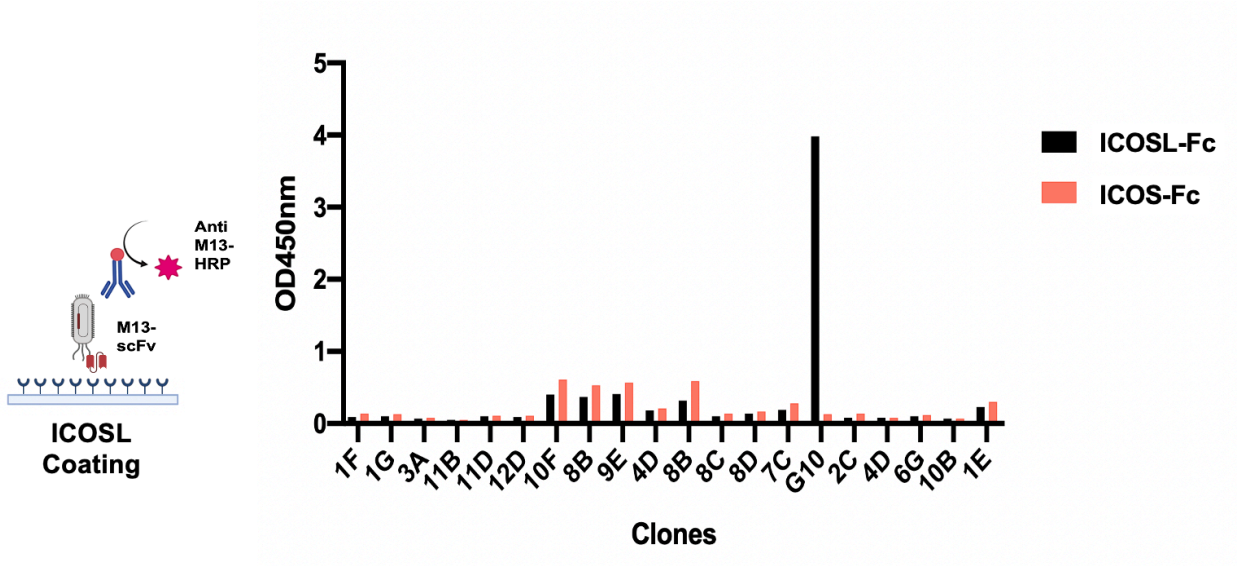

***Fig.23 Phage ELISA of the clones selected on the antigen coated on solid phase**. Phages were incubated with the antigen at a final concentration of 5 µg/ml. ICOS-Fc was used as negative control. Results show that only G10 clone is positive and specific for ICOSL-Fc*

presence of non-specific binding to the Fc fragment, ICOS-Fc was coated at the same concentration.

The binding between the phages and the antigen was detected with anti-M13 antibody HRP labeled secondary antibody that binds the G3P of the bacteriophage. As can be seen from the graph (Fig 23), the only positive clone is the G10 clone. It presents a signal on the ICOSL-Fc antigen and shows no binding on the ICOS-Fc molecule. This indicates that the negative selection process has been performed successfully. A possible explanation for this is that ICOSL-Fc is a highly glycosylated molecule. As a matter of fact, glycosylations can cause false positives due to the sticky nature of this macromolecule. Furthermore, it is possible to observe clones (10F, 8B, 9E,8B) that present a weak signal but also show a signal towards ICOS-Fc. These clones were not subsequently investigated

1.6 Characterization of the anti-ICOSL isolated clone G10

Given the positivity of the G10 clone, we wanted to investigate the specificity of the binding. In particular, to do this, the antibody was incubated with different antigens coated at the same concentration (5 µg/ml).

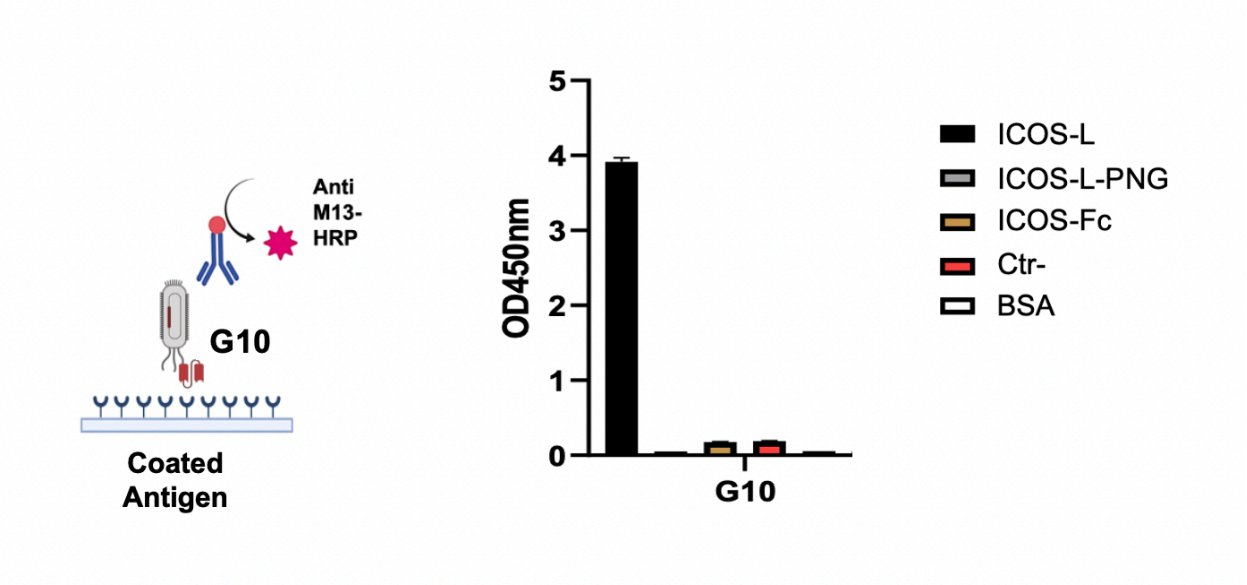

***Fig.24 Phage ELISA of G10 clone**. The specificity of the G10 clone was tested by phage ELISA on the solid phase. The antigens were coated at a concentration of 5 µg / mL. G10 shows positivity only on ICOSL and not on the other antigens. Furthermore, the G10 clone does not bind ICOSL treated with PNGASE.*

The antigens are ICOSL-Fc, ICOSL-Fc treated with PNGASE (an enzyme able to cut the glycosylation), ICOS-Fc, an unrelated antigen (ctr-), and BSA (Bovine serum albumin). As it is possible to observe from the graph (Fig.24), the G10 clone shows good specificity against the antigen of interest. As a matter of fact, the G10 has no signal on the other unrelated antigens. Intriguingly, we did not observe any signal in ICOSL-Fc-PNGASE as well.

This result is probably due to the fact that glycosylations play a fundamental role in antibody binding. This could have two possible explanations. First, glycosylations directly intervene in the binding between the antibody and the antigen. The second explanation may be the change in the folding of the antigen, which hides or makes the epitope inaccessible.

1.7 Recombinant monoclonal antibody production

Given the promising results obtained in specificity, it was decided to proceed with further characterization of the clone. Thus, we produced the G10 clone in a format similar to a full-length immunoglobulin: the scFv-Fc (schematic representation in Fig .25). The coding sequence of the scFv of the G10 clone was cloned into a mammalian

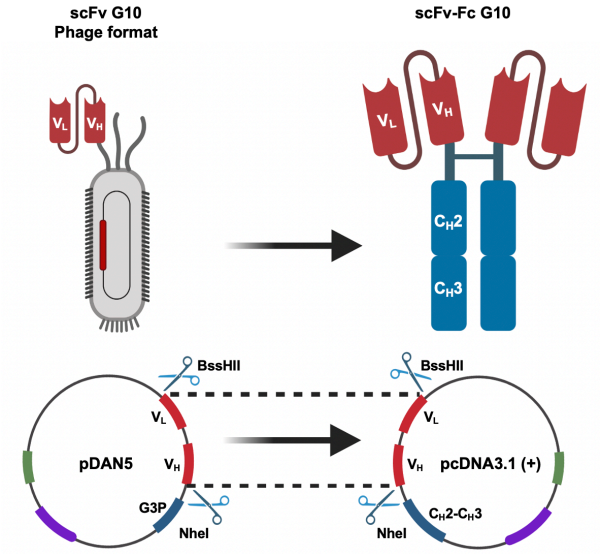

Fig.25 Schematic representation of cloning strategy. *Schematic representation of the cloning strategy that allows the switching from the scFv to the scFv-Fc. The coding sequence of the scFv is cut from the phagemid vector and cloned on the scFv-Fc expression vector.*

expression vector (pcDNA3.1 (+)) that allows the production of recombinant proteins in a eukaryotic system (the detailed structure of these vectors is given in [142]). To do this, both the phagemid (pDAN5), containing the scFv sequence of the G10 clone, and the eukaryotic expression vector (pcDNA3.1 (+)) were digested with the restriction enzymes BssHII and NheI, allowing the extraction of the scFv sequence and the preparation of the receiving vector.

In this case, the scFv was cloned into a vector presenting the human IgG C_H2-C_H3 (Fc) coding sequence. A schematic representation of the cloning strategy is given in Fig. 25.

Once cloning was done, the antibody fragment was produced through ExpyCHO, a commercial cell line optimized to ensure high production yields. The high titer protocol was used in 30 ml of culture, and scFv-Fcs production was evaluated eight days post-transfection.

To verify the scFv-Fc G10 production, the supernatant of the transfected cells was used for an ELISA test. The supernatant was diluted 1:10 and 1:50 in PBS and coated in an ELISA well,

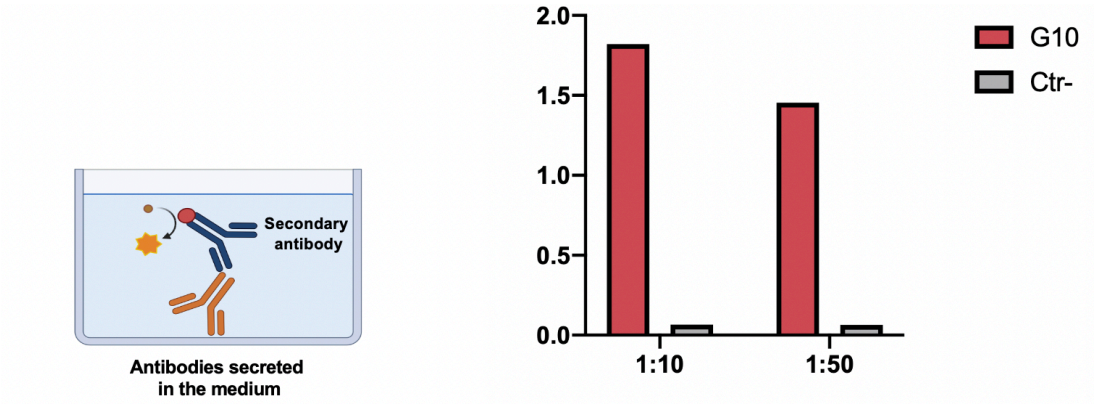

***Fig.26 ELISA test to verify the production of the G10 scFv-Fc**. The supernatant of the transfected cells was diluted 10 and 50 times before coating. The presence of the scFv-Fc of interest was detected using a an HRP-conjugated anti-human-Fc secondary antibody.*

and production was evaluated by an HRP-conjugated anti-human-Fc secondary antibody. The result is shown in Fig. 26. As can be seen, the G10 clone shows a signal in both dilutions indicating that the G10 is indeed produced.

Subsequently, the scFv-Fc has been protein A purified and quantified by densitometry. As shown from the SDS page (Fig. 27 a), the purified antibody (monomeric form composed of the variable domains and Fc fragment) shows two different bands under denaturing conditions. The first, with an apparent size of 60kDa, represents the entire scFv-Fc molecule. Instead, the band around 45kDa is the degradation form of the scFv-Fc molecule that probably has lost the variable domain (approximately 12-15 kDa).

As can be seen from the SDS page, the amount of non-degraded scFv-Fc is slightly higher than that of degraded.

This is also confirmed by the Western Blot (WB) analysis of the purified scFv-Fc using an anti-SV5 secondary antibody (the SV5 tag is at the end of the FC domain) (Fig. 27 b). It is possible to observe two bands with an apparent size of about 60kDa and one with a size of about 45kDa. The first represents the entire scFv-Fc, while the second represents the scFv-Fc molecule, presumably lacking a variable immunoglobulin domain (probably the V_L domain).

Only the full-length portion was considered for quantification of the antibody and the future test.

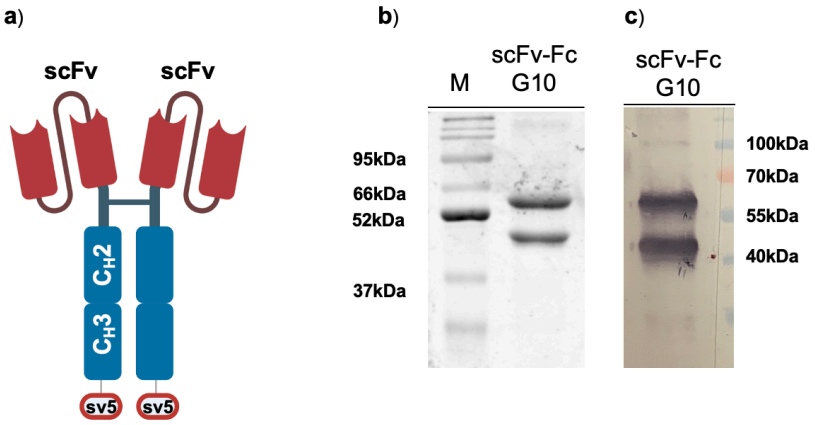

Fig.27 *a) Schematic representation of the scFv-Fc molecule. b) SDS-PAGE of the purified scFv-fc of the G10 clone. 2 µl of the purified scFv-Fc were loaded on gel and run in reducing conditions. c) anti SV5 WB analysis of the purified scFv-Fc of the G10 clone. Loaded 1µg of the purified scFv-Fc g10*

1.8 scFv-Fc G10 specificity

Once produced as scFv-Fc, the G10 clone was tested for its functionality. The first test was an ELISA test to verify that the format change did not result in a change in ICOSL antigen recognition. Several antigens were coated at a concentration of 5 µg/ml and

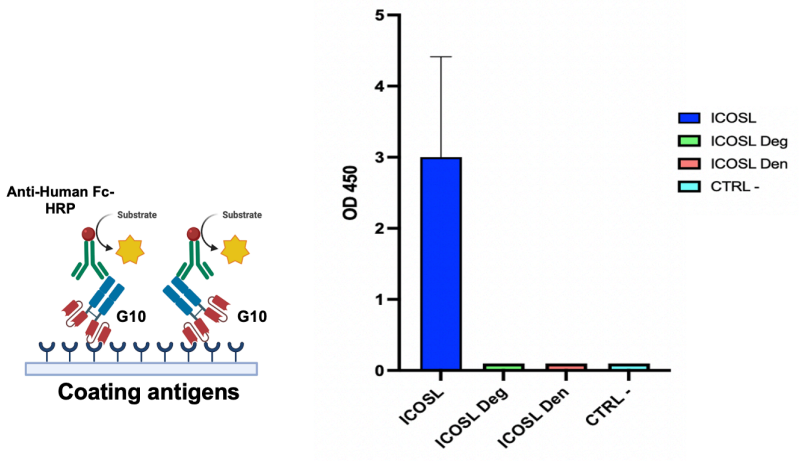

Fig. 28 ELISA of G10 clone for evaluation of the specificity*. The specificity of the G10 clone was tested by ELISA tes on the solid phase. The antigens were coated at a concentration of 5 µg / mL. G10 shows positivity only on ICOSL and not on the other antigens. Furthermore, the G10 clone does not bind ICOSL treated with PNGASE and with ICOSL treated with denaturing agents*

then incubated with scFv-Fc G10 at a concentration of 1 µg/ml. Binding was detected using an HRP-conjugated anti-human-Fc secondary antibody.

Due to the cross-reactivity due to the presence of the Fc fragment in the ICOSL-Fc antigen, the ICOSL-His tag was used for these experiments. For this experiment, ICOSL-His was deglycosylated but also reduced and denatured (using DTT and IDA) to test the antibody's ability to recognize the antigen in non-native form.

As it is possible to see from the results in Fig. 28, the G10 clone maintains its ability to bind ICOSL. The G10 clone shows no signal on PNGASE-treated ICOSL, confirming the critical role of glycosylation for binding. Interestingly, we cannot observe any signals in denatured ICOSL either. These results are essential for understanding the nature of the binding. The G10 bond appears to depend on glycosylation and folding of the antigen.

These data are also confirmed by Western Blot analysis. In fact, as shown in Fig. 29,

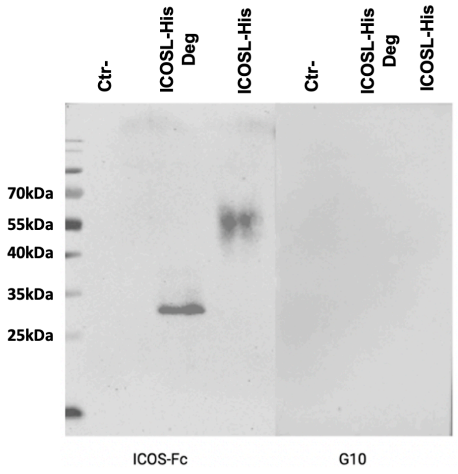

Fig.29 *Western blot analysis for evaluation of the binding specificity of clone G10. Loaded 500ng for each antigen and evaluated the binding of ICOS-Fc or G10 antibody using an anti-human-HRP secondary antibody.*

clone G10 does not bind either denatured or deglycosylated ICOSL-His. Curiously, ICOS-Fc, used as a positive control, binds all forms of ICOSL. This result provided important information about the nature of the binding between antigen and antibody. In fact, it is very probable that ICOS-Fc and the G10 clone bind different epitopes of the ICOSL molecule.

1.9 scFv-Fc G10 affinity

Once specificity was established, the dissociation constant at equilibrium (k_D) was calculated. The k_D is the ratio of the k_d (antibody dissociation rate) to the k_a (antibody association rate) between the antibody and the antigen. Its value is related to the antibody concentration, so the lower the k_D, the higher the affinity of the antibody [143].
This was performed with the BLI instrument OCTET® N1 (bio-layer interferometry).
This optical technique exploits the interference pattern of white light that is reflected between two surfaces: a layer of immobilized protein on the biosensor tip and an internal reference layer. When the molecules bind to the tip of the biosensor, they cause a change in the interference pattern, which is measured in real-time by the instrument.

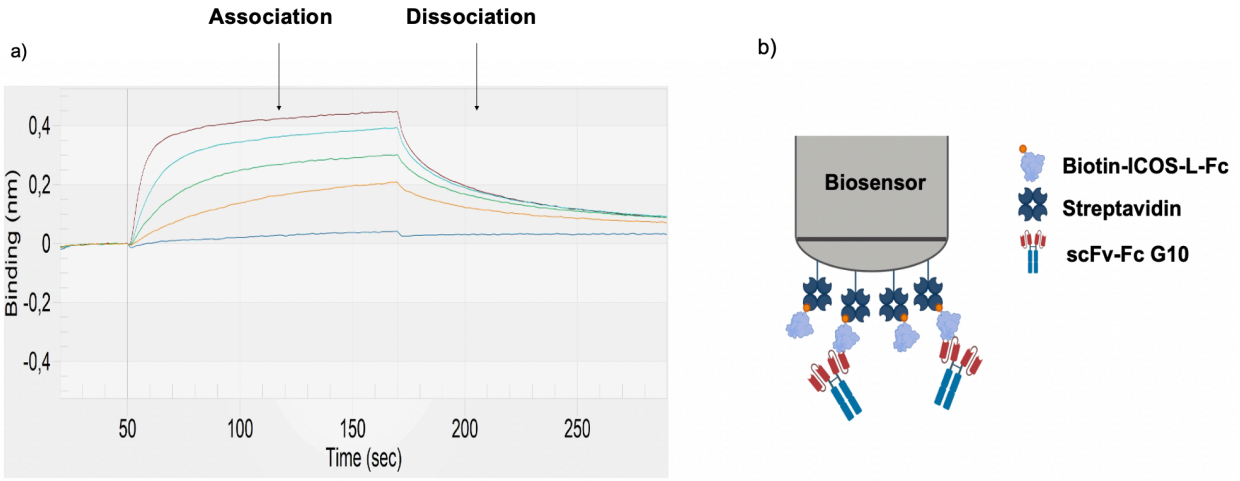

c)

ID	k_D	Ka 1/Ms	Kd 1/s
G10	87 nM	2.33 E5	2.04 E^{-2}

Fig.30 Calculation of the dissociation constant of clone G10. *The streptavidin functionalized biosensor was loaded with ICOSL-biotinylated at a concentration of 10ug / ml. the scFv-Fc G10 was subsequently added at different concentrations: 0,25,50,100,200 nM. The graph was obtained using the OCTET® N1 software. b) Schematic representation of the biosensor tip: Streptavidin-functionalized biosensor loaded with ICOSL-biot and subsequently incubated with G10 antibody for affinity assessment c) Table resuming KD, Ka and Kd values of the G10 clone*

In particular, a biosensor (OCTET® Sa Biosensor) functionalized with streptavidin was used. Therefore ICOSL-Fc was biotinylated and loaded on the biosensor at a

concentration of 10µg/ml. The tip of the biosensor was subsequently placed in contact (Association:120'') with a solution containing different concentrations of G10 scFv-Fc.
In fact, k_D analyses performed with varying concentrations of antibodies make the measurement more accurate. In detail, five different antibody concentrations were used: 0, 25, 50, 100, e 200nM. As can be seen from the graph in Fig.30 (a), as the concentration increases, the height of the curve increases, indicating a greater quantity of antibody that binds over time. Subsequently, the dissociation phase (120 '') was evaluated after washing. As shown in the table (Fig.30 b), the G10 clone has a high Ka value (fast association) but also a low Kd value (rapid dissociation) that leads to a K_D value of 87nM. This value is in line with the K_D values of other antibodies isolated from a naive library, which are between 10nM and 100nM.

2 Functional characterization of anti-ICOSL G10 clone

Since one of the objectives of this project is to isolate antibodies capable of functioning as the recombinant molecule ICOS-Fc, the second phase of this work has focused on the study of the functional characteristics of the antibody against ICOSL G10. In particular, its ability to inhibit the process of cell migration and osteoclastogenesis has been explored.

2.1 Surface recognition of ICOSL by flow cytometry

For functional testing, the G10 clone must be able to bind ICOSL on the cell surface. Therefore, the ability of clone G10 to bind ICOSL on the surface of ICOSL+ cells was then evaluated. Different ICOSL+ tumor cell lines were used for this analysis: OVCAR-3 cells (ovarian cancer) [144], MDA-MB cells (breast cancer) [145], PC3 cells (prostate cancer) [146], MCF7 (breast metastatic adenocarcinoma) [146], and BxPc3 (pancreatic cancer) [146].

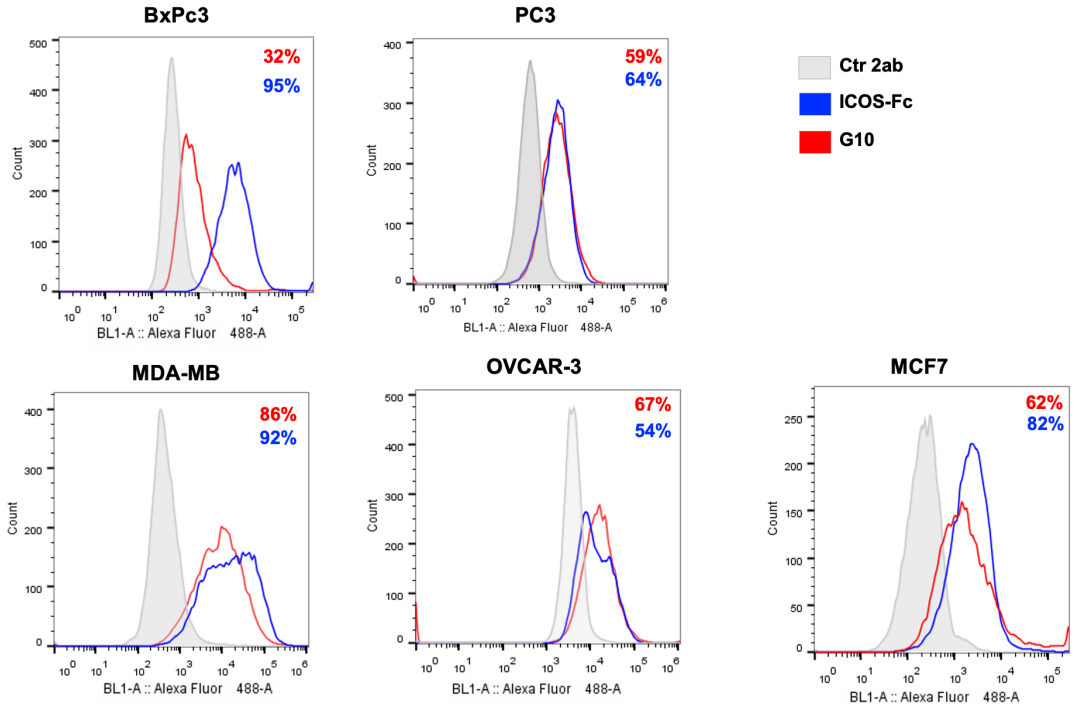

***Fig.31 Figure showing the histograms of ICOSL expression on different cell types**. Clone G10 and ICOS-Fc Positive Control were incubated with different cells (1.5 x 10^5 cells per condition) at a concentration of 15 µg / mL. The G10 shows positivity in all cell types with a value comparable to the positive control, except on BxPC3. Percentage of G10 positive population: BxPC3 32%, MDA-MB 86%, PC3 64%, OVCAR-3 67% and MCF7 60%.*

The cells were then incubated with scFv-Fc G10, and its binding was detected by an antibody labeled with Alexa 488 fluorophore, capable of recognizing the Fc region of the antibody. The ICOS-Fc molecule was used as a positive control for the effective success of the experiment. Both ICOS-Fc and scFv-Fc G10 were used at a concentration of 15µg/ml. As can be seen from the graphs in Fig. 31, by comparing the fluorescence signal of the G10 clone with that of the control (only secondary anti-human antibody), G10 binds ICOSL specifically on the cell surface. It is important to note that there are different degrees of positivity depending on cell types (BxPC3 32%, MDA-MB 86%, PC3 64%, OVCAR-3 67%, and MCF7 60%). This is due to the different degrees of ICOSL expression on the cell surface. Moreover, it can be noted that in almost all cases, except BxPc3 cells, the G10 fluorescence signal is comparable to that of the ICOS-Fc positive control. Therefore, the G10 clone recognizes ICOSL in its native form on the cell surface, making it a good candidate for osteoclast testing.

2.2 Wound healing assay

Once the ability of the G10 antibody to bind ICOSL on the cell surface was established, functional evaluation was performed.

Dianzani et al. [13] have demonstrated how the triggering of ICOSL on the cell surface by ICOS-Fc is able to inhibit the cell migration of different tumor cell lines. Interestingly, this effect was not attributable to ICOS-Fc toxicity because the proliferation and survival were not affected.

In the same way, we performed a cell migration test to study the effect of our anti-ICOSL G10 antibody on cell migration. We performed the scratch assay, an in vitro “wound healing” assay, on BxPC3.

Pancreatic cancer is one of the most aggressive tumors nowadays, exhibiting a high degree of tumor cell invasion into normal tissues and organs, making this cell type a good model for studying cell migration [147, 148].

For the wound healing assay, the cells were plated onto 12-well plates and grown to the confluence. A linear scratch was performed, whit a tip, on a confluent monolayer of the cell line and then cultured in 1% FBS-medium to minimize cell proliferation in the presence of ICOS-Fc (5mg/ml) or the antibody G10 (5mg/ml) for 24h. The control consists only of culture with 1% FBS medium. A microscopic analysis allowed the evaluation of cell migration. Through the ImageJ / Fiji® plugin

'Wound_healing_size_tool' [147], it was possible to calculate the area inside the scratch and compare it between treatments. As can be seen from the images (Fig.32a), the treatment causes the inhibition of cells' migration compared to the control. The control, after 24 hours, appears almost entirely closed; on the contrary, treated samples show a wider uncoated area.

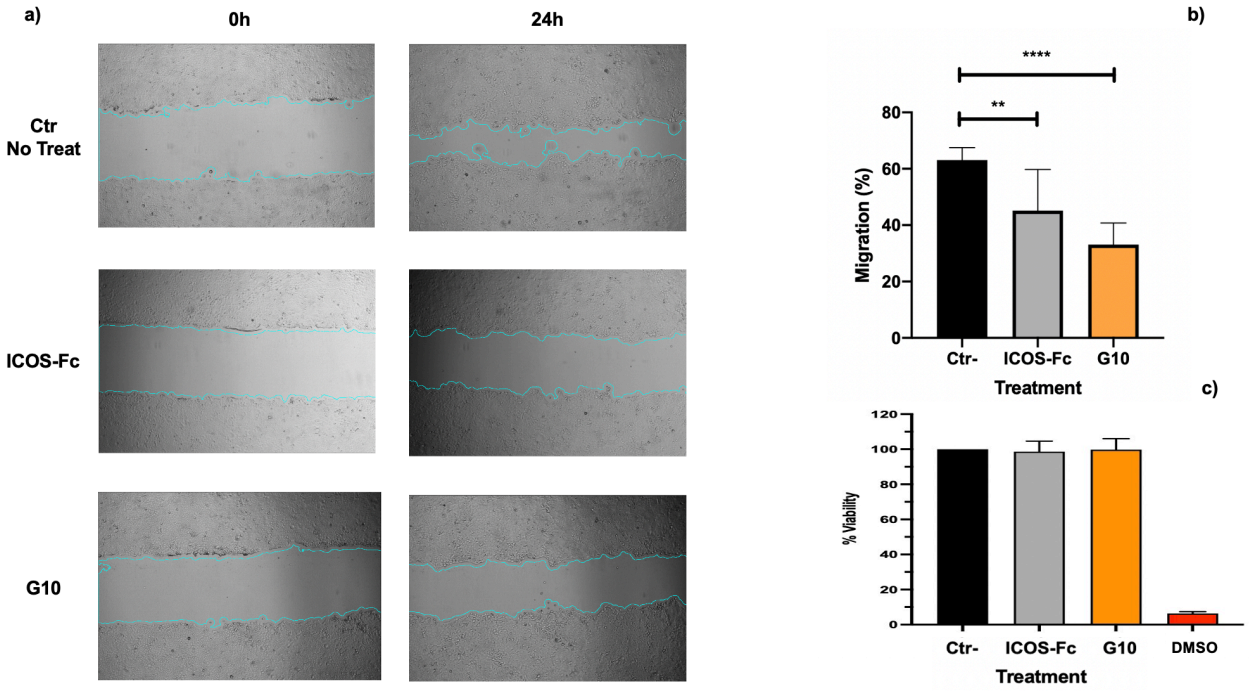

Fig.32 Effect of ICOS-Fc and anti ICOSL G10 antibody on the migration of the BxPc3, using a "wound-healing" assay. *The cells were grown to confluence on twelve-well plates. A scratch was made through using a pipette tip; the cells were washed and then cultured in the presence or absence of 2 mg/ml of ICOS-Fc and G10 antibody for 24 h. To monitor the migration the photographs were taken immediately after the scratch (0h) and at 24h. The wounded area was calculated by the ImageJ / Fiji® plugin 'Wound_healing_size_tool. Both treatments are effective in reducing cell migration compared to control. b) Representative histogram of the percentage of cell migration expressed as area* ***(0h - area24) / (area 0h)x100****. statistical analysis carried out through T-test towards the control. **= p<0.0099 and ****= p<0.0001. Representative panel of three distinct experiments. c) histogram representing the result of the MTT vitality test. Result expressed as % viability compared to the control without treatment. The treatments (ICOS-Fc and G10 antibody) did not show any variation in viability compared to the control*

This is also confirmed in the histogram, where the percentage of migration (expressed as area (0h - area24) / (area 0h) x100) of cells treated with ICOS-Fc or with G10 is significantly reduced if compared to the controls (Fig.32 b).

These data confirm the efficacy of our antibody, which shows a behavior similar to the ICOS-Fc molecule. Interestingly, the histogram makes it possible to appreciate a better outcome in inhibiting migration by G10 compared to ICOS-Fc.

Furthermore, to evaluate whether the inhibitory effect of migration depended only on the functional effect of the treatment and not on cell death, we performed an MTT viability assay. To perform this assay, cells were grown to confluence in a 96-well plate (three wells for each condition) in RPMI with 10% FBS. Then the cells were subjected to treatment with RPMI 1% FBS and 5 µg/ml of G10 antibody and ICOS-Fc for 24 hours (same conditions as the migration assay) (the viability control consists of cells grown in 1% RPMI FBS, on the other hand, the mortality control consists of cells treated with 10% DMSO + RPMI 1% FBS)

As can be seen from the graph (Fig. 32 c), the treatments do not cause changes in cell mortality compared to the control. Therefore, the migration is due to a functional effect of the treatment and not to a secondary effect caused by cell death.

2.3 Effects of ICOSL triggering on Onsteoclasts differentiation.

2.3.1 Osteoclastogenesis Assay

As already mentioned, the ICOS / ICOSL pathway is involved in the differentiation and activity of osteoclasts. Activation of ICOSL on the surface of MDOCs (monocyte-derived osteoclast-like cells) by ICOS-Fc inhibits their differentiation into mature osteoclasts. Also, it reduces the expression of enzymes necessary for their activity [32].

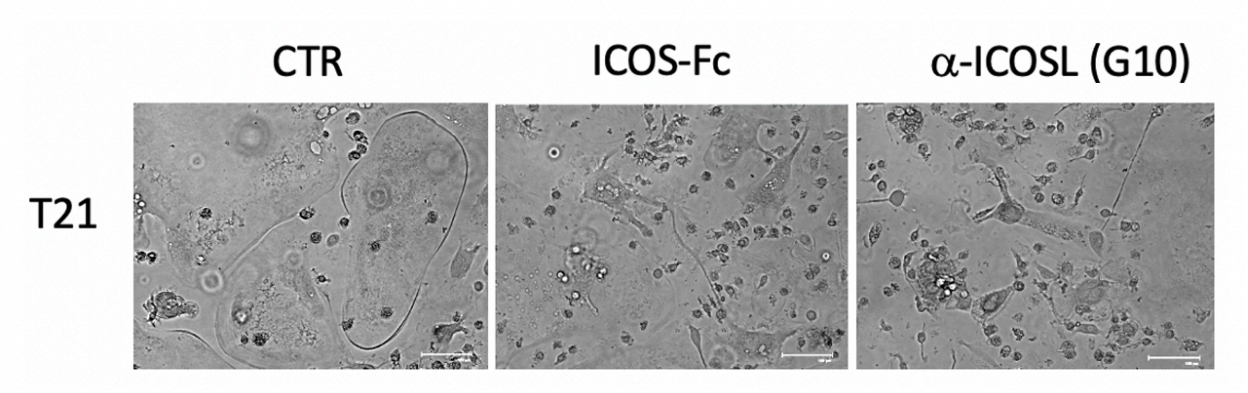

Fig. 33 Effect of treatment with ICOS-Fc and the G10 antibody on the osteoclastogenesis process. *Monocytes were induced to differentiate to MDOCs in the presence and absence of the ICOS or G10 antibody added from day 0 (T0–21 treatment).on day 21 the treated cells have a different morphology than the control. The control shows a typical progression towards the morphology of MDOCs, while the treated ones have a small and spindle shape consistent with inhibition of osteoclastogenesis. Representative panel of three distinct experiments*

The osteoclast is a multinucleated giant cell whose maturation consists of cell polarization with the formation of a ruffled membrane and the clear zone, which is the secretion site of TRAP, cathepsins, and metalloproteinases, crucial enzymes involved in the demineralization of the inorganic component of the bone [148]. In this work, we want to demonstrate that the anti-ICOSL antibody G10 can behave like ICOS-Fc in inhibiting osteoclasts' differentiation. To do this, an osteoclastogenesis assay was performed in collaboration with the company NOVAICOS. Monocytes were cultured for 21 days in a differentiation medium composed of M-CSF and RANK-L. Cells were treated with 2mg/ml of either ICOS-Fc or G10 antibody from day 0, and osteoclasts morphology was analyzed on day 21. Fig. 33 (microscope images) shows a notable difference between treated and untreated cells. In fact, on the 21st day, the untreated control shows the presence of giant cells showing the typical progression toward the MDOC morphology. At the same time, both ICOS-Fc and G10 antibodies show similar results; in fact, in the microscope images, there are no multinucleated cells but cells that have acquired a spindle morphology. These results are consistent with an inhibition of MDOC differentiation in mature osteoclasts.

2.3.2 TRAP Assay: evaluation of TRAP enzyme amount

To further investigate the functionality of the G10 clone, we also performed, in collaboration with the company NOVAICOS, a TRAP assay. This is highly expressed in mature osteoclasts and is contained within lysosomes and vesicles, ready to be released into the clear zone.

The presence of the TRAP protein and its quantity were analyzed by enzyme staining in osteoclasts. As before, the monocytes were cultured in the presence of growth factors and subsequently treated with ICOS-Fc and the G10 antibody from day 0. The evaluation of the TRAP enzyme was done on day 21. Again, it is possible to observe from Fig. 34 (a) that the control shows giant cells with a massive amount of TRAP protein (stained in black) in them. On the contrary, the two treatments show a robust inhibition of maturation. There is a smaller amount of multinucleated cells and a notable presence of cells with spindle-like cell morphology.

Furthermore, the amount of TRAP protein significantly decreased compared to the control. This is also confirmed by the histogram that shows the percentage of the multinuclear $TRAP^+$ cells at T21 (Fig. 34 b). The percentage of $TRAP^+$ cells is

comparable between the two treatments, showing a decrease of about 50% compared to the control.

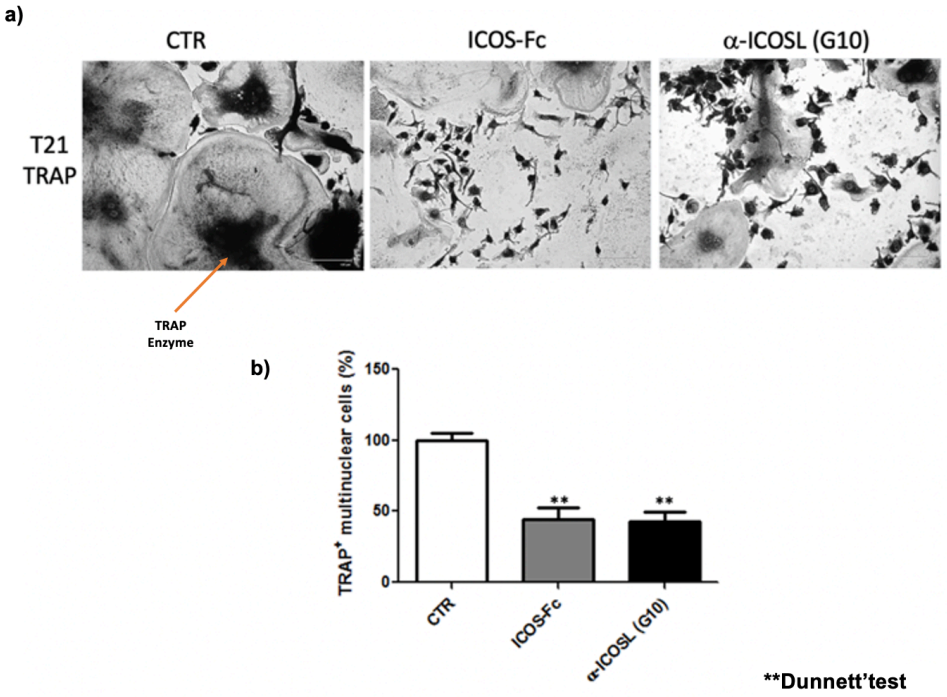

Fig. 34 Effect of ICOS-Fc and G10 antibody on MDOC differentiation*. Monocytes were i differentiated to MDOCs in the presence and absence of the two treatments reagents added from day 0 (T0–21 treatment).* ***a)*** *Microphotographs of TRAP staining at T21 were observed at original magnification x40 (representative of three experiments).* ***b)*** *Data are expressed as the mean +/- SEM of the percentage of inhibition versus the control (set at 100%) obtained in three independent experiments by counting 10 fields per sample (**p < 0.01 versus the control).*

2.3.3 Real-time PCR: evaluation of the expression level of NFATc1, OSCAR and STAMP genes

Since the osteoclasts differentiation depends on the upregulation of specific genes like DC-STAMP (necessary for the osteoclast precursor fusion), OSCAR (regulator of osteoclast differentiation), and NFATc1 (activation of genes needed for the production of TRAP and cathepsin enzyme), we decided, in collaboration with NOVAICOS, to assess the effect of the treatment on the expression of these genes by real-time PCR.

Similarly, monocytes were grown and matured into osteoclasts with or without treatment, and on day 21, the genes expression level was evaluated.

The results showed that ICOS-Fc and the G10 antibody treatment decreased the expression of all these mRNAs in the osteoclasts if compared with untreated cells (*=p <0.05, **=p<0.01 versus the control) (Fig. 35). Interestingly, the G10 clone presents a

better result in the inhibition of the genes OSCAR and NFAT-c1 compared to the ICOS-Fc molecule.

Once again, these data confirmed the goodness of the anti-ICOSL G10 antibody in inhibiting the processes of osteoclastogenesis and osteoclastic function. This was done by behaving similarly to the recombinant molecule ICOS-Fc, which has proven effective for these purposes. This lays new foundations for the continued characterization of this clone to further explore its potential.

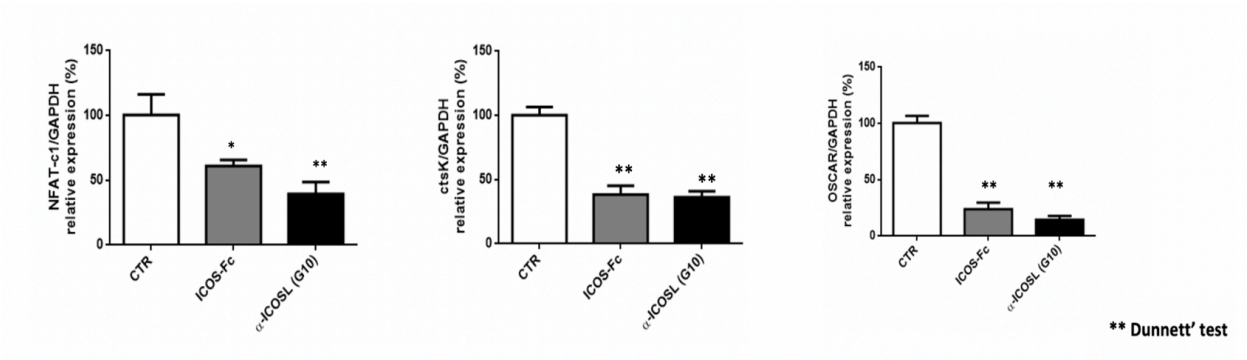

Fig.35 Effect of ICOS-Fc and G10 antibody on MDOC expression of OSCAR, NFATc1, and DC-STAMP*. Histograms show the real-time PCR data of expression of NFATc1 (sx panel), of ctsK (middle panel) and OSCAR (dx panel) on day 21. The treatments are effective in reducing the expression of genes involved in osteoclast maturation compared to the control. Furthermore, the G10 antibody is more effective in inhibiting NFAT-c1 and OSCAR. Data areexpressed as the mean +/- SEM from three independent experiments. The data are normalized for the expression in thecontrol cells (control expression set at 100%). *p < 0.05, **p < 0.01 versus the control.*

3 Improvement of G10 clone affinity

Given the promising data obtained from the G10 clone both in specificity tests and in functionality tests obtained with osteoclasts, the third phase was focused on improving the affinity of the G10 clone through the affinity maturation technique called chain shuffling.

3.1 Affinity maturation of the G10 clone and Antibody library construction

For the affinity improvement of the G10 clone, it was decided to use the chain shuffling technique [149]. The V_H sequence of the G10 clone was kept constant and randomly assembled with a V_L library deriving from the library naive (Fig. 36).

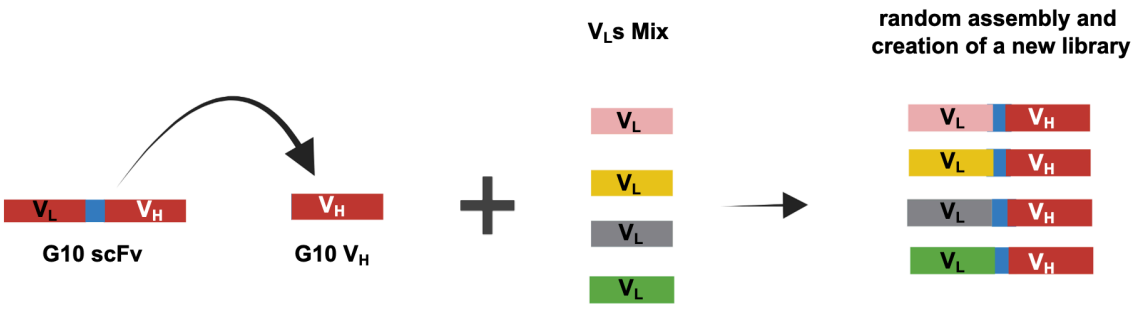

Fig.36 Schematization of the chain shuffle technique.
The heavy chain variable region (V_H) sequence was kept constant and randomly associated with a library of light chain variable regions (V_L) derived from the naïve library. In this way, it is possible to build mini-libraries of the clone G10 to look for variants that give greater affinity.

To do this, the V_H G10 sequence was amplified from the phagemid (pDan5) using specific primers.

A random assembly of the G10 V_H with a V_L library is done through an assembly PCR. The first rounds of this PCR protocol are composed of just annealing and denaturation steps, without adding any primers in the reaction. This step allows the annealing of the linker region through the overlap regions previously created. In this way, mixing the two V regions recreates the linker region that joins the two coding sequences. Once the V_H and V_L are randomly paired, another set of primers is used in order to amplify the entire scFv fragments. The correct success of the PCR reactions was verified by agarose gel

electrophoresis, as shown in Fig. 37 (a-b). The amplification of the V_Ls and the V_H of the G10 fragments have an aspected size of about 450 bp, while the assembly reaction led

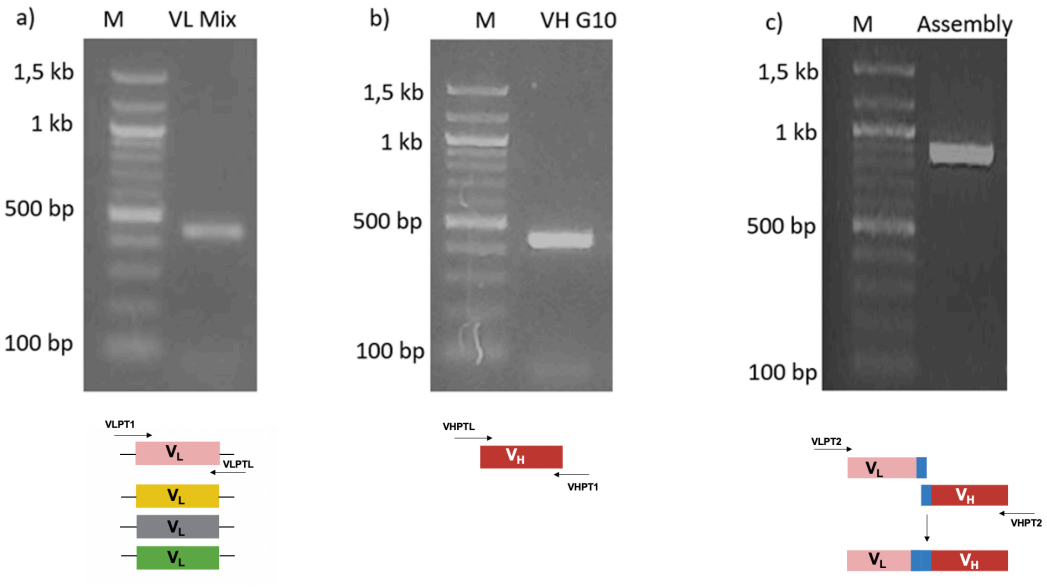

Fig. 37 Figure representing the phases of the chain shuffling technique*. The first step involves amplifying the G10's V_H and V_L mix. V_H amplification was achieved by VHPT1-VHPTL primers while V_Ls were amplified by VLPT2-VLPTL. The results of the amplifications are reported in the figures relating to the electrophoretic gel (a and b). The amplified products show an expected length of about 450 bp. The second phase involves the random assembly between the V_Ls sequences and the V_H of the G10 clone through the overlap region at the linker level. The assembly product is shown in (c). The fragment has an expected size of approximately 900 bp*

to the formation of a fragment of approximately 870 bp (Fig. 37 c) (sum of V_H, V_L, and linker).

Finally, for the construction of the V_L library of the G10 clone, both the phagemid and the PCR fragments resulting from the assembly reaction were digested with the restriction enzymes and the scFvs sequences were then cloned upstream of the G3P coding sequence and finally electroporated into electrocompetent *E. coli* cells (Fig.38). After 9 electroporations, we obtained a library of the size of $3x10^4$ clones. The resulting library is not the size we expected, but it still has a good size for selecting and isolating new clones.

The bacteria resulting from the electroporation were then collected and grown in a liquid medium. Subsequently, the plasmid DNA was extracted to obtain complete information about the scFvs library.

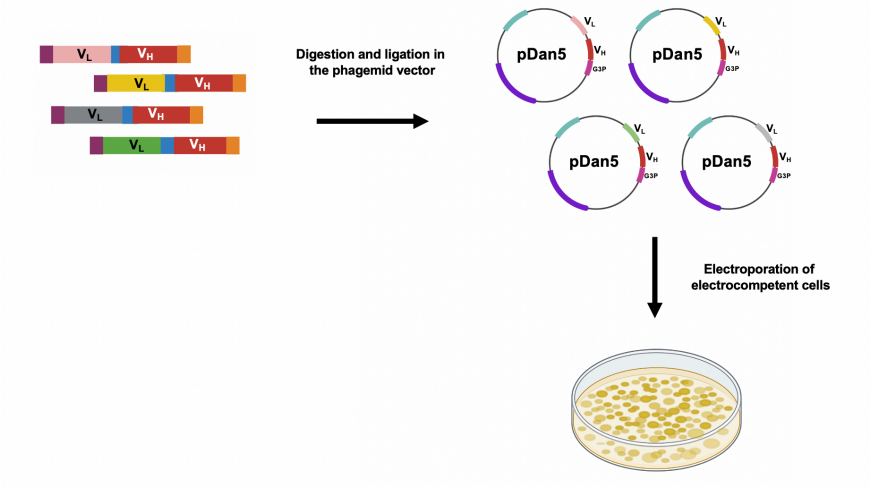

***Fig.38 Schematic representation of the building of the library**. The PCR fragments deriving from the PCR Assembly are digested with the enzymes BssHII and NheI and cloned inside the pDAN5 vector, which is also digested with the same enzymes. The plasmids were then electroporated into electrocompetent E. coli cells. A total of 9 electroporations were performed*

3.2 Transformation of the library into yeast

For the selection and isolation of new clones with increased affinity, we decided to use the yeast display technique.

This technique has characteristics that would allow us to isolate clones with the desired characteristics.

The yeast has a better quality of antibody exposure thanks to the post-transcriptional modification (glycosylation pattern similar to that of mammals), which improves its solubility (and stability). Furthermore, the presence of the endoplasmic reticulum (and molecular chaperones) allows the elimination of antibodies that have unstable sequences but also express complex clones for the prokaryotic system [126].

But above all, with the yeast display, through FACS, it is possible to select clones with greater affinity in real-time.

To switch to the yeast display system, the created mini library has been cloned into a vector (pDNL6) that allows the expression of scFvs as fusion proteins with the AGA2 protein. To do this, the scFvs were amplified, starting from the miniprep of the library, using specific primers (Fig.39).

The primers have bases homologous to those of the primers used to amplify the sequence of scFvs from the phagemid allowing to exploit of gap repair mechanism in

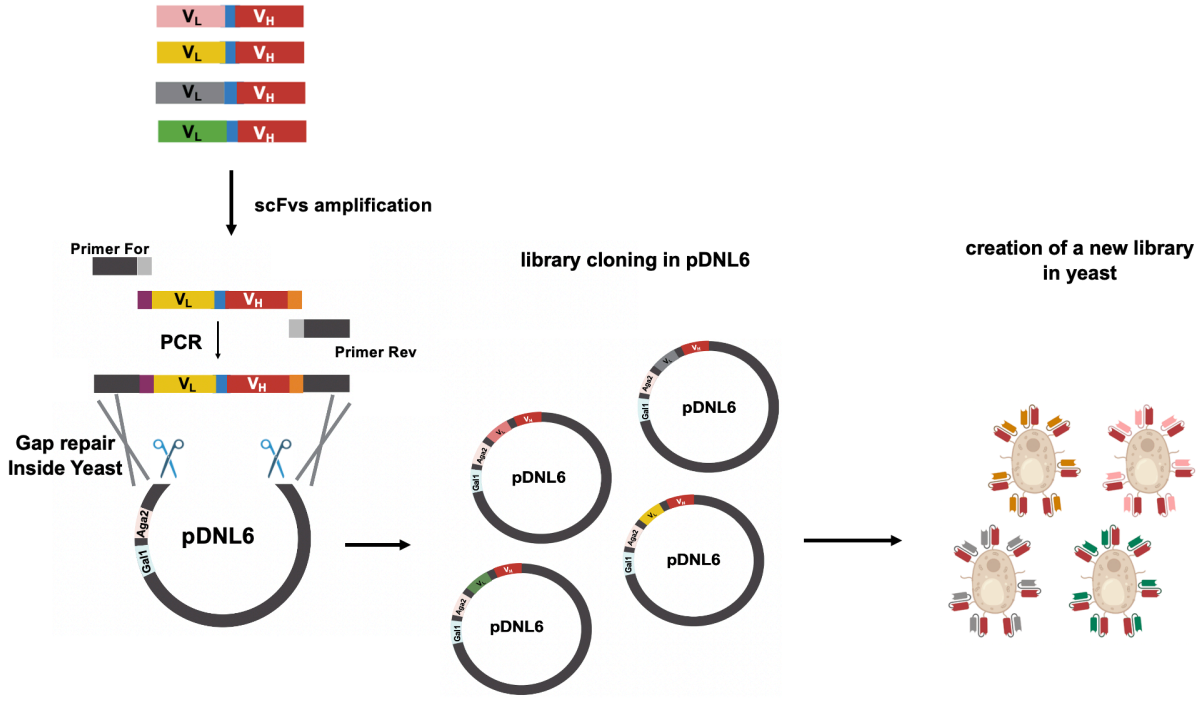

Fig. 39 Schematic representation of the gap repair process. *the genes were amplified using a pair of primers (pDAN_to_pDNL6 3' and pDAN_to_pDNL6 5) showing bases of homology with the vector to its cloning site (black) and regions of homology with the gene itself (grey). The amplified sequences were transformed into S. cerevisiae together with the vector digested with the enzymes BssHII and NehI. After transformation, the recombination process present in the yeast allows the recombination between the amplified gene and the vector. Finally the new created scFvs library is cloned into the pDNL6 vector and transformed into competent chemical yeast cells for library building.*

yeast, avoiding laborious in vitro purification and ligation of DNA [150]. In fact, these primers also have regions homologous to the vector in its cloning site. Thus, the resulting PCR product, composed of the scFvs flanked by the regions homologous to the vector's cloning site, is used for the yeast transformation together with the linearized vector. In this way, the recombination between the amplified fragments and the plasmid will occur in the transformed yeast, leading to the construction of the recombinant vector *in vivo.*

Finally, 500ng of digested vector and 1.5µg of amplified scFvs were added to the chemical yeast cells competent for the transformation process. The library obtained has a size of $5x10^4$ clones, a value comparable to that obtained in the transformation of the library into *E. coli*.

3.3 Analysis of the G10 library

In order to assess the quality of the mini-library, the yeast library was cultured in liquid culture for 48 hours, and subsequently, the expression of the scFvs on the yeast surface was induced. The expression of scFvs was verified by flow cytometry analysis,

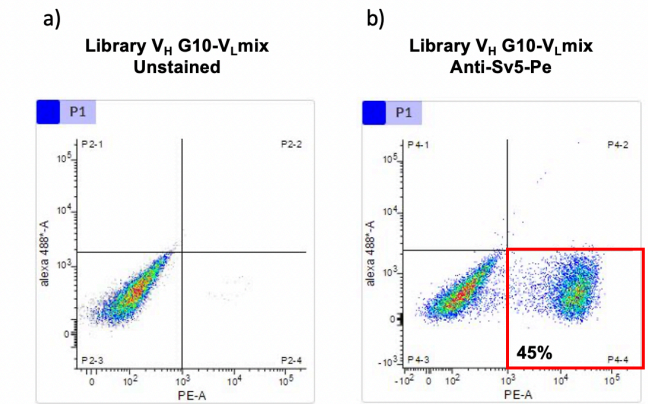

***Fig.40 Analysis of the expression of scFvs on the yeast surface**. a) Unstained library. b) Library incubated with anti SV5-Pe antibodies for expression control. About 45% of the population express the antibody fragment.*

marking with a fluorescent antibody labeled with PE (phycoerythrin) that recognizes the SV5 tag at the C-terminus. It is possible to observe in Fig.40 how the anti-SV5-PE binding is associated with a population shift along the x-axis, which represents the population expressing scFv, compared to the unmarked population. It can be observed that the percentage of positive cells for anti-SV5-PE is about 45%; this result confirms how yeast is an excellent tool for eliminating clones that have an unstable sequence and that do not reach the correct folding.

Furthermore, this provided us with information on the good construction of the library; in fact, almost 50% of the population expresses the scFv on the surface.

Once the expression was verified, the ability of the library to bind the antigen was evaluated. For this test, ICOSL-biotinylated, at different concentrations (1, 10, and 50 nM), was used to test the entire library's affinity level. The choice of these concentrations is based on the k_D of clone G10 (87nM) calculated by BLI. Since we aim to isolate clones with higher affinity, we decided to test lower antigen concentrations. Thus, a second label with Streptavidin-Alexa Fluor 488 was performed to observe the binding of the library with the biotinylated antigen. A greater amount of bound antigen is associated with an increase in the fluorescence signal along the y-axis (Fig. 41). The

upper right quadrant shows those clones showing double fluorescence signals (scFv expression and antigen binding). By observing this quadrant, it can be seen that at different antigen concentrations, there are different percentages of positive cells (Fig.41). At 1 nM of ICOSL-Bio, only 0,5% of the population recognize the antigen, at 10

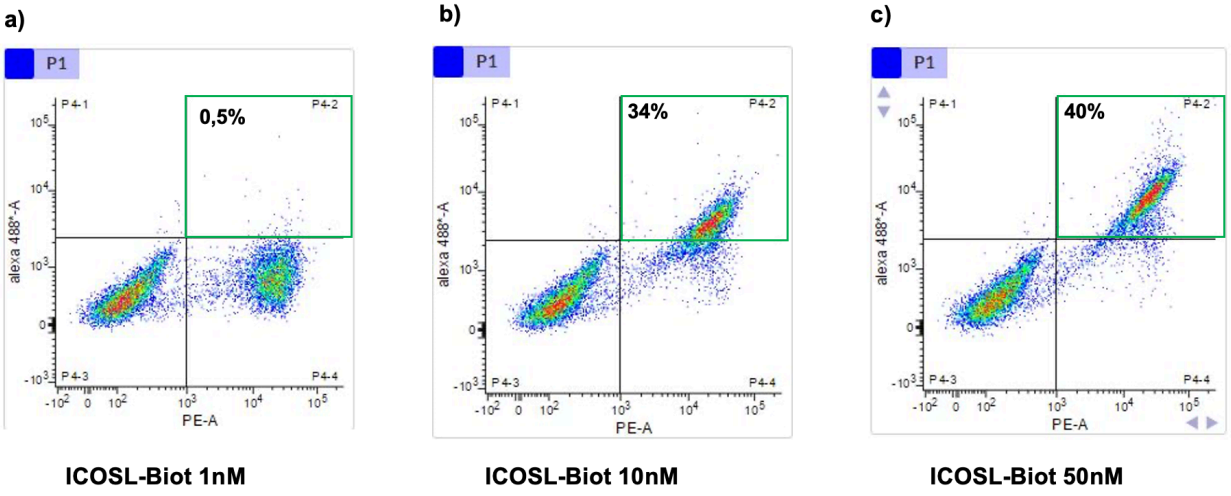

***Fig.41 Evaluation of the binding capacity of the antigen**. a) Library incubated with 1nM of ICOSL-biot. b) Library incubated with 10nM of antigen. c) library incubated with 50 nM of antigen. Anti-Sv5-Pe and streptavidin-alexa fluor 488 antibodies were used for staining. As it is possible to see as the antigen concentration increases, the percentage of the population that binds the antigen increases*

nM 34%, and at 50 nM 40% (almost the totality of the population that expresses the scFv). Although these two last populations have a similar positive population percentage, the mean fluorescence intensity is greater in the population incubated with the highest antigen concentration. The population appears, in fact, to be more shifted upwards in the quadrant, indicating only a greater quantity of antigen bound to single yeast cells due to the increased concentration of the antigen.

3.4 Selection of affinity maturated clones through cell sorting

Once the ability of the mini-library to bind the antigen was tested, it was decided to carry out a selection cycle using FACS. It was decided to choose the population incubated with 10nM of biotinylated antigen; at the 1nM antigen concentration, even if the positive clones probably have a higher affinity, the population is too close to the negative population, and there may be a risk of isolating false positives.

Furthermore, at the concentration of 50nM, we have no more information than at the concentration of 10nM.

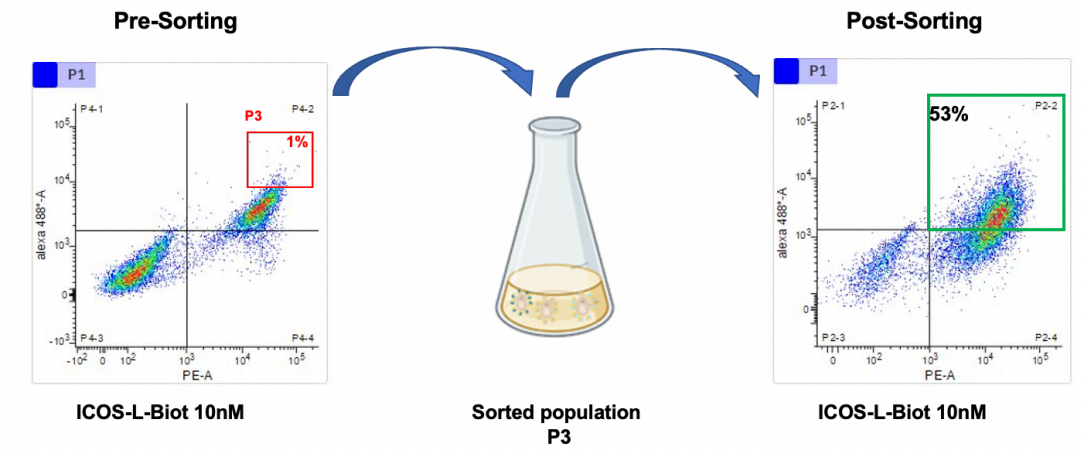

***Fig. 42 Schematization of the sorting process**. The yeast population incubated with 10 nM of ICOSL biot was used for the sorting process. The sorting gate has been opened in the upper part of the double positive population (red box). Specifically, 20,000 events were sorted by 1% of the population. After sorting, the population was evaluated for its binding capacity. it is possible to observe an enrichment of the double positive population quantity, compared to the pre-sorting*

Then, a specific population was sorted from the ICOSL-biot 10nM incubated library. In detail, 20,000 events (cells), corresponding to 1% of the population, were sorted from the highest portion of the double positive population (P3) (Fig.42). The gate (red squared in Fig.38) has been positioned at the top of the graph, as the clones with the greatest affinity are usually placed there. Basically, the greater the fluorescence, the greater the bound antigen. Finally, the P3 population was grown in culture and re-analyzed for expression level and antigen binding. As can be seen from Fig.42, there was an enrichment of the double positive population (53,8%) compared to the starting situation (40%), confirming the correct success of the sorting process.

3.5 Isolation and characterization of new anti-ICOSL clones.

Once the functionality of the sorted population was verified, the individual clones were isolated. To do this, the P3 population was diluted and grown at 30 ° C for 48 hours.
To carry out an initial screening, a total of 25 colonies were used for screening (Fig.43) and analyzed for diversity through the fingerprint technique. In particular, using a high cutoff frequency restriction enzyme, it was possible to observe different digestion

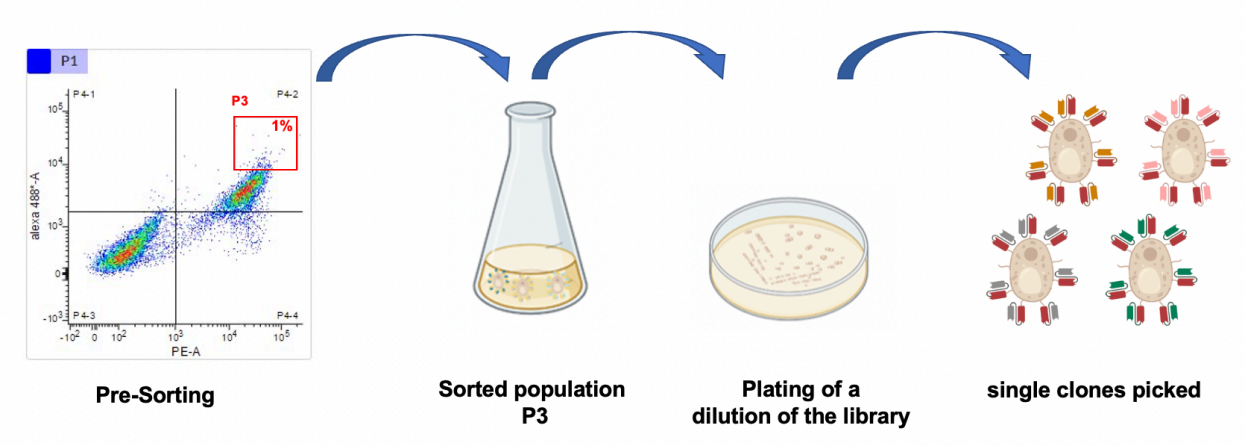

***Fig. 43 schematic representation of the isolation process of single anti-ICOSL clones**. A dilution of the P3 population was plated on a solid medium to obtain single colonies. 25 clones were selected and cultured for subsequent analysis*

patterns based on the nucleotide sequence of the individual clones. Therefore, the sequences of the scFvs were amplified (Fig. 44 a) and digested with the enzyme BstnI. As expected, some of the patterns were the same due to the enrichment of a small population during the sorting process. The general diversity has been summarized in Fig. 44 (b). It can be seen that although part of the sequence is the same in all clones

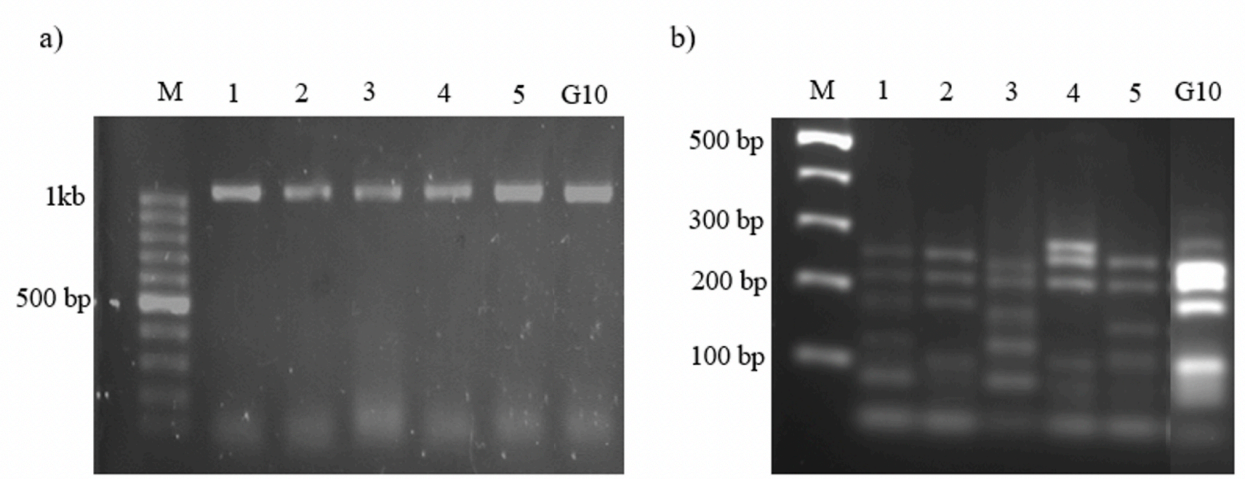

***Fig.44** a) amplification of the scFv sequence with pDNL6 For / Rev primers. b) Electrophoretic gel summarizing the diversity of anti ICOSL clones. Among the 25 clones only 6 showed different digestion patterns*

(V_H G10), the patterns are visibly different from each other. Five clones with different patterns were identified, while the clones with identical fingerprints were discarded.

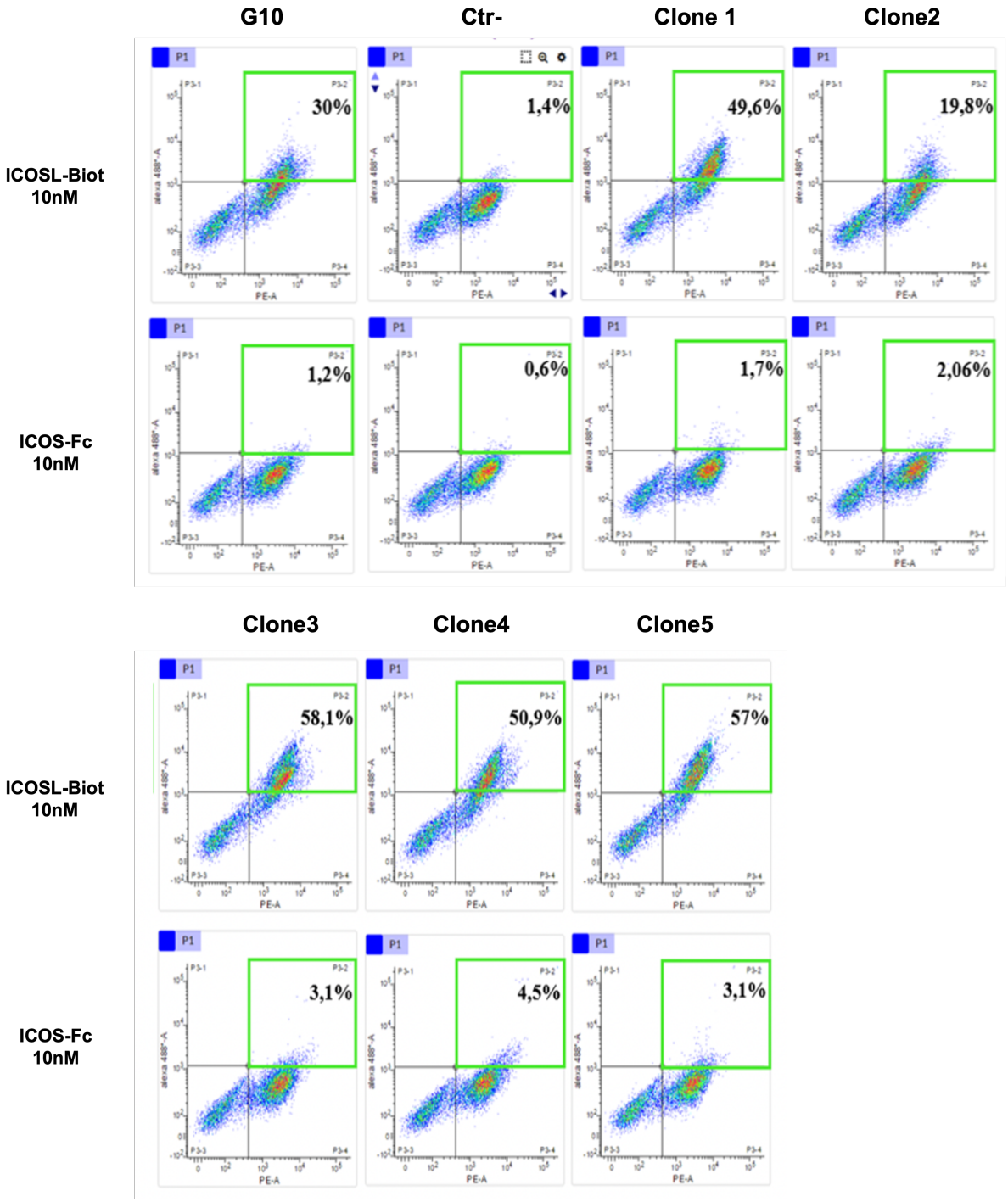

***Fig. 45 Analysis of the functionality of single anti-ICOSL clones**. Individual clones were incubated with 20nM of ICOSL biot antigen and ICOS-Fc non-related antigen and tested for their specificity. All samples were treated with two secondary antibodies: anti-Sv5-Pe (for scFvs expression) and streptavidin Alexa fluor 488 (for binding to the antigen). An unrelated antibody was used as a negative control. All six clones show a binding capacity to ICOSL-biot and not to ICOS. all, except clone 2, have a higher percentage of the population than the parental clone*

Given this, a flow cytometric analysis was performed to evaluate the binding specificity of the five clones compared to the parental G10 clone. These clones were incubated with ICOSL-Fc and ICOS-Fc at 10nM (Fig. 45). A clone presenting an unrelated scFv (Ctr-) was used as a negative control.
From the flow cytometric analysis, it was possible to observe that all the isolated clones are able to recognize and bind ICOSL-Fc but do not recognize ICOS-Fc (Fig.45). Watching the graphs, it is possible to observe how most of the clones, except clone 2, seem to have a greater positivity towards ICOSL-Fc than G10 clone. This may be caused both by a greater affinity of the new clones or by greater stability that determines a better expression on the yeast surface.

3.6 Affinity evaluation by yeast display

Once the effective binding capacity of the selected clones had been established, it was decided as a preliminary investigation to evaluate differences in affinity with respect to the parental clone G10. To do this, each clone was incubated with different concentrations of ICOSL-biotinylated (0, 10, 40, and 80 nM), and the binding capacity was evaluated by calculating the MFI (mean fluorescent intensity) of the positive population.
As shown in Fig.46, all clones show an increase in the population in the fourth quadrant as the concentration of the antigen increases. It is interesting to note that at the concentration of 10 nM, almost all clones have an almost identical positive population; only clone 5 already shows substantial differences; in fact, almost all of the sv5 positive population binds the antigen at a concentration of 10 nM. At the highest concentration tested (80nM), the new 3,4,5 clones would appear to have a more positive population than the parental clone G10. Only clone 1 has similar behavior to clone G10. These preliminary results, therefore, show a different behavior between the different clones. The result is that clone 3,4,5 may have a higher affinity than clone G10, while clone 1 may have a similar or slightly better binding affinity.
These results are an estimate of the affinity of the various clones, which will subsequently be investigated by BLI.

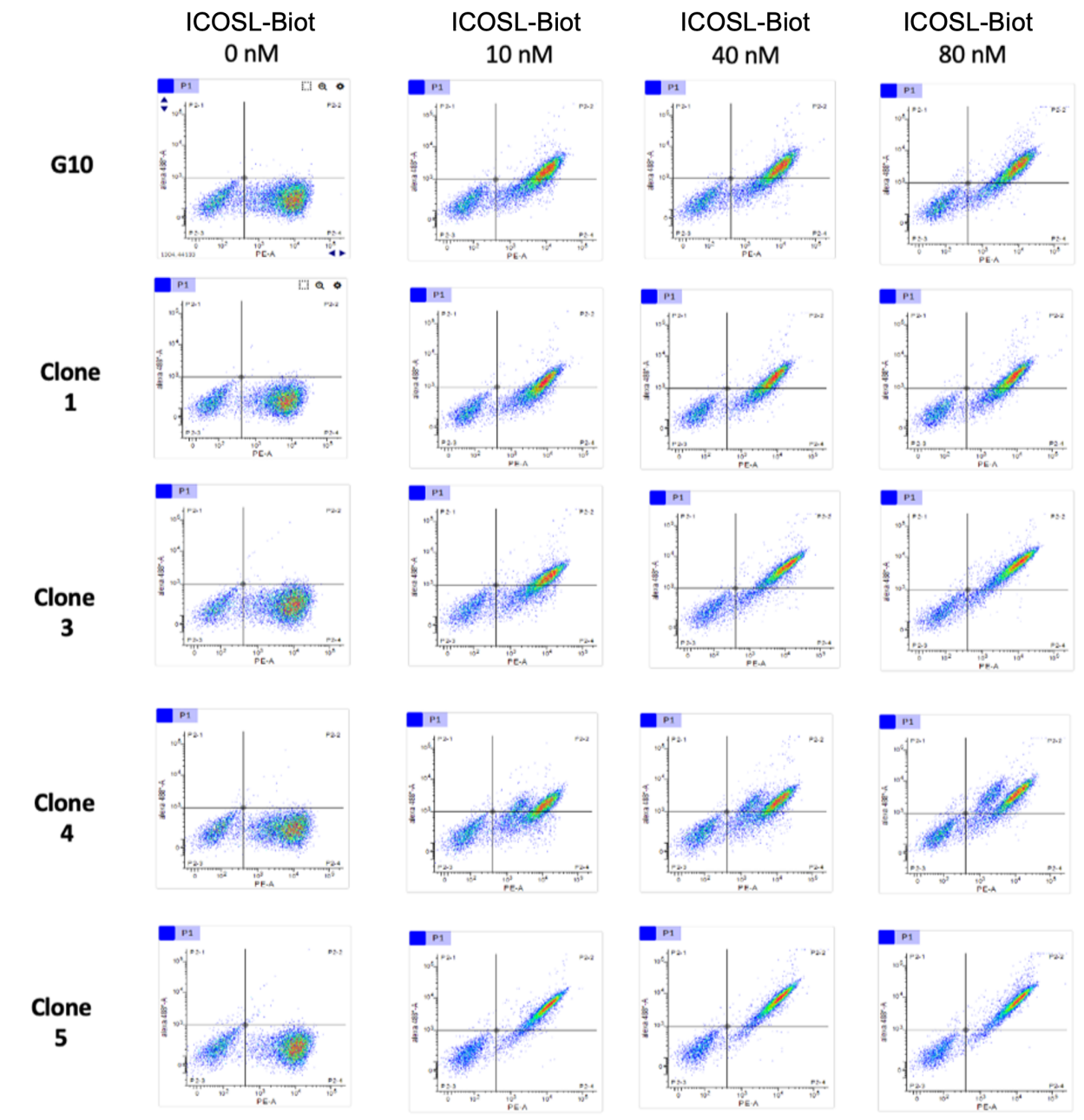

***Fig.46 Affinity evaluation of the selected clones**. Individual clones were incubated with 0, 10, 40, and 80 nM of ICOSL biot antigen. All samples were treated with two secondary antibodies: anti-Sv5-Pe (for scFvs expression) and streptavidin Alexa fluor 488 (for binding to the antigen). Clones 3,4,5 show a higher positive population than clone G10, while clone 1 shows a similar behavior*

3.7 Production of the new clones as scFv-Fc

To compare the affinity of the new clones with that of the parental clone G10, the new clones were produced as scFv-Fc. The scFvs were cloned into a vector presenting the human IgG C_H2-C_H3 sequence. Once cloning was done, the antibody fragment was

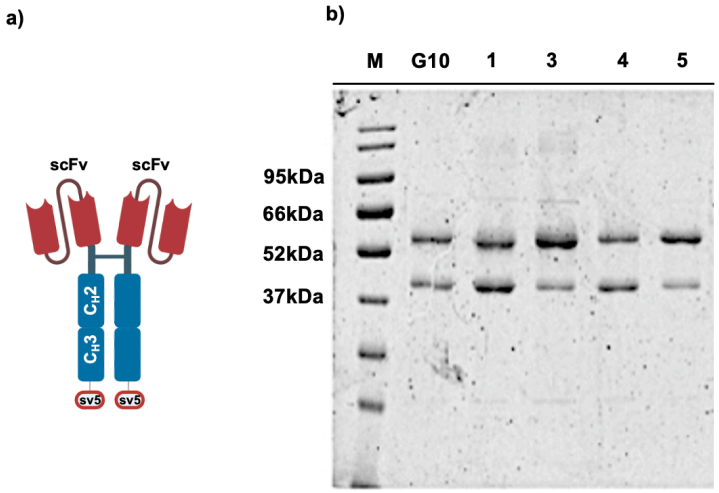

Fig.47 *a) Schematic representation of the scFv-Fc molecule. b) SDS-PAGE of the protein A purified of the clone 1, 3, 4,5, and G10. 2 µl of the purified scFv-Fc were loaded on gel and run in reducing conditions.*

produced through ExpyCHO, a commercial cell line optimized to ensure high production yields. The high titer protocol was used, and scFv-Fc production was evaluated eight days post-transfection. Subsequently, the scFv-Fc has been protein A purified and quantified by densitometry. As can be seen from the SDS page (Fig. 47), all antibodies were produced. As it is possible to see from Fig. 46, clones 5 and 3 were produced better than the others because they are probably more stable than the parental clone. The band corresponding to the loss of a variable region is less intense than the other clones. In contrast, clones 1 and 4 have higher antibody degradation than the intact antibody. For the quantification of the antibodies and for the future test, only the full-length portion of the antibody was considered.

3.8 k_D calculation: comparison between G10 and new clones

Once the effective ability to bind the antigen in solution in a specific way was established, the new clones were subjected to an affinity test. To prove that the affinity maturation process, through the chain shuffling technique, has worked, the affinities of the new clones must be better than the parental clone.

Even in this case, the OCTET® N1 instrument was used to calculate the affinity. In particular, a streptavidin functionalized biosensor was used to fix the biotinylated antigen. ICOSL-biot was loaded onto the tip at a concentration of 10 µg/mL, and then different concentrations of antibodies were added. Each antibody was used at 4 different concentrations: 0, 25, 50, 100, and 200 nM. Figure 48 (a) shows the graphs related to the calculation of the k_D of the single clones. While figure 48 (b) shows a

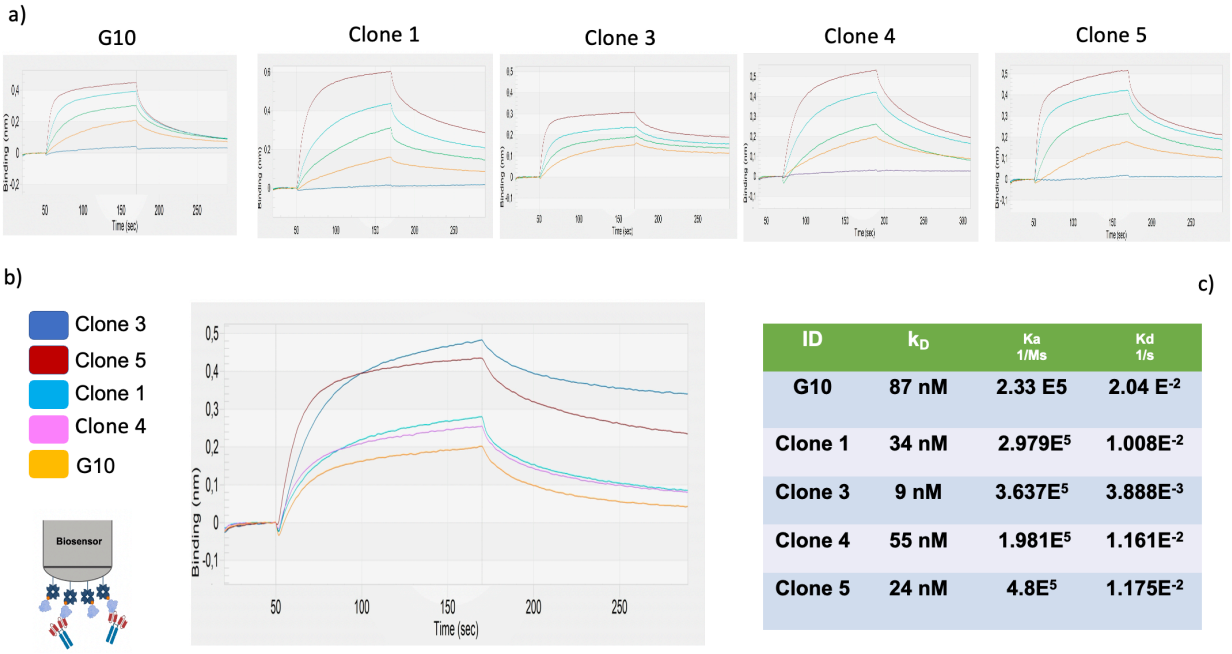

ID	k_D	Ka 1/Ms	Kd 1/s
G10	87 nM	2.33 E5	2.04 E^{-2}
Clone 1	34 nM	2.979E^{5}	1.008E^{-2}
Clone 3	9 nM	3.637E^{5}	3.888E^{-3}
Clone 4	55 nM	1.981E^{5}	1.161E^{-2}
Clone 5	24 nM	4.8E^{5}	1.175E^{-2}

Fig. 48 Calculation of the dissociation constant. *a)The streptavidin functionalized biosensor was loaded with ICOSL-biotinylated at a concentration of 10µg/mL. The scFv-Fcs were subsequently added at different concentrations: 0,25,50,100,200 nM (The program used is shown in Tab 3 in the materials and methods section). The graph was obtained using the OCTET® N1 software. b) summary graph of the kD of the different clones. The streptavidin functionalized biosensor was loaded with ICOSL-biot at a concentration of 10µg/mLand then antibodies at a concentration of 100nM were added. c) Table reassuming KD, Ka and Kd values.*

summary graph of all the clones. This allows us to appreciate the difference in affinity between the individual clones visually.

Observing the table (Fig.48c), it is possible to observe differences in the values of association and dissociation between the different clones. In fact, it is possible to note how clones 3 and 5 present the highest association values (indicating that they associate more rapidly with the antigen in the unit of time), while clones 4 and 1 present even lower values than clone G10 despite having a better K_D. The values of Kd, on the other hand, are different. In fact, clones 1 and 4 show lower values than clone G10, demonstrating a slower dissociation of the antigen and a higher affinity. Finally, clone 3 has the lowest kd value, while clone 5 has a value comparable to clones 1 and 4.

Finally, all the new clones show an improved k_D compared to the G10 (orange line in Fig. 48 b), indicating success in the affinity maturation process.

Notably, clone 3 has an affinity value approximately ten times higher than the parental G10 clone.

Conclusion

This work aimed to isolate, through in vitro display technology, antibodies able to replace the recombinant molecule ICOS-Fc in the treatment of osteoporosis. The first step was the selection of a naïve antibody phage library, previously built in our laboratory. The selection strategy was based on immobilizing the ICOSL-Fc antigen (provided by NOVAICOS srls) on a solid support. The selection process allowed the isolation of a single clone, G10, specific for ICOSL.

To further study the potential of this antibody fragment, the scFv sequence was cloned into pcDNA 3.1 (+) to obtain the scFv-Fc antibody format. Functionality and specificity were tested on ELISA assays with different ICOSL forms. From this test, the G10 clone demonstrated its ability to bind ICOSL. Interestingly, the absence of a signal indicated that the binding is highly dependent on glycosylation and the folding of the molecule.

A crucial part of the work was also to understand whether the G10 antibody was able to recognize ICOSL in its native conformation. To understand this, a cytofluorimetric analysis was performed on different ICOSL+ cell types. The results confirmed the good potential of this antibody, albeit with different percentages of positivity, the G10 clone is able to recognize ICOSL on the surface.

Finally, the capability of the G10 clone to inhibit osteoclastogenesis was performed.

The G10 antibody was compared in its functional activity with the ICOS-Fc molecule, which was found to be an effective treatment in previous studies [32]. In the osteoclastogenesis assay, clone G10 was found to have comparable capabilities to ICOS-Fc in decreasing osteoclast maturation. Furthermore, through an assay aimed at quantifying the TRAP enzyme inside osteoclasts, it was confirmed that clone G10 is able to inhibit osteoclast maturation. In fact, the amount of TRAP protein inside the osteoclasts was similar between the two treatments (clone G10 and ICOS-Fc) and lower than in the untreated sample. Furthermore, by staining the cells for the TRAP protein, it was again possible to observe a decrease in giant cells, with an increase in spindle cells, in the treated samples.

These results were also confirmed by analyzing the expression of some genes involved in the osteoclast maturation process. In particular, the genes analyzed are NFATc1, OSCAR, and STAMP. Interestingly, in all three genes analyzed, osteoclasts treated with ICOS-Fc and clone G10 showed lower gene expression levels than untreated ones.

Furthermore, the G10 antibody had a better ability to inhibit the NFATc1 and OSCAR genes than the ICOS-Fc molecule.

In light of these promising results, it was decided to improve the affinity of this clone through the chain shuffling technique.

To do this, the V_H sequence of clone G10 was randomly shuffled with a library of V_Ls from the naïve antibody library. This has led to the formation of a mini-library of $3x10^4$ clones. For the selection of new antibodies with greater affinity, it was decided to use the yeast display technique. This allowed us to exploit real-time sorting through the FACS technique. Once the library was validated, the selection process envisaged a sorting phase of 20,000 yeast cells presenting binding capacity against ICOSL. From this process, it was possible to isolate four different anti-ICOSL antibodies able to bind ICOSL. To further characterize them and to understand the success of the affinity maturation technique, the new clones were produced as scFv-Fc and subsequently calculated their affinity (K_D). In this work, the calculation of the K_D was performed by the Biolayer Interferometry technique. From the data analysis, it was possible to confirm the correct functioning of the chain shuffling technique; in fact, all new clones have better affinity if compared with the G10 parental clone.

The anti-ICOSL G10 clone proved to be a great candidate for our purposes. Indeed, these tests revealed its potential as a possible substitute for the recombinant molecule ICOS-FC in inhibiting osteoclast maturation and function and in the possible future treatment of osteoporosis.

In light of this, further functional characterizations will be needed. Among these, there is certainly the possibility of testing the molecule in a mouse model of osteoporosis in order to evaluate its ability to inhibit the disease and its toxicity.

Furthermore, it would be interesting to test the new clones, which have a better affinity than the parent clone, in functionality tests. In particular, it would be useful to understand whether or not an increase in affinity could give better functional effects than the starting clone G10 in the inhibition of osteoclast maturation and functionality

Bibliography

1. Sattler, S., The Role of the Immune System Beyond the Fight Against Infection. Adv Exp Med Biol, 2017. **1003**: p. 3-14.10.1007/978-3-319-57613-8_1

2. Manna, P.R., Z.C. Gray, and P.H. Reddy, Healthy Immunity on Preventive Medicine for Combating COVID-19. Nutrients, 2022. **14**(5).10.3390/nu14051004

3. Murphy, K.M., *Janeway's Immunobiology.* Garland Publishing, 2012

4. Turvey, S.E. and D.H. Broide, *Innate immunity.* J Allergy Clin Immunol, 2010. **125**(2 Suppl 2): p. S24-32.10.1016/j.jaci.2009.07.016

5. Bonilla, F.A. and H.C. Oettgen, *Adaptive immunity.* J Allergy Clin Immunol, 2010. **125**(2 Suppl 2): p. S33-40.10.1016/j.jaci.2009.09.017

6. Yatim, K.M. and F.G. Lakkis, A brief journey through the immune system. Clin J Am Soc Nephrol, 2015. **10**(7): p. 1274-81.10.2215/CJN.10031014

7. Bretscher, P.A., A two-step, two-signal model for the primary activation of precursor helper T cells. Proc Natl Acad Sci U S A, 1999. **96**(1): p. 185-90.10.1073/pnas.96.1.185

8. Sharpe, A.H. and G.J. Freeman, *The B7-CD28 superfamily.* Nat Rev Immunol, 2002. **2**(2): p. 116-26.10.1038/nri727

9. Greenwald, R.J., G.J. Freeman, and A.H. Sharpe, *The B7 family revisited.* Annu Rev Immunol, 2005. **23**: p. 515-48.10.1146/annurev.immunol.23.021704.115611

10. Parkin, J. and B. Cohen, *An overview of the immune system.* The Lancet, 2001. **357**(9270): p. 1777-1789.10.1016/s0140-6736(00)04904-7

11. Chattopadhyay, K., et al., Structural basis of inducible costimulator ligand costimulatory function: determination of the cell surface oligomeric state and functional mapping of the receptor binding site of the protein. J Immunol, 2006. **177**(6): p. 3920-9.10.4049/jimmunol.177.6.3920

12. Rujas, E., et al., Structural characterization of the ICOS/ICOS-L immune complex reveals high molecular mimicry by therapeutic antibodies. Nat Commun, 2020. **11**(1): p. 5066.10.1038/s41467-020-18828-4

13. Amatore, F., L. Gorvel, and D. Olive, Inducible Co-Stimulator (ICOS) as a potential therapeutic target for anti-cancer therapy. Expert Opin Ther Targets, 2018. **22**(4): p. 343-351.10.1080/14728222.2018.1444753

14. Hutloff A, D.A., Beier KC, et al, ICOS is an inducible T-cell co-stimulator structurally and functionally related to CD28. Nature, 1999

15. Yao, S., et al., B7-h2 is a costimulatory ligand for CD28 in human. Immunity, 2011. **34**(5): p. 729-40.10.1016/j.immuni.2011.03.014

16. Raineri, D., et al., Osteopontin binds ICOSL promoting tumor metastasis. Commun Biol, 2020. **3**(1): p. 615.10.1038/s42003-020-01333-1

17. Mages, H.W., et al., Molecular cloning and characterization of murine ICOS and identification of B7h as ICOS ligand. Eur J Immunol, 2000. **30**(4): p. 1040-7.10.1002/(SICI)1521-4141(200004)30:4<1040::AID-IMMU1040>3.0.CO;2-6

18. Occhipinti, S., et al., Triggering of B7h by the ICOS modulates maturation and migration of monocyte-derived dendritic cells. J Immunol, 2013. **190**(3): p. 1125-34.10.4049/jimmunol.1201816

19. Tang, G., et al., Reverse signaling using an inducible costimulator to enhance immunogenic function of dendritic cells. Cell Mol Life Sci, 2009. **66**(18): p. 3067-80.10.1007/s00018-009-0090-7

20. Dianzani, C., et al., B7h triggering inhibits umbilical vascular endothelial cell adhesiveness to tumor cell lines and polymorphonuclear cells. J Immunol, 2010. **185**(7): p. 3970-9.10.4049/jimmunol.0903269

21. Dianzani, C., et al., B7h triggering inhibits the migration of tumor cell lines. J Immunol, 2014. **192**(10): p. 4921-31.10.4049/jimmunol.1300587

22. Stoppa, I., et al., ICOSL Stimulation by ICOS-Fc Accelerates Cutaneous Wound Healing In Vivo. Int J Mol Sci, 2022. **23**(13).10.3390/ijms23137363

23. Hedl, M., et al., Pattern recognition receptor signaling in human dendritic cells is enhanced by ICOS ligand and modulated by the Crohn's disease ICOSLG risk allele. Immunity, 2014. **40**(5): p. 734-46.10.1016/j.immuni.2014.04.011

24. Strauss, L., et al., Expression of ICOS on human melanoma-infiltrating CD4+CD25highFoxp3+ T regulatory cells: implications and impact on tumor-mediated immune suppression. J Immunol, 2008. **180**(5): p. 2967-80.10.4049/jimmunol.180.5.2967

25. Martin-Orozco, N., et al., Melanoma cells express ICOS ligand to promote the activation and expansion of T-regulatory cells. Cancer Res, 2010. **70**(23): p. 9581-90.10.1158/0008-5472.CAN-10-1379

26. Giraldo, N.A., et al., Tumor-Infiltrating and Peripheral Blood T-cell Immunophenotypes Predict Early Relapse in Localized Clear Cell Renal Cell

Carcinoma. Clin Cancer Res, 2017. **23**(15): p. 4416-4428.10.1158/1078-0432.CCR-16-2848

27. Nagase, H., et al., ICOS(+) Foxp3(+) TILs in gastric cancer are prognostic markers and effector regulatory T cells associated with Helicobacter pylori. Int J Cancer, 2017. **140**(3): p. 686-695.10.1002/ijc.30475

28. Faget, J., et al., ICOS-ligand expression on plasmacytoid dendritic cells supports breast cancer progression by promoting the accumulation of immunosuppressive CD4+ T cells. Cancer Res, 2012. **72**(23): p. 6130-41.10.1158/0008-5472.CAN-12-2409

29. Le, K.S., et al., Follicular B Lymphomas Generate Regulatory T Cells via the ICOS/ICOSL Pathway and Are Susceptible to Treatment by Anti-ICOS/ICOSL Therapy. Cancer Res, 2016. **76**(16): p. 4648-60.10.1158/0008-5472.CAN-15-0589

30. Nicholson, S.M., et al., Effects of ICOS+ T cell depletion via afucosylated monoclonal antibody MEDI-570 on pregnant cynomolgus monkeys and the developing offspring. Reprod Toxicol, 2017. **74**: p. 116-133.10.1016/j.reprotox.2017.08.018

31. Fan, X., et al., Engagement of the ICOS pathway markedly enhances efficacy of CTLA-4 blockade in cancer immunotherapy. J Exp Med, 2014. **211**(4): p. 715-25.10.1084/jem.20130590

32. Gigliotti, C.L., et al., ICOS-Ligand Triggering Impairs Osteoclast Differentiation and Function In Vitro and In Vivo. J Immunol, 2016. **197**(10): p. 3905-3916.10.4049/jimmunol.1600424

33. Robling, A.G., A.B. Castillo, and C.H. Turner, Biomechanical and molecular regulation of bone remodeling. Annu Rev Biomed Eng, 2006. **8**: p. 455-98.10.1146/annurev.bioeng.8.061505.095721

34. Datta, H.K., et al., *The cell biology of bone metabolism.* J Clin Pathol, 2008. **61**(5): p. 577-87.10.1136/jcp.2007.048868

35. Mohamed, A.M., AN OVERVIEW OF BONE CELLS AND THEIR REGULATING FACTORS OF DIFFERENTIATION. 2007

36. Capulli, M., R. Paone, and N. Rucci, Osteoblast and osteocyte: games without frontiers. Arch Biochem Biophys, 2014. **561**: p. 3-12.10.1016/j.abb.2014.05.003

37. Florencio-Silva, R., et al., Biology of Bone Tissue: Structure, Function, and Factors That Influence Bone Cells. Biomed Res Int, 2015. **2015**: p. 421746.10.1155/2015/421746

38. Boivin, G., et al., The role of mineralization and organic matrix in the microhardness of bone tissue from controls and osteoporotic patients. Bone, 2008. **43**(3): p. 532-8.10.1016/j.bone.2008.05.024

39. Andersen, T.L., et al., A physical mechanism for coupling bone resorption and formation in adult human bone. Am J Pathol, 2009. **174**(1): p. 239-47.10.2353/ajpath.2009.080627

40. Franz-Odendaal, T.A., B.K. Hall, and P.E. Witten, *Buried alive: how osteoblasts become osteocytes.* Dev Dyn, 2006. **235**(1): p. 176-90.10.1002/dvdy.20603

41. Bonewald, L.F., Osteocytes as dynamic multifunctional cells. Ann N Y Acad Sci, 2007. **1116**: p. 281-90.10.1196/annals.1402.018

42. Kim, K., et al., NFATc1 induces osteoclast fusion via up-regulation of Atp6v0d2 and the dendritic cell-specific transmembrane protein (DC-STAMP). Mol Endocrinol, 2008. **22**(1): p. 176-85.10.1210/me.2007-0237

43. Yavropoulou, M.P. and J.G. Yovos, Osteoclastogenesis--current knowledge and future perspectives. J Musculoskelet Neuronal Interact, 2008. **8**(3): p. 204-16

44. Sodek, J. and M.D. McKee, Molecular and cellular biology of alveolar bone. Periodontol 2000, 2000. **24**: p. 99-126.10.1034/j.1600-0757.2000.2240106.x

45. Miyamoto, T., The dendritic cell-specific transmembrane protein DC-STAMP is essential for osteoclast fusion and osteoclast bone-resorbing activity. Mod Rheumatol, 2006. **16**(6): p. 341-2.10.1007/s10165-006-0524-0

46. Phan, T.C., J. Xu, and M.H. Zheng, Interaction between osteoblast and osteoclast: impact in bone disease. Histol Histopathol, 2004. **19**(4): p. 1325-44.10.14670/HH-19.1325

47. Genant, H.K., et al., Interim report and recommendations of the World Health Organization Task-Force for Osteoporosis. Osteoporos Int, 1999. **10**(4): p. 259-64.10.1007/s001980050224

48. Noh, J.Y., Y. Yang, and H. Jung, Molecular Mechanisms and Emerging Therapeutics for Osteoporosis. Int J Mol Sci, 2020. **21**(20).10.3390/ijms21207623

49. Rashki Kemmak, A., et al., Economic burden of osteoporosis in the world: A systematic review. Med J Islam Repub Iran, 2020. **34**: p. 154.10.34171/mjiri.34.154

50. Zhou, J., et al., Comparative efficacy of bisphosphonates in short-term fracture prevention for primary osteoporosis: a systematic review with network meta-analyses. Osteoporos Int, 2016. **27**(11): p. 3289-3300.10.1007/s00198-016-3654-z

51. Zhou, J., et al., Comparative Efficacy of Bisphosphonates to Prevent Fracture in Men with Osteoporosis: A Systematic Review with Network Meta-Analyses. Rheumatol Ther, 2016. **3**(1): p. 117-128.10.1007/s40744-016-0030-6

52. Hoppe, E., et al., Osteomalacia in a patient with Paget's bone disease treated with long-term etidronate. Morphologie, 2012. **96**(313): p. 40-3.10.1016/j.morpho.2012.08.001

53. Stains, J.P., et al., Molecular mechanisms of osteoblast/osteocyte regulation by connexin43. Calcif Tissue Int, 2014. **94**(1): p. 55-67.10.1007/s00223-013-9742-6

54. von Keyserlingk, C., et al., Clinical efficacy and safety of denosumab in postmenopausal women with low bone mineral density and osteoporosis: a meta-analysis. Semin Arthritis Rheum, 2011. **41**(2): p. 178-86.10.1016/j.semarthrit.2011.03.005

55. Walsh, M.C. and Y. Choi, Biology of the RANKL-RANK-OPG System in Immunity, Bone, and Beyond. Front Immunol, 2014. **5**: p. 511.10.3389/fimmu.2014.00511

56. Nakamura, T., et al., Estrogen prevents bone loss via estrogen receptor alpha and induction of Fas ligand in osteoclasts. Cell, 2007. **130**(5): p. 811-23.10.1016/j.cell.2007.07.025

57. Ettinger, B., et al., Reduction of vertebral fracture risk in postmenopausal women with osteoporosis treated with raloxifene: results from a 3-year randomized clinical trial. Multiple Outcomes of Raloxifene Evaluation (MORE) Investigators. JAMA, 1999. **282**(7): p. 637-45.10.1001/jama.282.7.637

58. Isaia, P.D.A.G.C., The use of raloxifene in osteoporosis treatment.pdf. 2013

59. Fiorilli, S., et al., Sr-Containing Mesoporous Bioactive Glasses Bio-Functionalized with Recombinant ICOS-Fc: An In Vitro Study. Nanomaterials (Basel), 2021. **11**(2).10.3390/nano11020321

60. Ma, H. and R. O'Kennedy, The Structure of Natural and Recombinant Antibodies. Methods Mol Biol, 2015. **1348**: p. 7-11.10.1007/978-1-4939-2999-3_2

61. Schroeder, H.W., Jr. and L. Cavacini, *Structure and function of immunoglobulins.* J Allergy Clin Immunol, 2010. **125**(2 Suppl 2): p. S41-52.10.1016/j.jaci.2009.09.046

62. Brezski, R.J. and G. Georgiou, Immunoglobulin isotype knowledge and application to Fc engineering. Curr Opin Immunol, 2016. **40**: p. 62-9.10.1016/j.coi.2016.03.002

63. Kapingidza, A.B., K. Kowal, and M. Chruszcz, *Antigen-Antibody Complexes.* Subcell Biochem, 2020. **94**: p. 465-497.10.1007/978-3-030-41769-7_19

64. Rothlisberger, D., A. Honegger, and A. Pluckthun, Domain interactions in the Fab fragment: a comparative evaluation of the single-chain Fv and Fab format engineered with variable domains of different stability. J Mol Biol, 2005. **347**(4): p. 773-89.10.1016/j.jmb.2005.01.053

65. Mondon, P., et al., Human antibody libraries: a race to engineer and explore a larger diversity. Front Biosci, 2008. **13**: p. 1117-29.10.2741/2749

66. Nelson, A.L., *Antibody fragments.* Landes Bioscience, 2010

67. Herrington-Symes, A.P., et al., Antibody fragments: Prolonging circulation half-life special issue-antibody research. Advances in Bioscience and Biotechnology, 2013. **04**(05): p. 689-698.10.4236/abb.2013.45090

68. Pande, J., M.M. Szewczyk, and A.K. Grover, Phage display: concept, innovations, applications and future. Biotechnol Adv, 2010. **28**(6): p. 849-58.10.1016/j.biotechadv.2010.07.004

69. Hassan M. E. Azzazy, W.E.H., Jr, Phage display technology clinical applications and recent innovations.pdf. Clinical Biochemistry, 2002

70. Hamers-Casterman, C., et al., Naturally occurring antibodies devoid of light chains. Nature, 1993. **363**(6428): p. 446-8.10.1038/363446a0

71. Muyldermans, S., *Nanobodies: natural single-domain antibodies.* Annu Rev Biochem, 2013. **82**: p. 775-97.10.1146/annurev-biochem-063011-092449

72. G, S., *The emergence of antibody fragments and derivates.* Innovation in pharmaceutical Tachnology.BioPharma UK, Biopharma, 2009: p. 46-48

73. Hairul Bahara, N.H., et al., Phage display antibodies for diagnostic applications. Biologicals, 2013. **41**(4): p. 209-16.10.1016/j.biologicals.2013.04.001

74. Kumar, R., et al., Phage display antibody libraries: A robust approach for generation of recombinant human monoclonal antibodies. Int J Biol Macromol, 2019. **135**: p. 907-918.10.1016/j.ijbiomac.2019.06.006

75. Smith, S.L., *Ten years of Orthoclone OKT3 (muromonab-CD3): a review.* J Transpl Coord, 1996. **6**(3): p. 109-19; quiz 120-1.10.7182/prtr.1.6.3.8145l3u185493182

76. Castelli, M.S., P. McGonigle, and P.J. Hornby, The pharmacology and therapeutic applications of monoclonal antibodies. Pharmacol Res Perspect, 2019. **7**(6): p. e00535.10.1002/prp2.535

77. Yasunaga, M., Antibody therapeutics and immunoregulation in cancer and autoimmune disease. Semin Cancer Biol, 2020. **64**: p. 1-12.10.1016/j.semcancer.2019.06.001

78. Scott, A.M., J.D. Wolchok, and L.J. Old, *Antibody therapy of cancer.* Nat Rev Cancer, 2012. **12**(4): p. 278-87.10.1038/nrc3236

79. Urquhart, L., Top companies and drugs by sales in 2019. Nat Rev Drug Discov, 2020. **19**(4): p. 228.10.1038/d41573-020-00047-7

80. Valldorf, B., et al., Antibody display technologies: selecting the cream of the crop. Biol Chem, 2022. **403**(5-6): p. 455-477.10.1515/hsz-2020-0377

81. Lu, R.M., et al., Development of therapeutic antibodies for the treatment of diseases. J Biomed Sci, 2020. **27**(1): p. 1.10.1186/s12929-019-0592-z

82. Kaplon, H., et al., *Antibodies to watch in 2020.* MAbs, 2020. **12**(1): p. 1703531.10.1080/19420862.2019.1703531

83. Kohler G, M.C., Continuous cultures of fused cells secreting antibody of predefined specificity. 1975

84. Samantha Zaroff, G.T., Hybridoma technology the preferred method for monoclonal antibody generation for in vivo applications. **BioTechniques**, 2019

85. Parray, H.A., et al., Hybridoma technology a versatile method for isolation of monoclonal antibodies, its applicability across species, limitations, advancement and future perspectives. Int Immunopharmacol, 2020. **85**: p. 106639.10.1016/j.intimp.2020.106639

86. Deantonio, C., et al., Phage display technology for human monoclonal antibodies. Methods Mol Biol, 2014. **1060**: p. 277-95.10.1007/978-1-62703-586-6_14

87. Kuhn, P., et al., Recombinant antibodies for diagnostics and therapy against pathogens and toxins generated by phage display. Proteomics Clin Appl, 2016. **10**(9-10): p. 922-948.10.1002/prca.201600002

88. Bradbury, A. and A. Pluckthun, Reproducibility: Standardize antibodies used in research. Nature, 2015. **518**(7537): p. 27-9.10.1038/518027a

89. Frenzel, A., et al., Designing Human Antibodies by Phage Display. Transfus Med Hemother, 2017. **44**(5): p. 312-318.10.1159/000479633

90. Presta, L.G., Engineering of therapeutic antibodies to minimize immunogenicity and optimize function. Adv Drug Deliv Rev, 2006. **58**(5-6): p. 640-56.10.1016/j.addr.2006.01.026

91. Hwang, W.Y. and J. Foote, *Immunogenicity of engineered antibodies.* Methods, 2005. **36**(1): p. 3-10.10.1016/j.ymeth.2005.01.001

92. Schaffitzel, C., et al., Ribosome display: an in vitro method for selection and evolution of antibodies from libraries. J Immunol Methods, 1999. **231**(1-2): p. 119-35.10.1016/s0022-1759(99)00149-0

93. Smith, G.P., Filamentous fusion phage: novel expression vectors that display cloned antigens on the virion surface. Science, 1985. **228**(4705): p. 1315-7.10.1126/science.4001944

94. Bazan, J., I. Calkosinski, and A. Gamian, Phage display--a powerful technique for immunotherapy: 1. Introduction and potential of therapeutic applications. Hum Vaccin Immunother, 2012. **8**(12): p. 1817-28.10.4161/hv.21703

95. Lim, B.N., et al., Principles and application of antibody libraries for infectious diseases. Biotechnol Lett, 2014. **36**(12): p. 2381-92.10.1007/s10529-014-1635-x

96. Alfaleh, M.A., et al., Phage Display Derived Monoclonal Antibodies: From Bench to Bedside. Front Immunol, 2020. **11**: p. 1986.10.3389/fimmu.2020.01986

97. Naranjo, L., et al., Recombinant Antibodies against Mycolactone. Toxins (Basel), 2019. **11**(6).10.3390/toxins11060346

98. Ledsgaard, L., et al., Basics of Antibody Phage Display Technology. Toxins (Basel), 2018. **10**(6).10.3390/toxins10060236

99. Rasched, I. and E. Oberer, Ff coliphages: structural and functional relationships. Microbiol Rev, 1986. **50**(4): p. 401-27.10.1128/mr.50.4.401-427.1986

100. Straus, S.K. and H.E. Bo, Filamentous Bacteriophage Proteins and Assembly. Subcell Biochem, 2018. **88**: p. 261-279.10.1007/978-981-10-8456-0_12

101. van Wezenbeek, P.M., T.J. Hulsebos, and J.G. Schoenmakers, Nucleotide sequence of the filamentous bacteriophage M13 DNA genome: comparison with phage fd. Gene, 1980. **11**(1-2): p. 129-48.10.1016/0378-1119(80)90093-1

102. Frenzel, A., T. Schirrmann, and M. Hust, Phage display-derived human antibodies in clinical development and therapy. MAbs, 2016. **8**(7): p. 1177-1194.10.1080/19420862.2016.1212149

103. Click, E.M. and R.E. Webster, Filamentous phage infection: required interactions with the TolA protein. J Bacteriol, 1997. **179**(20): p. 6464-71.10.1128/jb.179.20.6464-6471.1997

104. Huang, J.X., S.L. Bishop-Hurley, and M.A. Cooper, Development of anti-infectives using phage display: biological agents against bacteria, viruses, and parasites. Antimicrob Agents Chemother, 2012. **56**(9): p. 4569-82.10.1128/AAC.00567-12

105. Hess, G.T., et al., M13 bacteriophage display framework that allows sortase-mediated modification of surface-accessible phage proteins. Bioconjug Chem, 2012. **23**(7): p. 1478-87.10.1021/bc300130z

106. Jared Sheehan, W.A.M., *Phage and Yeast Display.* Microbiology Spectrum, 2015.10.1128/microbiolspec.AID

107. Fagerlund, A., A.H. Myrset, and M.A. Kulseth, Construction and characterization of a 9-mer phage display pVIII-library with regulated peptide density. Appl Microbiol Biotechnol, 2008. **80**(5): p. 925-36.10.1007/s00253-008-1630-z

108. Loset, G.A. and I. Sandlie, Next generation phage display by use of pVII and pIX as display scaffolds. Methods, 2012. **58**(1): p. 40-6.10.1016/j.ymeth.2012.07.005

109. Qi, H., et al., Phagemid vectors for phage display: properties, characteristics and construction. J Mol Biol, 2012. **417**(3): p. 129-43.10.1016/j.jmb.2012.01.038

110. Oh, M.Y., et al., Enhancing phage display of antibody fragments using gIII-amber suppression. Gene, 2007. **386**(1-2): p. 81-9.10.1016/j.gene.2006.08.009

111. O'Connell, D., et al., Phage versus phagemid libraries for generation of human monoclonal antibodies. J Mol Biol, 2002. **321**(1): p. 49-56.10.1016/s0022-2836(02)00561-2

112. Bradbury, A.R. and J.D. Marks, *Antibodies from phage antibody libraries.* J Immunol Methods, 2004. **290**(1-2): p. 29-49.10.1016/j.jim.2004.04.007

113. Carmen, S. and L. Jermutus, *Concepts in antibody phage display.* Brief Funct Genomic Proteomic, 2002. **1**(2): p. 189-203.10.1093/bfgp/1.2.189

114. Shim, H., *Antibody Phage Display.* Adv Exp Med Biol, 2017. **1053**: p. 21-34.10.1007/978-3-319-72077-7_2

115. Laustsen, A.H., et al., Pitfalls to avoid when using phage display for snake toxins. Toxicon, 2017. **126**: p. 79-89.10.1016/j.toxicon.2016.12.010

116. Chao, G., et al., Isolating and engineering human antibodies using yeast surface display. Nat Protoc, 2006. **1**(2): p. 755-68.10.1038/nprot.2006.94

117. Murtey, M.D. and P. Ramasamy, Sample Preparations for Scanning Electron Microscopy – Life Sciences, in Modern Electron Microscopy in Physical and Life Sciences. 2016.

118. Goffeau, A., et al., *Life with 6000 genes.* Science, 1996. **274**(5287): p. 546, 563-7.10.1126/science.274.5287.546

119. Duina, A.A., M.E. Miller, and J.B. Keeney, Budding yeast for budding geneticists: a primer on the Saccharomyces cerevisiae model system. Genetics, 2014. **197**(1): p. 33-48.10.1534/genetics.114.163188

120. Parapouli, M., et al., Saccharomyces cerevisiae and its industrial applications. AIMS Microbiol, 2020. **6**(1): p. 1-31.10.3934/microbiol.2020001

121. Gera, N., M. Hussain, and B.M. Rao, Protein selection using yeast surface display. Methods, 2013. **60**(1): p. 15-26.10.1016/j.ymeth.2012.03.014

122. Haber, J.E., Mating-type genes and MAT switching in Saccharomyces cerevisiae. Genetics, 2012. **191**(1): p. 33-64.10.1534/genetics.111.134577

123. Dranginis, A.M., Regulation of cell type in yeast by the mating-type locus.pdf. 1986

124. Lipke, P.N. and J. Kurjan, Sexual agglutination in budding yeasts: structure, function, and regulation of adhesion glycoproteins. Microbiol Rev, 1992. **56**(1): p. 180-94.10.1128/mr.56.1.180-194.1992

125. Feldhaus, M.J. and R.W. Siegel, Yeast display of antibody fragments: a discovery and characterization platform. J Immunol Methods, 2004. **290**(1-2): p. 69-80.10.1016/j.jim.2004.04.009

126. Boder, E.T., M. Raeeszadeh-Sarmazdeh, and J.V. Price, *Engineering antibodies by yeast display.* Arch Biochem Biophys, 2012. **526**(2): p. 99-106.10.1016/j.abb.2012.03.009

127. Feldhaus, M.J., et al., Flow-cytometric isolation of human antibodies from a nonimmune Saccharomyces cerevisiae surface display library. Nat Biotechnol, 2003. **21**(2): p. 163-70.10.1038/nbt785

128. Ferrara, F., M.F. Soluri, and D. Sblattero, Recombinant Antibody Selections by Combining Phage and Yeast Display. Methods Mol Biol, 2019. **1904**: p. 339-352.10.1007/978-1-4939-8958-4_16

129. Fei, C., et al., Potential Applications of Fluorescence-Activated Cell Sorting (FACS) and Droplet-Based Microfluidics in Promoting the Discovery of Specific Antibodies for Characterizations of Fish Immune Cells. Front Immunol, 2021. **12**: p. 771231.10.3389/fimmu.2021.771231

130. Sidhu, S.S. and F.A. Fellouse, *Synthetic therapeutic antibodies.* Nat Chem Biol, 2006. **2**(12): p. 682-8.10.1038/nchembio843

131. Pitaksajjakul, P., et al., Fab MAbs specific to HA of influenza virus with H5N1 neutralizing activity selected from immunized chicken phage library. Biochem Biophys Res Commun, 2010. **395**(4): p. 496-501.10.1016/j.bbrc.2010.04.040

132. Geisberger, R., M. Lamers, and G. Achatz, The riddle of the dual expression of IgM and IgD. Immunology, 2006. **118**(4): p. 429-37.10.1111/j.1365-2567.2006.02386.x

133. Erasmus, M.F., et al., A single donor is sufficient to produce a highly functional in vitro antibody library. Commun Biol, 2021. **4**(1): p. 350.10.1038/s42003-021-01881-0

134. Lim, C.C., Y.S. Choong, and T.S. Lim, Cognizance of Molecular Methods for the Generation of Mutagenic Phage Display Antibody Libraries for Affinity Maturation. Int J Mol Sci, 2019. **20**(8).10.3390/ijms20081861

135. Neylon, C., Chemical and biochemical strategies for the randomization of protein encoding DNA sequences: library construction methods for directed evolution. Nucleic Acids Res, 2004. **32**(4): p. 1448-59.10.1093/nar/gkh315

136. Rasila, T.S., M.I. Pajunen, and H. Savilahti, Critical evaluation of random mutagenesis by error-prone polymerase chain reaction protocols, Escherichia coli mutator strain, and hydroxylamine treatment. Anal Biochem, 2009. **388**(1): p. 71-80.10.1016/j.ab.2009.02.008

137. Unkauf, T., M. Hust, and A. Frenzel, Antibody Affinity and Stability Maturation by Error-Prone PCR. Methods Mol Biol, 2018. **1701**: p. 393-407.10.1007/978-1-4939-7447-4_22

138. Sblattero, D. and A. Bradbury, Exploiting recombination in single bacteria to make large phage antibody libraries. Nat Biotechnol, 2000. **18**(1): p. 75-80.10.1038/71958

139. Sblattero, D. and A. Bradbury, A definitive set of oligonucleotide primers for amplifying human V regions. Immunotechnology, 1998. **3**(4): p. 271-278.10.1016/s1380-2933(97)10004-5

140. Ingham, K.C., Precipitation of proteins with polyethylene glycol. Methods Enzymol, 1990. **182**: p. 301-6.10.1016/0076-6879(90)82025-w

141. Wen, J. and K. Yuan, Phage Display Technology, Phage Display System, Antibody Library, Prospects and Challenges. Advances in Microbiology, 2021. **11**(03): p. 181-189.10.4236/aim.2021.113013

142. Di Niro, R., et al., Construction of miniantibodies for the in vivo study of human autoimmune diseases in animal models. BMC Biotechnol, 2007. **7**: p. 46.10.1186/1472-6750-7-46

143. Hunter, S.A. and J.R. Cochran, Cell-Binding Assays for Determining the Affinity of Protein-Protein Interactions: Technologies and Considerations. Methods Enzymol, 2016. **580**: p. 21-44.10.1016/bs.mie.2016.05.002

144. Luth, J. and B. Barrier, CD28 and ICOS expression in human ovarian carcinoma cells. Cancer Research, 2007. **67**(9_Supplement): p. LB-341-LB-341

145. Ma, N., et al., ICOSL expressed in triple-negative breast cancer can induce Foxp3+ Treg cell differentiation and reverse p38 pathway activation. Am J Cancer Res, 2022. **12**(9): p. 4177-4195

146. Uhlen, M., et al., *Proteomics. Tissue-based map of the human proteome.* Science, 2015. **347**(6220): p. 1260419.10.1126/science.1260419, Human Protein Atlas proteinatlas.org

147. Pazienza, V., et al., Fasting cycles potentiates the efficacy of gemcitabine treatment in in vitro and in vivo pancreatic cancer models. Pancreatology, 2014. **14**(3).10.1016/j.pan.2014.05.753

148. Xu, D., et al., Cucurbitacin I inhibits the proliferation of pancreatic cancer through the JAK2/STAT3 signalling pathway in vivo and in vitro. J Cancer, 2022. **13**(7): p. 2050-2060.10.7150/jca.65875

149. Marks, J.D., Antibody affinity maturation by chain shuffling. Methods Mol Biol, 2004. **248**: p. 327-43.10.1385/1-59259-666-5:327

150. Bessa, D., et al., Improved gap repair cloning in yeast: treatment of the gapped vector with Taq DNA polymerase avoids vector self-ligation. Yeast, 2012. **29**(10): p. 419-23.10.1002/yea.2919